



Exploring the Fermentation Parameters of Kombucha on Caffeine and pH Using Experimental Design and the Feasibility of Raman Spectroscopy in Kombucha Analysis

Kellyn Tricia Co Ngo

Supervisor: Prof. Dr. Bjørn Grung (University of Bergen, Norway)



Erasmus Mundus Master in Quality in Analytical Laboratories (EMQAL)

September 27, 2023

Department of Chemistry

University of Bergen

Acknowledgements

This EMQAL master could not have been achieved without the support of the Erasmus+ Programme of the European Union and I am forever grateful for this opportunity.

I want to express my sincere appreciation to Professor Dr. Bjørn Grung, my supervisor. Your mentorship has been invaluable in guiding my research journey. Thank you for your support and patience.

I'm also grateful to Professor Svein Are Mjøs for providing me with laboratory space and accommodating my SCOBYs. Inger Johanne Fjellanger, Marit Bøe Vaage, and Reidun Alice Myklebust, thank you all for your patience in teaching and lending me laboratory equipment for the analysis of my Kombucha.

I'd like to extend my thanks to Anne-Kristine Nedrebø for sharing her experience in handling kombucha especially the SCOBYs and to Carl Eugen Johannesen from Bergen Kaffebrønneri (BKB) for supplying the necessary materials for this study and techniques on how to brew kombucha.

To my family and friends, your unwavering support means the world to me. I cannot adequately express my gratitude for your encouragement throughout this journey.

Disclaimer

The European Commission's support for the production of this publication does not constitute an endorsement of the contents, which reflect the views only of the authors, and the Commission cannot be held responsible for any use which may be made of the information contained therein.

Abstract

Kombucha shows promising growth potential due to its claimed health benefits. Through an experimental design, the impact of the fermentation parameters on color and appearance, pH and caffeine content was further understood with sample points of Day 1, 7, 10 and 14. Steeping time, steeping temperature, tea strength, starter-to-tea ratio, tea-to-liquid ratio, sugar content, and beaker size were employed on a 2^{7-4} design and its corresponding full fold-over. In addition, this study explores the feasibility of Raman spectroscopy for understanding and predicting kombucha behavior and validates an HPLC method for caffeine content analysis.

As expected during fermentation processes, pH declines rapidly in the first few days and gradually decreases later on. Identified significant variables vary among the sampling days, such as tea strength, sugar content and beaker size. The starter-to-tea ratio remained a significant parameter in the course of the fermentation.

In contrast, caffeine content was mostly consistent or decreased during the fermentation period except for a few experiments. Several of the identified parameters and interactions affect caffeine content; for example, steeping temperature, starter-to-tea ratio, tea strength, sugar content and interactions 1x5 (AxE) and 1x4 (AxD).

Savitzky-Golay 1st derivative, window 11, and at 2nd degree achieved modest separation of Set 3 from Sets 1 and 2 using PCA; however caffeine and pH were not the cause of the separation according to PLS. Unfortunately, Raman proved insensitive to kombucha's caffeine content and pH through spiking studies.

Overall, there is still a lot of work that can be done with this study. Execution of the experimental design, investigation of the microbial composition, and further exploration of the use of Raman spectroscopy are few of the recommendations for this study. Despite this, the study can serve as a foundation for future kombucha studies exploring the fermentation parameters and its effect on kombucha's chemical composition through experimental design.

Table of Contents

Acknowledgements	i
Disclaimer	ii
Abstract	iii
List of Figures	vii
List of Tables	x
List of Abbreviations	xi
1. Introduction	1
1.1 Kombucha	3
1.1.1 Physicochemical properties.....	3
1.1.2 Factors affecting fermentation.....	6
1.2 Experimental design	9
1.3 Chemical instrumentation and analysis	11
1.3.1 High performance liquid chromatography/ high pressure liquid chromatography (HPLC)	11
1.3.2 Raman spectroscopy	15
1.4 Multivariate analysis	22
1.4.1 Principal component analysis.....	22
1.4.2 Partial least squares regression (PLS-R).....	23
2 Experimental	24
2.1 Experimental design	24
2.2 Brewing	27
2.2.1 Materials.....	27
2.2.2 Brewing method	27
2.3 Sampling	27
2.4 pH	28
2.5 Caffeine content by HPLC	28
2.5.1 Materials.....	29

2.5.2	Method validation using the column available	29
2.5.3	Adjusting chromatographic gradient conditions	30
2.5.4	Converting from standard addition to external calibration	32
2.5.5	Final HPLC procedure for caffeine content.....	32
2.6	Raman spectroscopy	32
2.7	Multivariate analysis.....	32
3	<i>Results and discussion</i>	34
3.1	Physical properties of kombucha	34
3.2	pH.....	36
3.2.1	Factors affecting pH.....	40
3.3	Caffeine	46
3.3.1	Method validation of caffeine content by HPLC.....	46
3.3.2	Conversion from standard addition to external calibration method	47
3.3.3	Caffeine content	50
3.3.4	Factors affecting caffeine content.....	53
3.4	Raman spectroscopy	54
3.4.1	Raw data	54
3.4.2	Exploratory analysis.....	57
3.4.3	Data preprocessing.....	58
3.4.4	Partial least squares	63
4	<i>Conclusion</i>	66
5	<i>Recommendations.....</i>	67
6	<i>References.....</i>	68
7	<i>Appendix.....</i>	78
7.1	Brewing	78
7.2	Color and Appearance.....	79
7.3	Pictures of kombucha.....	81
7.4	pH.....	83

7.5	Method validation	84
7.5.1	Linearity and range.....	84
7.5.2	Precision	85
7.5.3	Accuracy	85
7.6	Caffeine Content	86
7.7	Experimental Design pH	87
7.7.1	pH day 1.....	87
7.7.2	pH day 7.....	89
7.7.3	pH day 10.....	93
7.7.4	pH day 14.....	97
7.8	Experimental Design Caffeine	99
7.8.1	Caffeine day 1.....	99
7.8.2	Caffeine day 7.....	101
7.8.3	Caffeine day 10.....	102
7.8.4	Caffeine day 14.....	103
7.9	Pre-processing	104
7.10	PLS tabular results	107

List of Figures

Figure 1: Fermentation pathway of yeast and AAB during kombucha fermentation ¹⁰	4
Figure 2: Model matrix of a factorial design ⁴⁰	9
Figure 3: 2 ⁷⁻⁴ fractional factorial design	10
Figure 4: Overview of an HPLC work flow ⁴²	11
Figure 5: HPLC chromatogram of caffeine	13
Figure 6: Electronic transitions of Raman spectroscopy ⁵²	16
Figure 7: Schematic diagram of Raman spectroscopy ⁵³	17
Figure 8: Spectrum composition of Raman ⁶²	19
Figure 9: Light scattering after laser exposure on a sample ⁵¹	20
Figure 10: Sampling point withdrawal from each experiment	28
Figure 11: Set 2: Experiment 1 over the course of the 14 days	35
Figure 12: pH profile trend Set 1.....	37
Figure 13: pH profile trend Set 2.....	37
Figure 14: pH profile trend Set 3.....	38
Figure 15: Predicted versus measured for pH day 1 with the significant variables	41
Figure 16: Response residuals for pH day 1 with the significant variables	41
Figure 17: Screening variables for pH Day 1	42
Figure 18: Normal probability plot of screening variables for pH day 1	43
Figure 19: Half normal probability plot for pH day 1	43
Figure 20: Regression coefficients for pH from day 1, day 7, 10 and 14.....	45
Figure 21: Chromatogram of kombucha for caffeine content.....	50
Figure 22: Caffeine profile over 14 days Set 1	51
Figure 23: Caffeine profile over 14 days Set 2	51
Figure 24: Caffeine profile over 14 days Set 3	52
Figure 25: Regression coefficients for caffeine content from day 1, day 7, 10 and 14.....	54
Figure 26: Sample Raman spectra of kombucha.....	56
Figure 27: Sample Raman spectra of kombucha zoomed in.....	56
Figure 28: Score plot of all samples and replicates without pre-treatment	57

Figure 29: Score plot of unprocessed raman spectra, removing outlier.....	58
Figure 30: Example of a rolling ball spectra	59
Figure 31: Raman spectra pre-processed using Savitzky-Golay.....	60
Figure 32: PCA plot for all samples and replicates of kombucha.....	60
Figure 33: Loadings plot of the kombucha samples	61
Figure 34: Score plot of raman spectra for pH.....	62
Figure 35: Score plot of raman spectra for caffeine	62
Figure 36: Various Raman spectra of caffeine content in kombucha	64
Figure 37: Raman spectra of kombucha spiked with acetic acid (HAc) and NaOH	65
Figure 38: Set 1 Day 7: Experiments 1 ,4, 7 and 6.....	81
Figure 39: SCOBY to be laid on one of the Kombucha set-ups	81
Figure 40: Random kombucha experiments.....	82
Figure 41: Set 2, Day 10, Experiments 1 to 10 (Exp 8-3) in sample bottles	82
Figure 42: Calibration curve peak area vs caffeine concentration (ppm).....	84
Figure 43: Residual plot of calibration curve from Figure 43.....	84
Figure 44: Predicted versus measured pH day 1 all screening variables	87
Figure 45: Response residuals of pH day 1- all screening variables.....	88
Figure 46: Screening variables for pH difference Day 7 and Day 1 (77.51%).....	89
Figure 47: Normal probability plot of screening variables for pH day 7-day 1	89
Figure 48: Predicted vs Measured for pH day 7- pH day 1- all significant variables	90
Figure 49: Response residuals pH day 7- pH day 1-all significant variables.....	90
Figure 50: Predicted versus Measured pH day 7- pH day 1, 6 significant variables.....	91
Figure 51: 6 Significant variables under pH day 7 - pH day 1 (75.76%).....	91
Figure 52: Response Residuals Day 7, 6 significant variables	92
Figure 53: Predicted vs Measured pH day 10-all significant variables.....	93
Figure 54: Half normal probability for screening significant variables Day 10	94
Figure 55: Screening variables for pH of Day 10 (98.53%).....	95
Figure 56: Predicted vs Measured Day 10 - 4 significant variables.....	96
Figure 57: Response residuals pH Day 10-4 significant variables	96

Figure 58: Predicted vs Measured pH day 14-all significant variables.....	97
Figure 59: Screening variables for pH of Day 14 (73.79%-all significant variables	97
Figure 60: Predicted vs. Measured for pH Day 14-4 significant variables.....	98
Figure 61: Response residuals for pH Day 14 - 4 significant variables	98
Figure 62: Screening variables for Caffeine content day 1	99
Figure 63: Half normal probability plot of Caffeine Day 1	99
Figure 64: Predicted versus Measured for Caffeine day 1	100
Figure 65: Screening variables for significant variables for caffeine day 7- caffeine day 1	101
Figure 66: Predicted vs measured caffeine day 7- caff day1	101
Figure 67: Screening variables caff day 10 - caff day 1 (explains: 99.08%).....	102
Figure 68: Screening variables caffeine day 14- caffeine day 1 (98.42%).....	103
Figure 69: PCA scores PC1 and PC3, Savitzky Golay window 11, 1st derivative	104
Figure 70: PCA scores PC1 and PC2, Savitzky Golay window 11, 1 st derivative	104
Figure 71: Component Information Table for the Savitzky Golay Differentiation 1 st Derivative Window 11 Degree 2 1 st replicates only.	105
Figure 72: Predicted versus Measured for Savitzky Golay Differentiation 1 st Derivative Window 11 Degree 2 with the cross-validation set	105
Figure 73: Predicted versus measured for Savitzky Golay Differentiation 1 st Derivative Window 11 Degree 2 with the predicting set	106

List of Tables

Table 1: Values of the coded levels for the seven parameters.....	24
Table 2: Reduced fractional design and fold-over design at Resolution III.....	25
Table 3: Experimental design conducted for Set 1	26
Table 4: Chromatographic Conditions from the original method to the converted.....	30
Table 5: Equations for converting HPLC gradient method ⁸⁰	31
Table 6: Method Validation Parameters with their Corresponding Procedure	31
Table 7: Identified significant variables affecting pH on days 1, 7, 10 and 14.....	44
Table 8: Method validation for caffeine content criteria and values	47
Table 9: Descriptive statistics for conversion of standard addition to external calibration	47
Table 10: Identified significant variables affecting caffeine on days 1, 7, 10 and 14.....	53
Table 11: Naming format of the Raman spectra from kombucha	55
Table 12: Actual Values for Brewing kombucha in the Experimental Design	78
Table 13: Organoleptic properties of different kombucha set-ups (Sets 1-3) and time points	79
Table 14: Obtained pH results for Sets 1, 2 and 3 over 1st, 7th, 10th and 14th day	83
Table 15: Raw data for precision study of caffeine content	85
Table 16: Data for accuracy studies of kombucha for caffeine content	85
Table 17: Obtained caffeine content (ppm) results for Sets 1, 2 and 3 over 1st, 7th, 10th and 14th day	86
Table 18: Examples of Pre-preprocessing techniques on the Raman spectra for pH.....	107
Table 19: Examples of Pre-preprocessing techniques on the Raman spectra for caffeine.....	107

List of Abbreviations

AAB	Acetic acid bacteria
BKB	Bergen Kaffebränneri
CCD	Charged -Coupled Device
CV	Coefficient of Variation
DAD	Diode Array Detector
EMSC	Extended Multiplicative Scatter/Signal Correction
US FDA	United States Food and Drug Administration
FO	Fold Over
HAC	Acetic Acid
HPLC	High Performance Liquid Chromatography
ICH	International Council for Harmonisation of Technical Requirements for Pharmaceuticals for Human Use
p-MC	p-value Monte Carlo
MSC	Multiplicative Scatter/Signal Correction
Obj-FO	Object Foldover
PC	Principal Component
PCA	Principal Component Analysis
PDA	Photodiode Array
PLS	Partial Least Squares
PTFE	Polytetrafluoroethylene
R²	Coefficient of Determination
R²CV	Coefficient of Determination Cross Validation
R²P	Coefficient of Determination Prediction
RMSECV	Root Mean Square Error Cross Validation
RMSEP	Root Mean Square Error Prediction
SC	Standard Calibration
SCOBY	Symbiotic Culture of Bacteria and Yeast

SD	Standard deviation
SERS	Surface-Enhanced Raman Spectroscopy
UV	Ultraviolet
UV-Vis	Ultraviolet-Visible

1. Introduction

Kombucha is a slightly fermented tea traditionally prepared by combining tea, sugar, a starter culture and laying a symbiotic culture of bacteria and yeast (SCOBY) on the surface of the liquid. The SCOBY is a cellulose pellicle made up of a symbiotic culture of bacteria and yeast (*Acetobacter xylinum*, *A. xylinoides*, or *Bacterium gluconicum*, and yeasts such as *Saccharomyces cerevisiae*, *S. ludwigii*, *Zygosaccharomyces bailii*, *Z. rouxii*, *Schizosaccharomyces pombe*, *Torulasporea delbrueckii*, *Brettanomyces bruxellensis*, *B. lambicus*, *B. custersii*, *Candida sp.*, or *Pichia membranaefaciens*). It is responsible for the aerobic fermentation often lasting for 7 to 12 days, resulting to a healthy, sweet, slightly sour, and effervescent drink^{1,2}. Microbial activity is claimed to enhance the health benefits compared to its unfermented counterpart^{3,4}. Fermentation parameters such as sugar concentration, vessel surface area, and substrate type can influence the fermentation product. Yet, it is certain that it contains organic acids, sugars, vitamins, amino acids, biogenic amines, purines, pigments, lipids, proteins, some hydrolytic enzymes, ethanol, caffeine, carbon dioxide, polyphenols, anions, minerals, D-saccharic acid-1, 4-lactone and bacterial metabolites which may have health benefits⁷.

Its claimed health benefits include anti-microbial, anti-carcinogenic, anti-diabetic capabilities, and treatment for gastric ulcers, and liver detoxification⁶. Due to growing number of consumers leaning towards a healthier lifestyle, kombucha has seen exponential economic growth in recent years. This shift in consumer preference has led several global companies, such as The Coca-Cola Company, to invest in kombucha shares and expand their product portfolio. Furthermore, the global market size of kombucha in 2019 was USD 1.84 billion. By 2027, predictions show an increase to USD 10.45 billion or a compound annual growth rate of 23.2%⁷.

Kombucha's economic potential has spurred the growth in kombucha studies, such as challenging the traditional use of black and green tea to more novel beverages such as milk, coffee, and soymilk and the addition of flavorings such as lavender, peach, and raspberry^{8,9}. Becoming a potential mainstream drink highlights the importance of scaling up studies and quality control measures to ensure consistent quality kombucha production in highly dynamic fermentation

systems. This study aims to use the less studied white tea as a substrate with the following objectives:

- Explore the profile of the kombucha white tea's appearance, pH, and caffeine content of white tea with sampling on day 1, day 7, day 10, and day 14.
- Screen significant fermentation variables of kombucha in line with the pH and caffeine content through fractional factorial design.
- Explore the capability of Raman spectroscopy to understand Kombucha's fermentation behavior and predict its caffeine content and pH.

To determine caffeine content, it is also an objective to develop a working analytical method through HPLC.

An essential aspect of the fermentation process is the microbial parameters of kombucha, especially the SCOBY and starter. These were not taken into consideration due to the time restraints and the knowledge of the experimenter.

1.1 Kombucha

1.1.1 Physicochemical properties

1.1.1.1 Appearance and color

One of the first noticeable things is that the physical attributes of a food product are the first line of defense for safety. The color and appearance can also affect its marketability. While several studies have been made on the fermentation parameters and health benefits, few studies have considered kombucha's appearance and color¹⁰.

A range of different methods have been employed such as observing subjectively¹¹, having a panel of personnel evaluating the desirability¹² to using instruments such as chromameters and UV-Vis spectrophotometer⁴. Kombucha can appear either clear or turbid. Turbidity can come from the aggregated proteins, polyphenols, and cellulose fibers from the acetic acid bacteria. Extracted polyphenols also contribute to the color of the tea^{10,13}.

1.1.1.2 pH

pH indicates the activity of hydrogen ions, but in most applications, the concentration of hydrogen ions is most often used. pH uses a scale of 0 to 14, where lower than 7 indicates the acidity and higher than 7 basicity when temperature is at 25°C¹⁴ but it can also go beyond this scale. Apart from the growth of microorganisms, pH can also influence and modify the chemical structure of some chemical compounds.

The relationship between pH and kombucha is most prominent during the fermentation process. In most studies, fermentation occurs between 7 to 14 days at temperature between 20 to 30 °C, where the pH decreases over time. Fermentation starts when the SCOBY is laid on the drink's surface, added with a small portion of old kombucha or starter to lower the pH. When the SCOBY is in contact, its consortium of bacteria and yeast metabolizes the drink's components. The SCOBY has reproduced itself during fermentation with a daughter tea fungus membrane. At the microbial and chemical level (Figure 1), the bacteria and yeast cells from the SCOBY metabolize sucrose to fructose and glucose. From fructose and glucose, organic acids such as gluconic and

acetic acid are produced, resulting in a decrease in the pH of kombucha. Acetic acid is the most dominant acid in kombucha when sucrose is used^{5,15}.

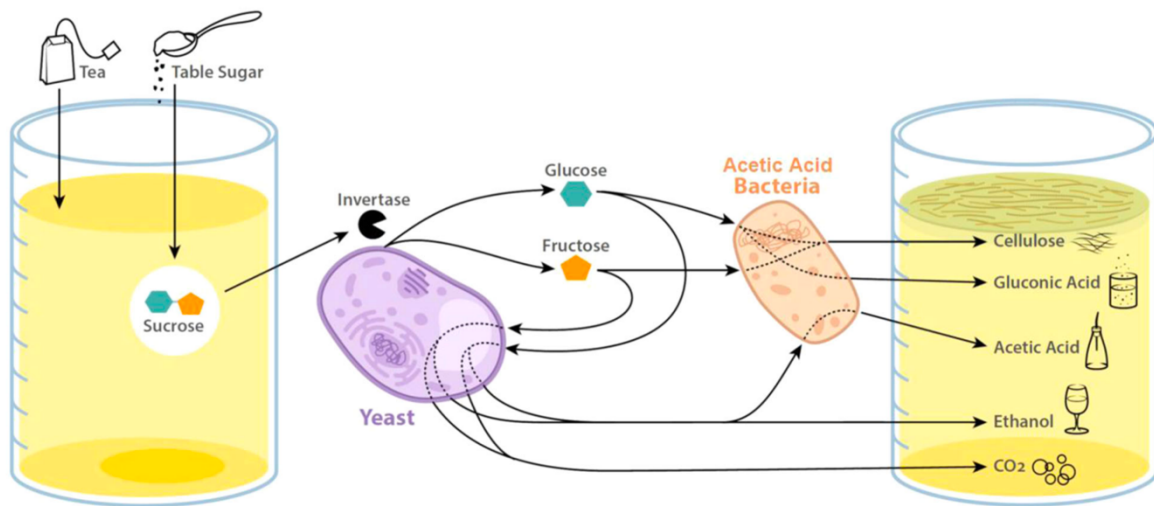


Figure 1: Fermentation pathway of yeast and AAB during kombucha fermentation¹⁰

pH plays a vital role in the development and health of microorganisms in kombucha. Different studies suggest different pH ranges for acetic acid bacteria (AAB) to live, but at a pH lower than 3; it is still capable of growing and producing a daughter SCOBY. On the other hand, yeasts thrive around pH 5 and convert sugar to alcohol and carbon dioxide^{12,16}. Hence, the decrease in pH to a specific range can signal certain processes occurring during the fermentation. Sudden drop of the pH at the start from 6.0 to 4.0 would most probably relate to the start of inoculation. Another would be the proliferation of critical microorganisms to convert glucose to gluconic acid, hence increasing the organic acid content contributing to a decline in pH¹⁶.

In relation to microorganisms, pH is often linked to kombucha's antimicrobial properties, which can avoid the growth of a wide range of harmful bacteria⁵. US FDA does not require temperature control for food with a lower pH than 4.6. Regulation for this type of food just requires the presentation of pH at safe levels, at most pH 4.6. At this pH, harmful bacteria cannot thrive; thus, these types of food do not require any preservatives¹⁷. Therefore, it is crucial to ensure that the pH drops to 4.6 after adding the starter to inhibit the growth of harmful bacteria^{16,17}. The pH and titratable acidity are used in tandem to determine the completion of fermentation and for quality control purposes¹⁸.

One manifestation of an acidic pH in a drink is its smell and taste profile. The first few days of fermentation would exhibit fruity and sweet notes, and as the fermentation progresses, sour notes similar to vinegar will develop². Thus, home fermenters usually use sourness as the basis to end their brewing. On the other hand, for industrial breweries and brewers with pH instruments, the range usually falls between pH 2.5 and 3.5¹⁹.

While a lower pH can be perceived as an increased presence of organic acids and pronounced anti-microbial properties, too low can make the drink lose its desirability¹². Also, consuming food products with too low a pH can lead to enamel degradation of the teeth and acidosis⁵.

1.1.1.3 Caffeine

Caffeine is a xanthine alkaloid found in plants such as coffee, tea, and cocoa consumed by humans. It is also a known contributor to the bitter taste and can enhance the flavor of tea. Humans primarily consume caffeine as a stimulant for the nervous system for improved work efficiency and sharper attention^{5,20}.

Tea leaves consist of 3-6% caffeine, mainly contributing to the caffeine content of kombucha tea. Caffeine content differs between different types of tea leaves which are classified by their physical appearance and the processing of the tea plant. While it is not a popular substrate compared to black and green tea, white tea was used in this study because of its mild taste and availability. White tea has the most delicate buds and leaves covered in thin white hairs⁵. It does not undergo oxidation but a delicate drying process that protects the sensitive chemical components from degradation, resulting in a milder taste than the more popular black and green tea. Compared to its more popular counterparts, this variety possesses the highest concentration of antioxidants and high catechin content⁵.

Caffeine provides the yeast and bacteria with the nitrogen necessary for metabolic processes and building new cells and energy for them so they can undergo the fermentation process^{5,21,22}. Because of this, a myth among kombucha brewers is that caffeine stimulates the fermentation

process of kombucha²³. Studies report a range of caffeine content due to different fermentation parameters^{6,24}, however they show decreased or constant caffeine content during the fermentation period²⁵. Some studies suggest that caffeine is converted to other compounds such as theophylline and methylxanthine and can be absorbed by the SCOBY during prolonged fermentation^{26,23}.

1.1.2 Factors affecting fermentation

Kombucha differs significantly from its unfermented counterpart drinks through its physical characteristics and nutritional content contributed by the SCOBY and fermentation process. Different fermentation parameters can lead to various other fermentation pathways, yielding various metabolites in kombucha. In this study, the fermentation factors are time, steeping temperature, steeping time, the ratio of liquid and beaker, the concentration of tea leaves, the ratio of starter and tea, the concentration of sugar, and the size of beaker. This study explores the application of experimental design to explore the fermentation parameters with pH and caffeine as the response variables on white tea kombucha.

1.1.2.1 Steeping temperature and steeping time

Not many studies have been conducted on the effect of steeping temperature and steeping time on kombucha tea. However, since the SCOBY acts on the chemical compounds from the substrate, studies on the impact of these parameters on tea are used. Studies have shown that steeping temperature and time affect the extraction by increasing solubility and movement of tea compounds from leaves to water, thus increasing antioxidant activity and flavonoid content^{27,28}. These implications on kombucha include more components for the SCOBY to work on due to the extraction from tea leaves.

1.1.2.2 Ratio of liquid and beaker, and beaker size

With the growing demand for kombucha, several research have been conducted on the possibility of using other substrates, optimal fermentation time and temperature, effect of sugar concentration, and so on. However, most studies were conducted on a 0.5 L to 1 L laboratory scale^{11,29,30}. Two important issues arise from this.

Scaling from small to industrial volumes is not as straightforward, especially for products that undergo fermentation. The bigger volume slows heat and mass transfer in scaled-up productions, resulting in differing physical, chemical, and biological characteristics between a small and large set-up. Agitation is often executed to at least minimize this problem. However, agitation can be difficult for kombucha since it can break the cellulose formation of the SCOBY. The SCOBY resides at the drink's surface while the some yeast particles from the SCOBY can be dispersed throughout the liquid. This results in uncertainty in the solution's homogeneity, which can impact the kombucha's properties³¹. Oxygen supply is another issue, as it can also affect the optimal sensory and healthy kombucha drink. Acetic acid bacteria, in particular, is aerobic; thus, its activity relies on oxygen supply, which can be affected by the surface area of the liquid and volume of the liquid^{10,32}.

1.1.2.3 Ratio of starter and tea (ml of starter/ ml of brewed tea)

A starter's role is essential as this initiates the pH drop of the tea and the fermentation process along with the laying of the SCOBY on the surface. Adding a suitable amount allows the safe production of kombucha without using preservatives, as meeting the pH of at most 4.6 inhibits the growth of harmful microorganisms¹⁷. While transferring kombucha pellicles to another batch and using old kombucha works, it suffers from the lack of control over the microbial composition of kombucha and consistency in the production of kombucha¹⁹.

Several studies that brew their own kombucha observed a sudden drop in the pH right after addition around to 6.0 to 4.0^{16,25,32}. Starters have also been found to spur the fermentation process¹⁰, increase the content of desirable chemical compounds, and improve the functional and sensory qualities of kombucha^{15,33}.

1.1.2.4 Concentration of tea leaves

White tea is the least processed with minimal fermentation among its other relatives. Young leaves and new growth buds are used and immediately dried to protect them from oxidation. This results in a light, delicate, and sweet taste that is different from its other close relatives. Beneficial compounds have been identified and separated, including polyphenols (16–26%), carbohydrates

(20–25%), amino acids (6–9%) and peptides, alkaloids (2–5%), volatile compounds (0.047%), organic acids, minerals, nucleosides, caffeine and catechins such as epigallocatechin, epicatechin gallate and epigallocatechin gallate. Health benefits include anti-oxidation, anti-inflammatory, anti-diabetes, anti-cancer, anti-obesity and antihyperlipidemic activities^{5,34–36}.

In kombucha, the purpose of tea leaves is to provide nitrogen and minerals for the microorganisms. Dried tea leaves contain 21-28% protein and amino acids, making up 6% w/w of the extract solids¹⁹. As of writing, no studies have been conducted on the influence of tea leaves concentration in kombucha tea fermentation.

1.1.2.5 Concentration of Sugar

Sugar serves as the carbon source for producing organic acids in the fermentation process of kombucha¹⁹. The microorganisms in the drink convert sucrose to glucose and fructose, then to ethanol, carbon dioxide, and glycerol. AAB converts these products to acetic acid which promotes the yeast to produce more ethanol¹³. Studies have shown that lower sugar concentration results in a lower pH value due to increased organic acid content^{16,37}.

1.1.2.6 Fermentation time

Fermentation time is critical to kombucha's sensory quality, chemical components, and health benefits. Different studies claim different periods of maximum fermentation times of kombucha from 7 days, 15 days, 60 days, or even 760 days^{1,38}. But most commonly, fermentation ends in 7 to 15 days. Prolonging fermentation can increase kombucha's antioxidant properties but results in an undesirable acidic drink with potentially harmful levels of organic acids for direct consumption³⁸.

The beverage is observed to have a refreshing fruity taste around the 6th to 10th day. However, a prolonged fermentation time leads to an unpleasant and vinegary taste¹. In terms of microbial load, they grow in number as the days pass and then equilibrate. Optimal fermentation time also differs depending on the substrate used. The fermentation pathway and duration in kombucha

made from black and green tea vary from each other²⁵. Thus, in this study, it is expected that white tea will behave differently from its more popular counterparts.

1.2 Experimental design

Experimental design is a systematic, efficient method to collect data and generate new knowledge by studying the relationship between several factors and responses. The process of executing experimental design is described briefly:

1. Identifying significant factors that may affect the responses and the result of the experiment
2. Implementing a proper design to minimize the effects of uncontrolled factors
3. Using statistics to determine the degree of importance of a variable³⁹.

Screening experiments, such as factorial design, are conducted to determine experimental factors and possible interactions that have a significant impact to the experiment. Factorial designs allow the study of several factors that are varied together and the discovery of interactions between factors that may affect the result of the experiment⁴⁰.

Experimental factors are the factors being investigated. If there are k selected factors at two levels being investigated, there are 2^k experiments. When three factors ($k=3$) are chosen, eight experiments will be executed, resulting in a full-factorial design (Figure 2).

Model matrix and the yield response

Exp.	I	x_1	x_2	x_3	$x_1 x_2$	$x_1 x_3$	$x_2 x_3$	$x_1 x_2 x_3$
1	+	-	-	-	+	+	+	-
2	+	+	-	-	-	-	+	+
3	+	-	+	-	-	+	-	+
4	+	+	+	-	+	-	-	-
5	+	-	-	+	+	-	-	+
6	+	+	-	+	-	+	-	-
7	+	-	+	+	-	-	+	-
8	+	+	+	+	+	+	+	+

Figure 2: Model matrix of a factorial design⁴⁰

A third-order polynomial explains the 2^3 design (1) where, main effects and interactions can be computed. The main effects refer to x_1 to x_3 , while interactions are the combinations of the

effects, such as x_1x_2 and, etc. The b values are the effect values computed to evaluate its significance in the experiment. The signs of the effects show how it affects the model, whether it is positive (+) or negative (-).

$$y = b_0 + b_1x_1 + b_2x_2 + b_3x_3 + b_{12}x_1x_2 + b_{13}x_1x_3 + b_{23}x_2x_3 + b_{123}x_1x_2x_3 \quad (1)$$

Adding more factors increases the number of experiments required and can become unmanageable. A fractional factorial design is a fraction of the full-factorial design and can still achieve the goals of the experiment. From 128 experiments in a 2^7 design, it can be reduced to 8 experiments, 2^{7-4} or 1/16 of the experiment.

Exp. no.	I	x_1	x_2	x_3	x_4	x_5	x_6	x_7
		a	b	c	ab	ac	bc	abc
1	1	-1	-1	-1	1	1	1	-1
2	1	1	-1	-1	-1	-1	1	1
3	1	-1	1	-1	-1	1	-1	1
4	1	1	1	-1	1	-1	-1	-1
5	1	-1	-1	1	1	-1	-1	1
6	1	1	-1	1	-1	1	-1	-1
7	1	-1	1	1	-1	-1	1	-1
8	1	1	1	1	1	1	1	1

Figure 3: 2^{7-4} fractional factorial design

In Figure 3 all seven factors are varied independently of each other, so they are still orthogonal. However, a drawback of fractional factorial design is that the true effects of the factors are confounded with the interaction effects. Additional experiments are required to separate the main effects from the interactions⁴⁰.

Confounding patterns are determined by the generator of the experimental design. One of the most common screening designs is a Resolution III design, where main effects are confounded with two-factor interactions. It is possible to separate the significant main effect from the aliased interactions by a fold-over design. This is an accompanying design where each factor has its level reversed compared to the original design. This separates all the main effects from the confounding interactions⁴¹.

There are multiple ways to determine the significant variables from a study. One way is to use the normal probability plot of effects. The effects that follow a straight line in the plot are negligible

effects, since they have zero means and small variances. Significant effects are the ones that do not fall on the straight line. Another similar method is the half normal probability plot where it plots the absolute value of the effect estimates to the cumulative normal probabilities⁴¹.

1.3 Chemical instrumentation and analysis

1.3.1 High performance liquid chromatography/ high pressure liquid chromatography (HPLC)

Chromatography is a common and powerful method to separate components of a sample through the distribution of the sample between two immiscible phases: stationary and mobile phase. The chemical interaction of the sample between these two phases allows the analyte's separation, identification, determination, and quantification. In HPLC, polarity is one of the governing chemical principles. There are two phases which are depending on the polarity of the stationary phase. The normal phase has a polar stationary phase and a non-polar mobile phase. On the contrary, the more commonly used reversed-phase employs a non-polar stationary phase and a polar mobile phase.

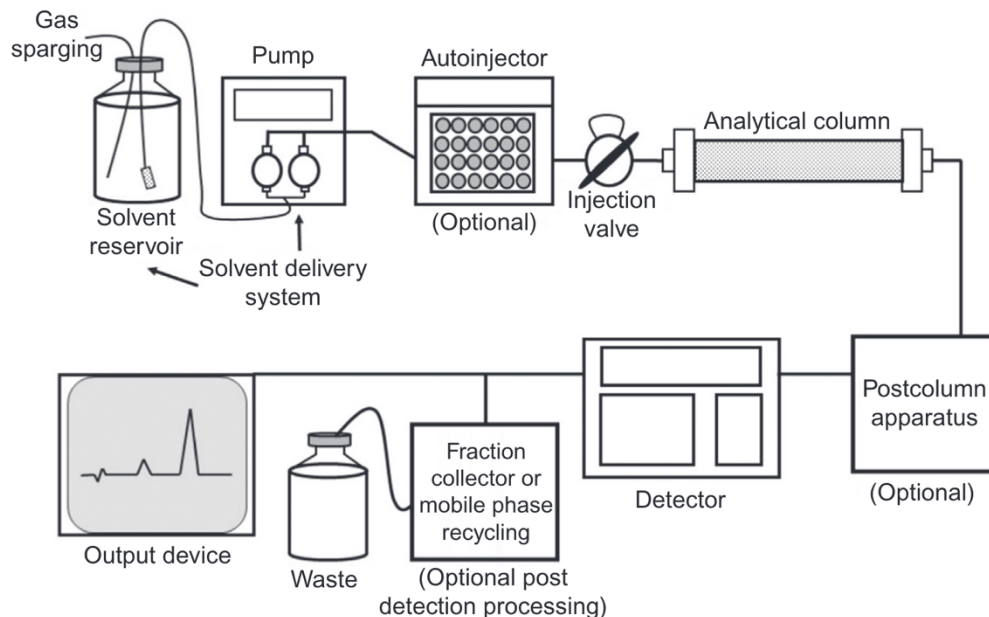


Figure 4: Overview of an HPLC work flow⁴²

Figure 4 shows that the instrument starts with a pump to provide pressure for the mobile phase to flow through the system, allowing the sample to be transported through the system. There are

two types of mobile phase elution: isocratic and gradient flow. Isocratic flow is the elution of the mobile phase at a constant composition, while gradient flow has two or more solvent systems, making the chemical composition of the mobile phase differ during the analysis⁴². The solvent systems employed during a gradient elution analysis have differing polarity. There are several advantages, such as a reduction in the total run time and enhanced peak resolution^{43,44}.

The mobile phase carries the sample to the column packed with the stationary phase. As stated earlier, the mobile phase in reversed-phase chromatography is polar while the stationary phase (column) is nonpolar. The sample separates according to polarity where the polar compounds will flow with the mobile phase to the detector, and the nonpolar compounds will interact with the stationary phase, taking longer to reach the detector¹⁴.

A specific response is generated when the desired analyte reaches the detector. One typical detector is the diode-array detector (DAD) which allows gathering of data in a wide range of wavelength, including UV-absorbing compounds, such as alkenes, aromatics, and compounds that have multiple bonds between C and O, N, or S⁴². Lastly, a software then allows the interpretation of the results usually through a chromatogram obtained (Figure 4).

A chromatogram is a graphical representation of response versus time (Figure 5). The retention time on the x-axis is the time elapsed between injection to the column and when it reaches the detector. As the compounds travel down the column and reach the detector one by one, the chromatogram can reflect several peaks at different retention times. An ideal peak in a chromatogram is a Gaussian curve at baseline. The peaks in the chromatogram can be used for qualitative or quantitative analysis. For qualitative analysis, the profile and position of the peaks on the retention time axis are used, while for quantitative analysis, the peak area is often used over the peak height of the compound of interest.⁴⁵

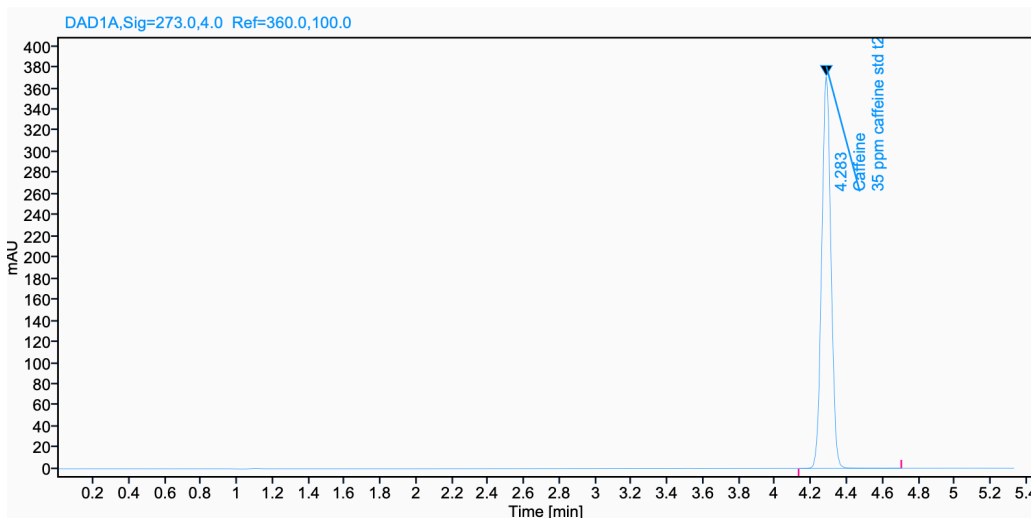


Figure 5: HPLC chromatogram of caffeine

1.3.1.1 Method validation

Method validation is critical to ensure that a method is suitable for its intended purpose. Since the use of the validated method is for the assay of caffeine in kombucha, the selected parameters used in this study are the following: selectivity, accuracy, precision, linearity, and range, which are based on International Council for Harmonisation of Technical Requirements for Pharmaceuticals for Human Use (ICH) guidelines⁴⁶.

1.3.1.1.1 Selectivity

Selectivity is the ability of the method to distinguish the analyte of interest from other particular analytes under given conditions¹⁴. In chromatography, selectivity can be determined through resolution and/or comparison of the peak with the chromatogram of the standard. Resolution is the quality of separation of the peaks by considering the distance between the peaks maxima and the average peak widths with at least a resolution of 1.5 from its neighboring peaks¹⁴.

1.3.1.1.2 Linearity

Linearity measures the proportionality of the response (y) to the analyte's concentration (x) through a calibration curve. A typical test for linearity is the square of the correlation coefficient or R^2 (Equation 2)¹⁴. An $R^2 \geq 0.99$ is often deemed to have a good linearity for many intended purposes. However, this number can be misleading. Errors from both the response and

concentration of analyte can arise from random errors. Thus, the residuals can be plotted to check that there are no systematic errors.

1.3.1.1.3 Precision

Precision is a method validation parameter that describes the degree of agreement among the independent measurements obtained during the analysis of a given sample through a given analytical procedure⁴⁷. It relates to random errors, measures of dispersion or spread around the mean value and is usually expressed by standard deviation.

While there are different kinds of precision depending on how the results are obtained, only repeatability is relevant in this study, where the results are obtained under the same conditions. One way to express repeatability is by coefficient of variation (CV) (Equation 2), where SD is standard deviation and x_m is the arithmetic mean of the sample^{14,46,47}.

$$CV = \frac{SD}{x_m} \times 100\% \quad (2)$$

1.3.1.1.4 Accuracy

Accuracy is the degree of agreement between the obtained measurement and the expected or true value¹⁴. There are several ways to determine the accuracy of a method. One way is to use the standard addition method and report the result as recovery(R)⁴⁶ (Equation 3), where c_{det} is concentration determined while c_{theor} is concentration determined theoretically.

$$R = \frac{c_{det}}{c_{theor}} \times 100\% \quad (3)$$

1.3.1.2 Calibration methods

Calibration is a process relating the actual physical quantity (such as mass, volume, force, or electric current) to the quantity indicated on the scale of an instrument. Indirect calibration methods of standard addition and external calibration will be discussed in this section.

1.3.1.2.1 External calibration

External calibration is an indirect calibration method that uses a series of increasing standard solutions and a blank to fit the best line that fits the experimental points using the least-squares method. The calibration curve equation is often $y=mx+b$ where sample responses are interpolated. In the least-squares method, the assumption is that the errors in y are much greater than in x -axis⁴⁸.

1.3.1.2.2 Standard addition

In standard addition, calibration occurs by adding increasing quantities of the analyte of interest to the sample. The known added quantity and unknown concentration of the sample are the same analyte. Increasing instrument signals are observed as there is an increase in the total quantity of the analyte. This calibration method is useful for complex matrices with high interferences to correct for matrix effects¹⁴. A disadvantage is that it is quite time-consuming, especially when there are several samples, as this is done per sample.

Briefly, standard addition starts with measuring the same amount of sample in each container. An increasing amount of standard is added to each sample, starting with zero. The analytical signal versus the concentration of analyte added is plotted on a calibration curve. Extrapolation to the point where $y=0$ on the x -axis is employed to determine the sample's concentration from the calibration curve^{14,39}.

1.3.2 Raman spectroscopy

1.3.2.1 Theory and instrumentation

Raman is a vibrational spectroscopic analytical technique that comes from the change in the polarizability of the molecular bonds. Polarizability is a characteristic of all molecules, but it is more prominent in non-polar bonds such as C-C, single or multiple bonds. Water has a weak Raman effect because of its lack of polarizability. Since water is the main solvent of kombucha, Raman can be a suitable analytical instrument.^{49,50}

Raman spectroscopy uses the interaction of the molecules of the sample with the incident laser beam where the molecules become excited and can go to virtual excited states and after which return to their original state, emitting a photon of light (Figure 6)⁵¹.

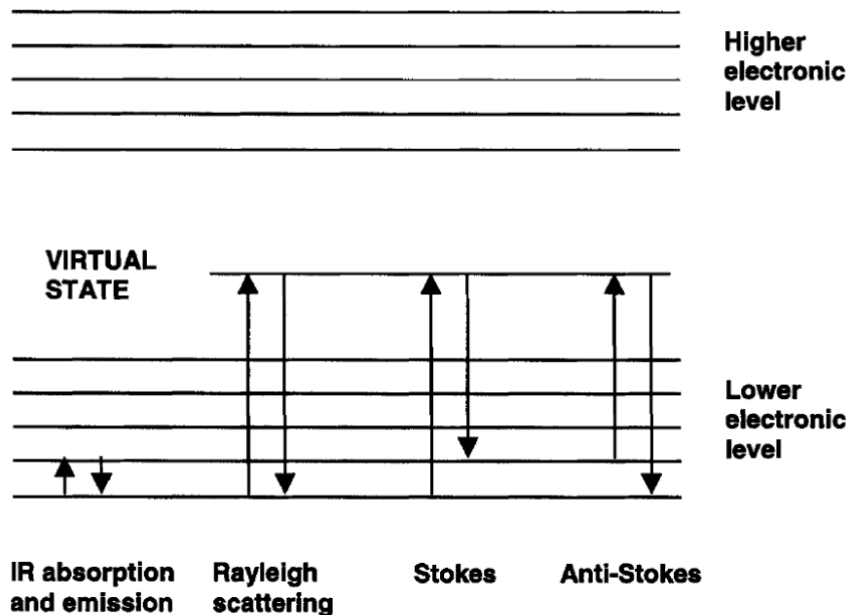


Figure 6: Electronic transitions of Raman spectroscopy⁵²

Most of the scattering in Raman spectroscopy falls under Rayleigh scattering. In Rayleigh scattering, the molecule returns to its original energy level, and the photon released has the same energy (frequency) as the incident light that excited it. This phenomenon results in elastic scattering, where the scattered light has the same frequency as the incident light^{49,52,53}.

Only a small fraction of the photons does not follow elastic scattering. Thus, Raman scattering is very weak compared to Rayleigh scattering. There are two types of Raman scattering: Stokes and Anti-Stokes. In Stokes scattering, the scattered photons fall to a lower frequency than the incident laser beam. It creates a difference between the frequency of the incident laser beam and scattered photons, which is denoted by the Raman shift (cm^{-1}), and the fingerprint of the molecule⁵⁴. Anti-stokes Raman scattering also happens when the incident photons excite the molecule to the excited state. But in contrast, the scattered photons have a higher frequency than the incident laser beam. Both Stokes and Anti-Stokes scattering give vital information depending

on their application, but due to the prevalence at room temperature, Stokes scattering is more used and is often the focus of Raman spectroscopy⁵⁴.

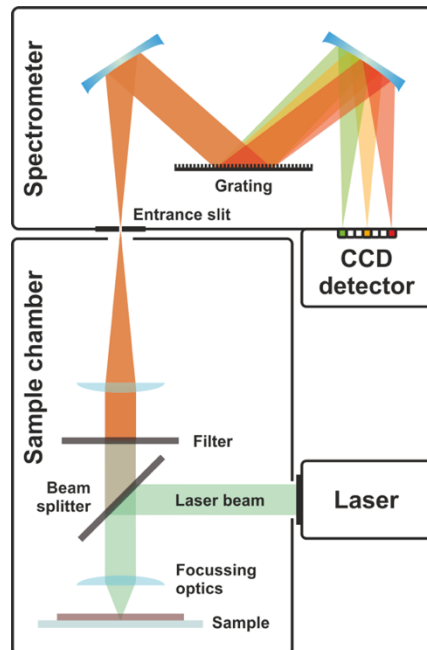


Figure 7: Schematic diagram of Raman spectroscopy⁵³

Raman starts with an excitation source through a laser beam and is directed to a beam splitter (Figure 7). Through the beam splitter, a portion of the light is projected to the sample through focusing optics. The focusing optic concentrates the laser on the sample for a more efficient Raman signal generation. It passes through a filter, other focusing optics and beams directed to the spectrometer. The filter blocks the scattered light from Rayleigh and only allows the passage of Raman scattering photons to the spectrometer. It houses the lens and grating, where the Raman scattered photon is dispersed to different wavelengths, thus recording the Raman spectra. Finally, the Raman signal is detected by the charged-coupled devices (CCD), thus transforming the intensity of Raman-scattered light to different Raman shift values through Raman peaks on a Raman spectra^{53,55}. A Raman spectra show the Raman shift or wavenumber (cm^{-1}) in the x-axis while intensity in the y-axis.

Raman spectroscopy has its advantages and disadvantages. It is easy to use, quick, non-destructive, and requires minimal sample preparation^{52,56}. This analytical technique can be

conducted directly on the sample with its packaging such as glass or plastics⁵². Pairing with multivariate analysis, it can replace expensive and destructive sampling because of its cost-effectiveness and time-saving⁵⁷. Disadvantages include high background interference such as fluorescence, which can destroy the sample if the laser is too much, and it may require several modes of operation and laser wavelengths to cover all applications^{57,58}.

As of writing, no papers exist using Raman spectrometry in the analysis of kombucha. However, a close relative of kombucha is wine, which is predominantly water, along with ethanol, and other components such as glycerol, sugars, polyols, phenols, minerals, organic acids, and volatile compounds⁵⁹. Raman spectroscopy for wine analysis is just starting to grow because of its recent developments in improving the instrument itself. Applications of Raman spectroscopy with chemometrics on wine range from identification and determination of chemical compounds, quality control and wine discrimination studies⁵⁰.

In the following sections, only a brief overview is provided as a Sirius 13.0 was heavily used to process the spectra and conduct multivariate analysis.

1.3.2.2 Outlier detection

Outlier detection is vital to the creation of predictive models⁶⁰. Outliers are data that go against expectations from a group of data; however, detected outliers should not be removed just because they are different from the rest. Severe burning effects and device artifacts are examples that can allow for the removal of these outliers. Nevertheless, these can also come from the system or the experimental design itself and thus cannot be removed because of its nature.

There are multiple ways to detect outliers, and it is usually an iterative process to ensure that they are outliers.

1. Visual inspection is where a spectra differs visually from the other spectra.
2. Principal Component Analysis, where scores that are far away from the group are usually outliers

1.3.2.3 Spectrum processing

Spectrum processing removes data artifacts in Raman spectra, such as baseline, scatter effects, and noise caused by the instruments and experiments (Figure 8). Especially with the small peaks of Raman spectra, spectra processing is an iterative process with data analysis to separate and preserve the Raman spectra of the samples for creating proper models⁶¹.

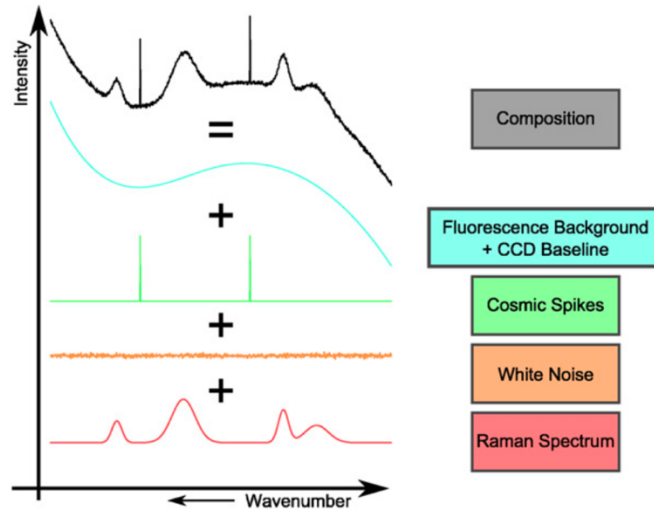


Figure 8: Spectrum composition of Raman⁶²

1.3.2.3.1 Baseline

A common artifact in Raman spectra is baseline changes due to background. Having a proper baseline ensures proper comparison and analysis between samples. In Raman, one common background artifact is fluorescence.

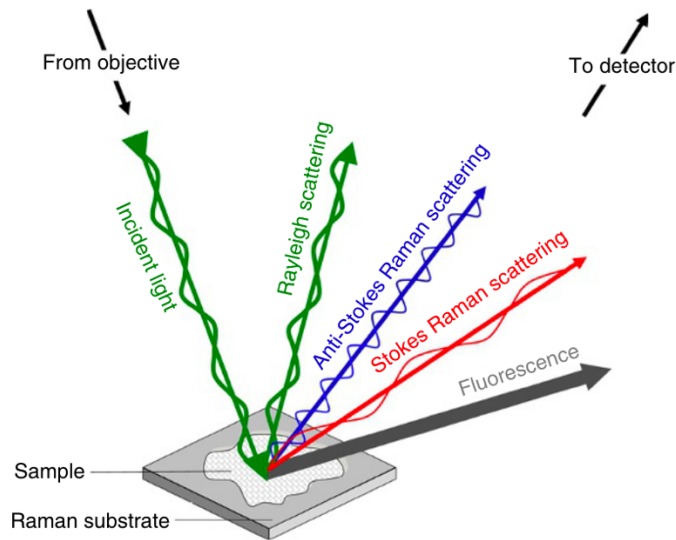


Figure 9: Light scattering after laser exposure on a sample⁵¹

Figure 9 illustrates the different types of light scattering after incident light hits the sample. Raman scattering and fluorescence frequently coincide when laser excitation is close to an electronic transition. Fluorescence occurs when electrons return to the ground state but emit photons at a longer wavelength. When laser excitation and fluorescence coincide with each other, the fluorescence can hinder the small Raman peaks since fluorescence has several orders of higher magnitude than Raman⁶³. A manifestation of fluorescence in Raman is a broad and strong fluorescence band which can go as 10^4 greater than the Raman signal, resulting to a spectra with small peaks and a curved slope baseline (Figure 8). Often, sources of fluorescence can come from the analyte or impurities of the sample^{51,62,64}.

These are some methods to reduce fluorescence:

1. Rolling ball

A ball with a radius larger than the Raman linewidths but smaller than the radius of curvature of the background is rolled under the spectra. The difference between the radii retains the spectra's shape by smoothing the spectra's curvature but not penetrating the Raman peaks.⁶⁵⁻⁶⁷.

2. Savitzky-Golay Derivatives

This algorithm derives an adjusted polynomial to fit several small data windows that mimic the spectra. Apart from reducing background, it also reduces the signal-to-noise ratio. The most common derivatives used are first and second order. First-order eliminates the vertical baseline offset while the second-order derivative removes the vertical baseline offset and the slope⁶⁸.

1.3.2.3.2 Scatter effects

Scatter effects are inherent to all light-based analytical techniques, such as Raman spectroscopy. Scattering manifests as changes in the spectral intensity despite the same sample or samples with the same concentrations. This can come from instrument effects and the heterogeneity of the sample. Heterogeneity comes from the difference in trajectory of light between the molecules of each sample and the detector. Scatter effects are often corrected by comparing signal intensities to a reference signal⁶⁸.

These are some pre-processing techniques used to reduce scatter effects:

1. Multiplicative Scatter/Signal Correction (MSC)

It estimates the regression coefficients with a reference spectrum or a mean spectrum. The regression coefficients should theoretically capture the influence of multiplicative scatter effects. From this, each spectra is adjusted by subtracting the estimated intercept and dividing by the slope^{68,69}.

2. Extended Multiplicative Scatter/Signal Correction (EMSC)

EMSC is highly used for spectral data due to its ability to separate physical light scattering effects from chemical light absorbance effects. As an extension of MSC, it can identify and retain desired effects while eliminating unwanted effects^{69,70}.

1.3.2.3.3 Noise

Noise is a common artifact for analytical techniques, manifested as fast and random spectral variations. A common approach to noise is smoothing the signals, such as the Savitzky-Golay algorithm. While smoothing decreases uncorrelated data, this can also lead to over-smoothing and losing information⁶⁴.

1.4 Multivariate analysis

With the ever-increasing sophistication and multi-analyte capability of instruments, more and more data can be extracted, and new information can be obtained with the correct tools. Multivariate analysis involves the analysis of multiple variables to make associations and predictions to explain phenomena. Chemometrics uses multivariate analysis to handle large quantities of chemical data, (i) to design or select optimal measurement procedures and experiments, (ii) to provide maximum relevant chemical information by analyzing chemical data and (iii) to obtain knowledge about chemical systems^{39,71}.

1.4.1 Principal component analysis

Principal Component Analysis (PCA) is an exploratory and unsupervised data analysis that uses principal components to visualize and reduce the dimensionality of a large correlated dataset while retaining as much information as possible³⁹. It explains data through principal components which consist of linear combinations of the original variables and go to the direction of the largest remaining variance in the data. The first principal component on the x-axis represents the largest source of variance, retaining most of the correlations in the original dataset. The second principal component explains the second largest variance, and so on. PCA is a tool for variable reduction because of the orthogonality of the principal components³⁹, enabling the removal of PCs that explain a relatively small variance thus simplifying the dataset⁷².

The output of PCA is typically visualized using two-dimensional plots known as score plots and loadings plots. A score plot displays the samples in the principal components' space to visualize sample similarities, groupings and detect outliers. Thus, a group of samples that cluster closely together means that they share similar variables and patterns with each other. In reverse, a sample that is significantly away from the group can be an outlier^{73,74}. A loadings plot shows the variable space, highlighting which variables are influential and rich in information, complementing the sample distribution observed in the score plot.

1.4.2 Partial least squares regression (PLS-R)

Partial least squares regression (PLS-R) is a supervised method which creates a linear model to describe the relationship between the predictor matrix (X) and the response vector (y), making it possible to predict y from X. The decomposition of X during regression is guided by the variations in y, resulting to the maximization of the covariance between X and y. Thus, the variation in X correlating with y is captured. To maximize the covariance, the calibration should represent samples that covers the variations of y and of future samples^{69,75}.

Generating an accurate PLS model often requires an iterative process and a performance criterion. Model creation starts with dividing the dataset to calibration and prediction sets. One of the methods to create a model is through cross validation which optimizes the number of latent variables for each PLS model. Latent variables are variables that are estimated indirectly from variables that are measured or observed directly using a mathematical model^{76,77}.

To check the robustness of the model, the following parameters were used in this study:

1. Root Mean Square Error of Prediction (RMSEP)

It is the root mean square standard error of prediction which evaluates the accuracy of the PLS model by the prediction error

2. Root Mean Square Error of Cross Validation (RMSECV) which is similar to RMSEP but by the error of cross validation

3. Correlation

There are several similarities between the outputs of PCA and PLS-R such as scores plot, loadings plots. One most used in this study is the predicted versus measured which evaluates the model through its capability to predict the result of the sample from the model against the reference or original result.

2 Experimental

2.1 Experimental design

Kombucha's projected potential has spurred a growing interest in its fermentation parameters and health benefits. Thus, this study aims to use experimental design to explore the main effects and interactions of several factors on pH, and caffeine content of kombucha on the 1st, 7th, 10th, and 14th day of fermentations.

Table 1 lists the seven parameters investigated with their corresponding values used to execute the experimental design. These values were based on the actual brewing parameters of BKB Kaffebrännereri when they made their product, except for the beaker size, which was based on the beaker sizes available at the University of Bergen. Actual weight and volume of the materials (ex. volume of starter, weight of tea leaves, weight of sugar and etc.) used in the experiment are found in the Appendix: 7.1 Brewing.

Table 1: Values of the coded levels for the seven parameters

	BKB Values	Low	High
(A) Steeping Time (mins)	10	5	15
(B) Steeping Temperature (°C)	90	60	95
(C) Ratio of Liquid & Beaker (mL of liquid/total mL capacity of beaker)	0.75	0.6	0.8
(D) Ratio of Starter and Tea (mL of starter/ mL of brewed tea)	0.2	0.125	0.5
(E) Strength of Tea (g/L of liquid)	5	2.5	10
(F) Concentration of Sugar (g/ L of liquid)	80	60	120
(G) Beaker size (L)	200	0.8	3

The ratio of liquid and beaker is calculated by multiplying the total volume capacity by the corresponding values. The value obtained here is the total liquid used to compute the values in the ratio of starter and tea, strength of tea, and concentration of sugar (4), where r is the radius of the selected beaker and h is the height of the beaker.

$$\text{Volume of liquid in beaker} = (\text{corresponding ratio level})\pi r^2 h \quad (4)$$

A saturated 2^{7-4} design with a Resolution III (Table 2) with its full fold-over (FO) was generated using Sirius 13.5.

Table 2: Reduced fractional design and fold-over design at Resolution III

	(A)	(B)	(C)	(D)	(E)	(F)	(G)
Set 2							
Exp 1	—	—	—	+	+	+	—
Exp 2	+	—	—	—	—	+	+
Exp 3	—	+	—	—	+	—	+
Exp 4	+	+	—	+	—	—	—
Exp 5	—	—	+	+	—	—	+
Exp 6	+	—	+	—	+	—	—
Exp 7	—	+	+	—	—	+	—
Exp 8-1	+	+	+	+	+	+	+
Exp 8-2	+	+	+	+	+	+	+
Exp 8-3	+	+	+	+	+	+	+
Set 3 (full fold-over of Set 2)							
FO-Obj 9	+	+	+	—	—	—	+
FO-Obj 10	—	+	+	+	+	—	—
FO-Obj 11	+	—	+	+	—	+	—
FO-Obj 12	—	—	+	—	+	+	+
FO-Obj 13	+	+	—	—	+	+	—
FO-Obj 14	—	+	—	+	—	+	+
FO-Obj 15	+	—	—	+	+	—	+
FO-Obj 16-1	—	—	—	—	—	—	—
FO-Obj 16-2	—	—	—	—	—	—	—
FO-Obj 16-3	—	—	—	—	—	—	—

Three sets of brewing with 10 experiments each were conducted in this study. A full fold-over of the design was executed later on in the study to further understand the main effects and interactions. Experiment 8 and FO-Obj 16 were replicated thrice. In executing the screening of the variables, the first replicate was used (Set 2: Exp 8-1 and Set 3: FO-Obj 16-1) and the second and third replicates are used to confirm the variables. In the PCA and PLS all three replicates were included. Table 3 shows the experimental design executed and the date of brewing for Set 1. Set

1 had a mistake in the execution of the experimental design where the signs under the strength of tea from Experiments 5 to 8, including the replicates of Experiment 8, were switched to their opposite; thus, the whole design was repeated (Table 2, Table 3). Despite this, results from Set 1 were continued to be collected. Thus, Set 2 and its fold-over are used to analyze the experimental design, while Set 1 supports observations and conclusions. The letters representing the variables are found in Table 1.

- Set 1 – October 8, 2022 to October 21, 2022

Table 3: Experimental design conducted for Set 1

	(A)	(B)	(C)	(D)	(E)	(F)	(G)
Exp 1	-	-	-	+	+	+	-
Exp 2	+	-	-	-	-	+	+
Exp 3	-	+	-	-	+	-	+
Exp 4	+	+	-	+	-	-	-
Exp 5	-	-	+	-	+	-	+
Exp 6	+	-	+	-	-	-	-
Exp 7	-	+	+	-	+	+	-
Exp 8-1	+	+	+	+	-	+	+
Exp 8-2	+	+	+	+	-	+	+
Exp 8-3	+	+	+	+	-	+	+

- Set 2 – November 1, 2022 to November 14, 2022
- Set 3- February 18, 2023 to March 03, 2023

The aliases generated by Sirius from the experimental design are the following:

- $BxD = BxD + CxE + FxG$
- $AxC = AxG + BxG + DxG$
- $AxD = AxG + CxF + ExG$
- $AxG = AxG + BxC + DxG$
- $AxE = AxG + BxF + DxG$
- $AxF = AxG + BxE + CxD$
- $AxB = AxG + CxG + ExF$

Third-order and higher-order interactions were disregarded since these are usually small.

The results were processed with Sirius 13.5. Data used in the software were the values from Table 1; thus the variables were standardized to ensure that only the contributions of the factors are considered and not how big the actual values is compared to the others.

2.2 Brewing

2.2.1 Materials

Bergen Kaffebränneri (BKB) provided the white tea leaves infused with peach flavoring, SCOBY, and the initial starter for Set 1. For Set 2 and Set 3, the starters were from previously brewed kombucha. For example, the starter culture used in Set 2 was from the kombucha set-up in Set 1. The SCOBY's from previous brewing were utilized for the succeeding brews. White granulated sugar was purchased from the supermarket.

2.2.2 Brewing method

Sugar was added with a concentration of 60 g/L or 120 g/L and dissolved by continuous stirring using a magnetic stirrer while maintaining 60 or $95\pm 2^{\circ}\text{C}$ water in a suitable beaker. The tea leaves (2.5 g/L or 10 g/L) were added and stirred for 5 or 15 minutes, depending on the steeping time of the set-up. The tea leaves were immediately filtered out with a funnel to the corresponding beaker (800 or 3000 mL). The liquid was then left to cool at room temperature for two hours. After cooling, the starter was poured into the brewed tea and stirred. Next, the pH was obtained for the first day. Then, 50 mL of the sample was withdrawn for caffeine content determination. After gathering data for the first day withdrawal point, the SCOBY was laid on top of the tea, after which a cheesecloth was put on top of the beaker. The set-up was stored in a dark and dry area at room temperature ($20\text{-}23^{\circ}\text{C}$) during the 14 day fermentation period.

2.3 Sampling

Samples of 50 mL were withdrawn from each experiment on Days 7, 10, and 14. Before withdrawing the sample for the corresponding day, the appearance and color were determined subjectively by placing a white bond paper at the base and back of the beaker. The experiments were stirred for ten minutes at the lowest speed with a stirrer and spin bar, careful not to disturb the SCOBY on the surface. The 5 mL aliquots were withdrawn from the beaker as illustrated in Figure 10. The samples were stored in a freezer at -20°C to stop further fermentation.

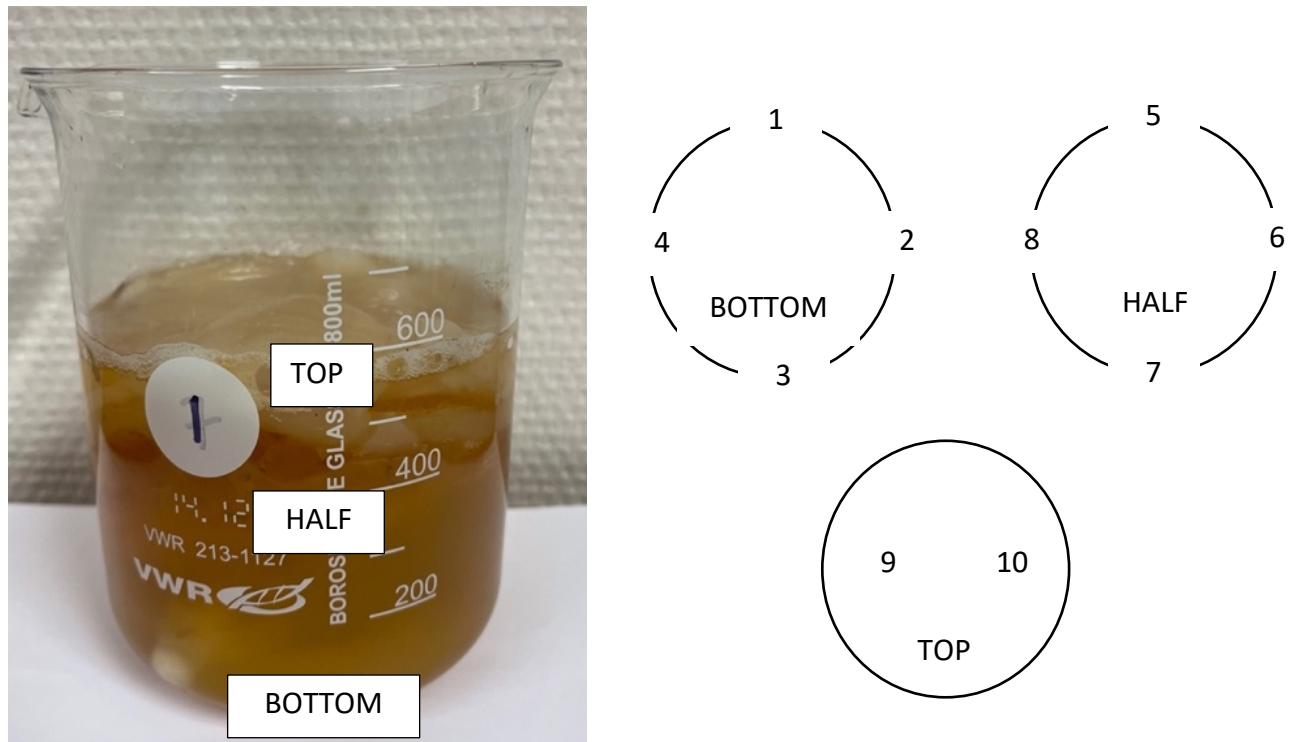


Figure 10: Sampling point withdrawal from each experiment (Left: Full beaker-view with sampling levels, Right: Cross-sectional view with sampling points)

To compare the laboratory-brewed kombucha, two bottles were obtained from BKB, stirred together for one hour, and two 50 mL samples were taken and stored at -20°C.

2.4 pH

The pH was measured on the 1st, 7th, 10th and 14th day using the 848 Titriplus Metrohm pH meter. It was calibrated before every use with Sigma Aldrich buffers 4.0 and 7.0. The pH for the first set was done in one trial, while the second and third sets were of triplicates and in a random order. The first set starter and BKB sample was also taken in one replicate, while the starters for the second and third set were also measured in triplicates.

2.5 Caffeine content by HPLC

The procedure in determining caffeine content was lifted from Miranda et al²⁴. Two steps were done prior to determining the caffeine content in Kombucha. First, due to column availability, conversion of the chosen method to new chromatographic conditions was conducted. Because

of the conversion, method validation was followed according to the ICH guidelines⁷⁸ and Shrestha et al.⁷⁹ When this has been accomplished, converting from standard addition to external calibration was conducted to save time and resources.

2.5.1 Materials

Caffeine standard (reagent grade), methanol (HPLC grade), and phosphoric acid (reagent grade) were from Sigma-Aldrich (Oslo, Norway). Samples were filtered with a Millex Syringe Filter, Hydrophilic PTFE, Non-sterile (cat no. SLLHH13NL). Caffeine content by HPLC was analyzed using the Agilent 1260 Infinity 2, which is equipped with the following: Agilent 1260 G4212B DAD detector, Agilent Quarternary Pump G7117A, and Agilent Sampler G7129A. The caffeine of kombucha was separated with an InfinityLab Poroshell 120 EC-C18 (4 μ m, 100 mm x 4.6 mm). For the method validation and conversion of the standard addition to external calibration purposes, old kombucha which was previously frozen was used.

2.5.1.1 Preparation of standard stock solution and working standard

For the method validation and converting of the procedure from standard addition to external calibration, three standard solutions of 1000 ppm caffeine standard solution were prepared in nanopure water. Serial dilution with the following concentrations: 2, 4, 8, 12, 16, 22, 24, 26, 30, 35, 40, 45, 50, 55, 60 ppm caffeine to construct a calibration curve.

2.5.1.2 Sample preparation for standard addition

Aliquot of 1 mL kombucha at room temperature was diluted to a 10 mL volumetric flask with nanopure water. Samples were filtered with 0.45 μ m PTFE syringe filter, and 1 mL was added to four 1.5 mL HPLC vials. Three of the vials were spiked with 100 ppm caffeine standard to a final concentration of 5, 10 and 15 ppm.

2.5.2 Method validation using the column available

Table 4 shows the chromatographic conditions of the original method²⁴ converted based on the dimensions of the column available. Equations used in converting the original procedure are in Table 5⁸⁰.

Table 4: Chromatographic Conditions from the original method to the converted

Original Procedure ²⁴		Converted				
Detector	PDA Detector					
Wavelength	273 nm					
Column	Phenomenex C18 RP (5µm, 150 mm x 4.6 mm)	InfinityLab Poroshell 120 EC-C18 (4 µm, 100 mm x 4.6 mm)				
Column Temp	Room temperature					
Mobile Phase	(A) 0.1% H ₃ PO ₄ in H ₂ O (B) MeOH					
Flow	Gradient					
Gradient Program	mins	%A	%B	mins	%A	%B
	0	80	20	0	80	20
	6	60	40	3.2	60	40
	9	80	20	4.8	80	20
	10	80	20	5.33	80	20
Flow rate	0.75 mL/min		0.94 mL/min			
Run time	10 mins		5.33 mins			
Injection vol.	20 µL		13.3 µL			
Calibration method	Standard addition		External calibration			

The parameters chosen according to ICH under assay are: selectivity, linearity and range, repeatability, and accuracy⁷⁸. Intermediate precision was not performed anymore due to time constraints.

2.5.3 Adjusting chromatographic gradient conditions

Unavailability of the exact column is sometimes inevitable. Compared to isocratic conditions, gradient conditions are more challenging because there is a need to consider the changing mobile phase composition, which significantly impacts the separation of the analytes. This profile of the gradient mobile phase composition should apply to the new column to have the same performance as the original column. Converting other parameters such as gradient program, flow rate, injection volume, and run time must be considered to compensate for the changes in the column dimension⁸⁰. Table 5 lists the equations used to obtain the values used to convert the original method suitable to the available column (Table 4).

Table 5: Equations for converting HPLC gradient method⁸⁰

	Equation	
Flow rate	$F_2 = F_1 \times \left[\frac{dc_2^2 \times dp_1}{dc_1^2 \times dp_2} \right]$	(5)
	<p>F₁= flow rate indicated in the original journal (mL/min)</p> <p>F₂= adjusted flow rate (mL/min)</p> <p>dc₁= internal diameter of the column indicated in the original journal (mm)</p> <p>dc₂= internal diameter of the column used (mm)</p> <p>dp₁= particle size indicated in the original journal (µm)</p> <p>dp₂= particle size of the column used (µm)</p>	
Gradient program	$t_{G_2} = t_{G_1} \times \left(\frac{F_1}{F_2} \right) \left[\frac{dc_2^2 \times L_2}{dc_1^2 \times L_1} \right]$	(6)
	<p>t_{G₂}= new time point (mins)</p> <p>t_{G₁}= time point of the gradient from the original journal (mins)</p> <p>L₁= column length indicated in the original journal (mm)</p> <p>L₂= new column length (mm)</p>	
Injection Volume	$V_{inj2} = V_{inj1} \times \left[\frac{dc_2^2 \times L_2}{dc_1^2 \times L_1} \right]$	(7)
	<p>V_{inj1}= injection volume indicated in the original journal (µL)</p> <p>V_{inj2}= adjusted injection volume (µL)</p>	

Table 6 lists the method validation parameters, and their corresponding procedures.

Table 6: Method Validation Parameters with their Corresponding Procedure

Parameter	Procedure
Selectivity	Inject kombucha and compare with 35 ppm caffeine standard.
Linearity & Range	Inject 2, 4, 8, 12, 16, 22, 24, 26, 30, 35, 40, 45, 50, 55, 60 ppm caffeine, with three trials for each concentration.
Accuracy	Kombucha was spiked with 100 ppm with a final concentration of 5 ppm, 10 ppm and 15 ppm. Recovery studies were conducted.
Repeatability	Six injections of one kombucha standard were injected, and the CV was determined from here.

2.5.4 Converting from standard addition to external calibration

To save on resources and time, the calibration method from standard addition was converted to external calibration. The procedure followed was lifted from Rodriguez et al⁸¹.

There were three calibration curves in triplicates:

- Standard calibration curve (obtained from linearity and range)
- Standard addition curve which was based on the original journal²⁴
- Variations in the concentration of the sample (0.5 mL, 1.0 mL, 1.5 mL, and 2.0 mL of sample in 10 mL and diluted with water)

2.5.5 Final HPLC procedure for caffeine content

Sample of one mL was pipetted to a 10mL volumetric flask then diluted with nanopure water and filtered with 0.45- μ m PTFE syringe filter to an HPLC vial. However, for experiments that required more than 10 g of tea leaves, it was noticed that there is a need to dilute further (Experiments 8-1, 8-2, 8-3, Obj-FO 10, Obj-FO 13) by diluting 5-mL in 10-mL since they were out of range. The converted method found in Table 4 is used to analyze caffeine content.

2.6 Raman spectroscopy

The samples were thawed overnight at room temperature. Before measurement, they were shook to homogenize them. RamanRxn 1 Analyzer with a trapezoidal probe was used in this experiment. The probe of the Raman was directly put in the sample container with settings of accumulation of 50 and laser at 50. Every after sample, the probe was cleaned with distilled water and dried with Kimwipes. The samples were read in a dark room, at random order, with the triplicates not being close to each other.

2.7 Multivariate analysis

Raman spectra of the kombucha samples were subjected to Principal Component Analysis and Partial Least Squares-Regression using Sirius 13.5 version (Pattern Recognition Systems AS, Bergen, Norway) to create multivariate models.

Creating a quality model has several factors, such as the composition of the calibration and validation sets and pre-processing methods. The order of the pre-processing methods also affects the quality of the model generated.

Raman spectra have common data artifacts that affect the model's quality and predictability, such as fluorescence and offsets. Thus, several pre-processing methods and combinations that were available in Sirius were explored, such as different rolling ball circle filter radii, first to the fourth order of Savitzky-Golay derivatives, MSC and EMSC.

Because of instrument or sampling errors, having outliers is also inevitable during the data acquisition process. Outliers influence the model generated, which must be treated cautiously. In this study, there are three replicates for each Raman sample. The outliers have been identified before and after the pre-processing method through visual comparison of the spectral replicates, principal component analysis, and partial least squares. For the visual comparison of the replicates, three of the replicates were selected, and the spectra that seemed to differ the most in intensity was treated as an outlier. Lastly, for PLS, the groupings from the selected components were chosen, along with the predicted versus measured from the training set and residuals versus leverage.

A dataset with a matrix of 375x11520 was used for PCA. The Raman variables were mean-centered and no variable weighting was carried out.

Due to the difficulty in understanding the behavior of the experimental design through the PCA, PLS was attempted for both datasets (375x11521) with the parameters set at 0.401 significance test of model dimension and cross-validation method using four groups and repeated 40 times. The variance explained, and the p-MC were compared. The goal is to have a big difference in the variance between the real and dummy datasets and a p-MC value close to zero (0.0). When a model meets these criteria, the quality of the PLS model will be judged by the RMSECV and RMSEP, with a preference for lower values.

3 Results and discussion

The power of the experimental design in a complex set-up like kombucha is the possibility of understanding how the parameters influence each other.

A total of three sets of brewing were conducted.

- Set 1 – October 8, 2022 to October 21, 2022
- Set 2 – November 1, 2022 to November 14, 2022
- Set 3 – February 18, 2023 to March 03, 2023

Under each parameter, there is a:

- a table or graph of the results and observations
- a table of the identified significant variables on Days 1, 7, 10, and 14
- a graph of regression coefficients showing the behavior of the seven variables and the interactions during fermentation

3.1 Physical properties of kombucha

While checking for smell and taste would be ideal for this study, only color and turbidity by sight were conducted subjectively. Figure 11 shows the change in appearance and color of Set 2 Exp 1 during fermentation. The beaker is put on a white background in a well-lit environment to describe the color and turbidity. Appendix: 7.2 Color and Appearance has a table describing the colors observed on Days 1, 7, 10 and 14. Pictures of other kombucha are at Appendix: 7.3 Pictures of kombucha.

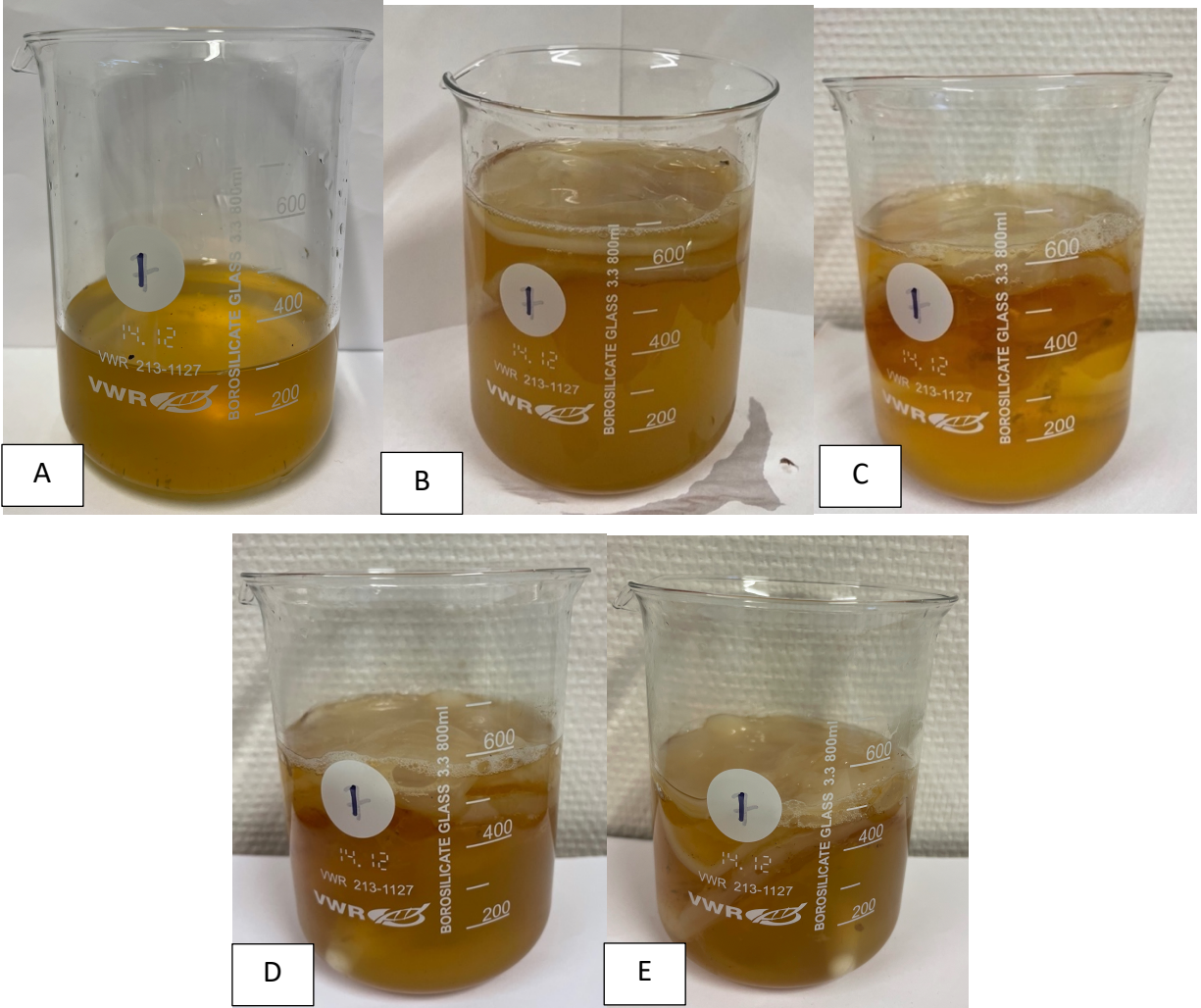


Figure 11: Set 2: Experiment 1 over the course of the 14 days (A) before adding starter and SCOBY (B) Day 1 (C) Day 7 (D) Day 10 (E) Day 14

It was observed that the addition of the starter to the brewed tea results to a change in color and appearance of the tea. On the seventh day, most of the kombucha samples have a new thin film or SCOBY forming on the surface, signaling the production of carbon dioxide³⁰. Deposits are also found at the base, which were absent on the first day.

Only a few studies have been conducted on the color and appearance of kombucha. Color of kombucha mainly comes from the extracted polyphenols of tea. Relating to the execution of the experimental design, the set-ups with a low steeping time and steeping temperature (Set 2:

Experiment 2, Set 2: Experiment 7, Set 3: FO-Obj 16) had lighter color intensity, leaning to shades of yellow while the ones with high steeping time and steeping temperature have shades of red and brown (Set 2: Experiment 8, Set 3: FO-Obj 13).

Seemingly consistent with other studies, majority of the set-ups seem to turn lighter throughout fermentation (Set 2: Experiment 4 to 6, Set 3: FO-Obj 12, Set 3: FO-Obj 14). Observations by Chakravorty et al, noted a significant decrease in color as the total phenolic concentration increased. They pointed to the conversion of thearubigin to theaflavin for the lightening of the color from reddish brown to light brown^{6,13}. The decrease in pH was also pointed as a cause of color lightening since the activity of the consortium could depolymerize or alter the pigments of the tea¹⁰. However, a more quantitative approach is recommended for such as using chromameters and UV-Vis spectrophotometer⁴.

Turbidity has also decreased as the fermentation progressed. Previous studies suggest that the suspension consists of microorganisms, large molecules such as proteins, polyphenols, and cellulose fibers synthesized by acetic acid bacteria¹³. The findings in this study is in contrast with a study done by Amarasinghe et al¹¹, where they have observed an increasing turbidity as the fermentation progresses to eight weeks. It is suggested that increasing turbidity is a result of the creation of the daughter SCOBY. In this study, the color was determined before carefully stirring the samples and allowing the particles to settle at the base, making most of the set-ups clear before stirring. Amarasinghe et al does not state when the turbidity was determined.

3.2 pH

The pH of kombucha during its fermentation has been widely studied and researched as it is vital to the growth of microorganisms and serves as quality control for kombucha. The actual table of values is in Appendix: 7.4 pH. In this study, pH was measured on the 1st, 7th, 10th and 14th day.

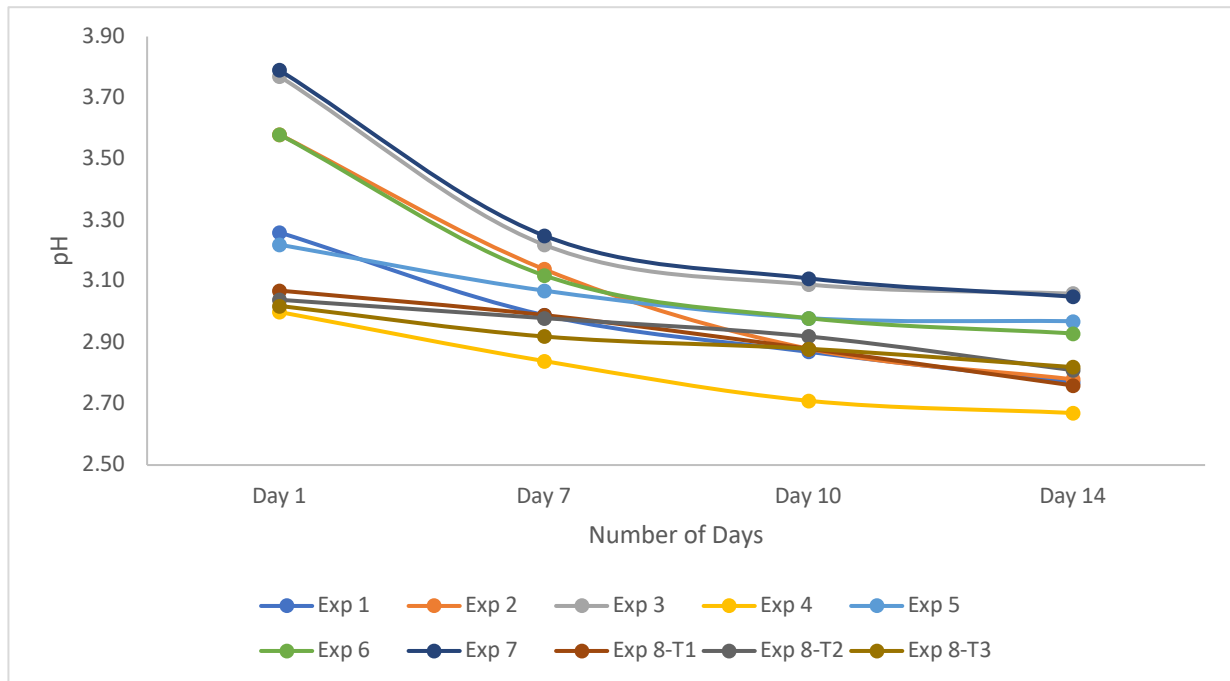


Figure 12: pH profile trend Set 1

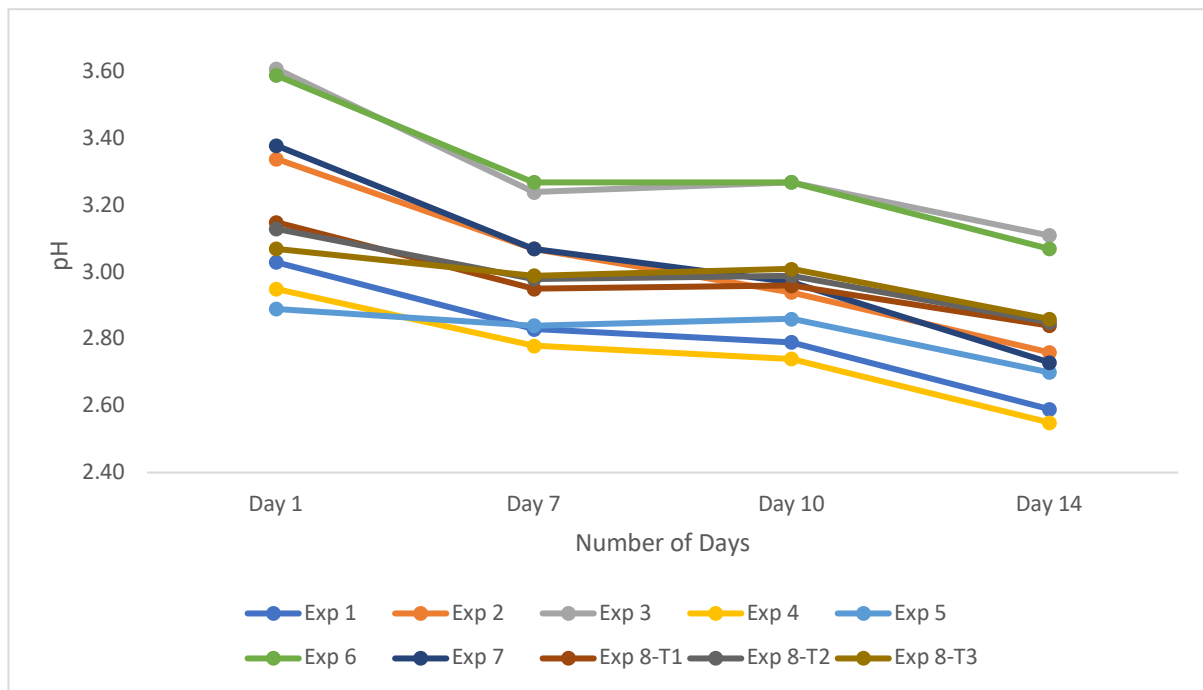


Figure 13: pH profile trend Set 2

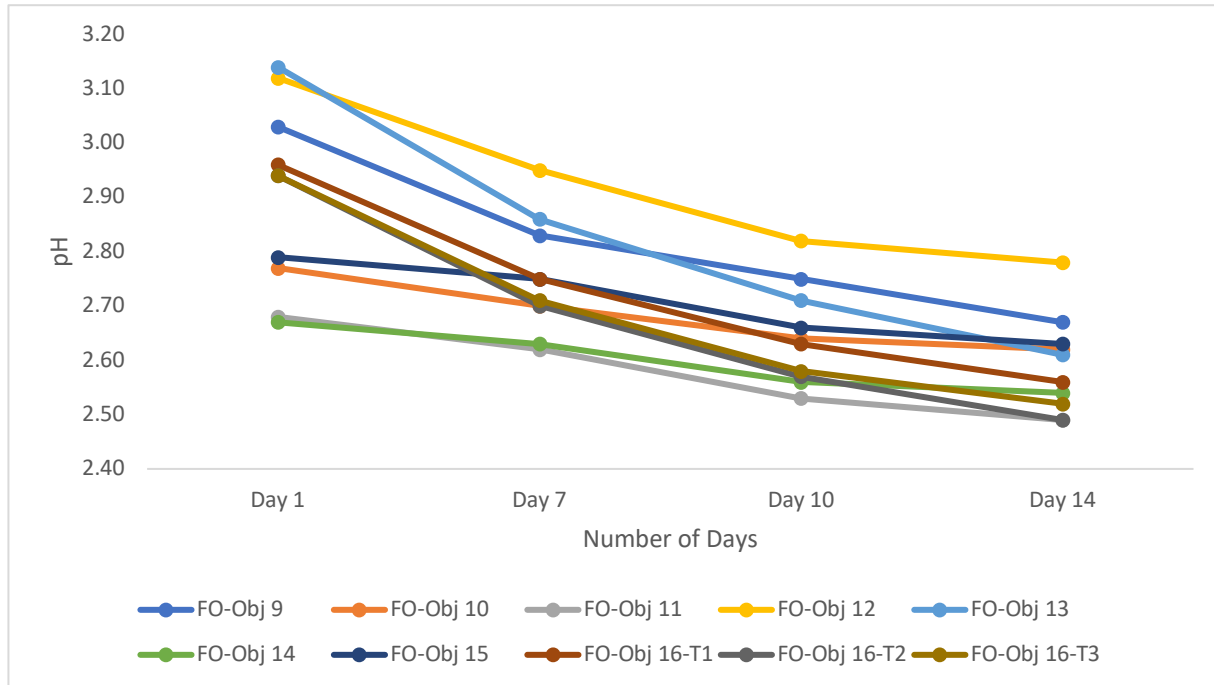


Figure 14: pH profile trend Set 3

Figure 12 to 14 compare the pH profile of the experiments from the experimental design to each other in each set. The pH on the first day shows that the kombucha samples start fermenting at a pH below 4.5, implying that the starter added is enough and has a suitable pH. Furthermore, they all fall within the recommended threshold of the US FDA for not using preservatives and time and temperature control for inhibition of harmful microorganism growth¹⁷.

Another observation is that Set 3 has a lower pH range than Set 1 and Set 2 which is linked to the starter having a lower pH of 2.52 than the other two sets, showing that the pH of the starter is important in the fermentation process.

In addition, most measurements are lower than the BKB sample of 3.22 for Day 1 where the BKB sample was fermented for 16 days. However, in this experiment, all samples under Set 3 have a lower pH than the BKB sample at Day 1, which can be again attributed to the lower pH of the starter. In Set 1 and Set 2, the set-ups on Day 1 with a positive ratio to starter and liquid exhibited lower pH than 3.22 (Exp 1, 4, 5 and 8), even though the starter for Day 1 was the same as what BKB used for this batch of kombucha. However, at Day 7, most samples were already below 3.22,

suggesting that decline in pH may be faster in a laboratory set-up compared to BKB. A hypothesis could be the type and size of the container where BKB uses a 200 L wooden keg while the laboratory set-up uses 800 mL and 3 L glass beakers.

Moving to the profile of the pH trend among the samples, the general profile of the pH trend is a quick drop in pH from Day 1 to Day 7 and slows down as the fermentation progresses further, and is also observed in previous studies^{32,82}. Previous studies indicate that the gradual decrease observed in Days 7 to 14 is due to the buffering capacity of kombucha and its interaction with the tea⁸³. According to Cvetković et al³², carbon dioxide is released in the first two to three days contributing to the rapid decline of pH. The water solution with carbon dioxide dissociates to the amphiprotic hydrocarbonate anion (HCO_3^-) which reacts with the hydrogen ions present in the solution from the organic acids., thus creating a buffering system, contributing to the slow drop of pH in the succeeding days³².

However, some set-ups do not follow this trend: Set 1: Experiment 8, Set 2: Experiment 5, and Set 3: Experiments 14 and 15. They exhibit a pH change at most 0.05 in a span of 7 days. Looking into the experimental design, a combination of a high ratio of starter and tea with a large beaker contributes to this trend. All the set-ups except Set 3: Experiment 15 use a lower concentration of tea leaves. An explanation for this could be that the low brewing temperature affected the extraction of the compounds, affecting the fermentation process and resulting in a stagnant pH drop in seven days. Interestingly, Set 1: Experiment 5 and Set 2: Experiment 8 do not exhibit this trend. The design shows they have a high concentration of tea leaves, a high ratio of starter to tea, and a big beaker size; thus, the concentration of tea leaves affects the pH profile. Another hypothesis could be that the starter has enough concentration of organic acids from the start to create a buffer in these set-ups, thus having minimal changes in the pH.

Another aspect is the profiles of Set 1: Experiments 2 and 7, Set 2: Experiments 2 and 7, and Set 3: FO-Obj 13 and FO-Obj 16. They exhibit a big difference in the pH change between day 7 and day 10. In most studies, the fermentation period ends between these days, or there is only a

gradual change. Comparing their parameters, they have a low ratio of starter and tea and a high sugar concentration. An implication of this is that there is so much food for the microorganisms to consume, and the bacteria multiply more to yield more acid during this time. However, FO-Obj 16 possesses all the fermentation parameters at the low side.

The observed trends suggest that pH is affected by the size of the beaker, strength of tea, ratio of starter and tea, and sugar concentration.

3.2.1 Factors affecting pH

To further understand the behavior of kombucha fermentation parameters, a screening fractional factorial design was conducted to see which parameters affect the pH as the days pass.

The starters used for the sets are different, affecting the experimental design results since these starters were not executed in a typical design with blocking, where this should have been divided accordingly based on the chosen design. Thus, the variable relating to the starter will always be a significant variable also by virtue of the design. Another consequence is the predicted versus measured graph. Figure 15 highlights the separation between the sets where Set 3 is above the regression line while Set 2 is below. Hence, the model predicts lower values for the pH in Set 2, while higher values for the pH in Set 3, which is also reflected in the response residuals (Figure 16). Even if the insignificant variables have been removed from the design, a clear division between the sets has been consistently observed, which is most evident for Day 1.

Day 1: pH, Significant variables only, Predicted vs Measured, RMSEC = 0.190,(1 Comp)

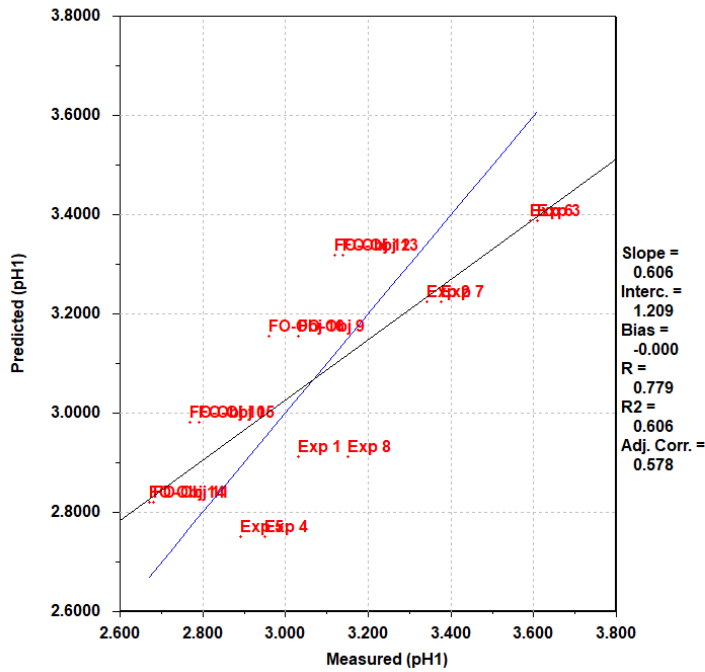


Figure 15: Predicted versus measured for pH day 1 with the significant variables

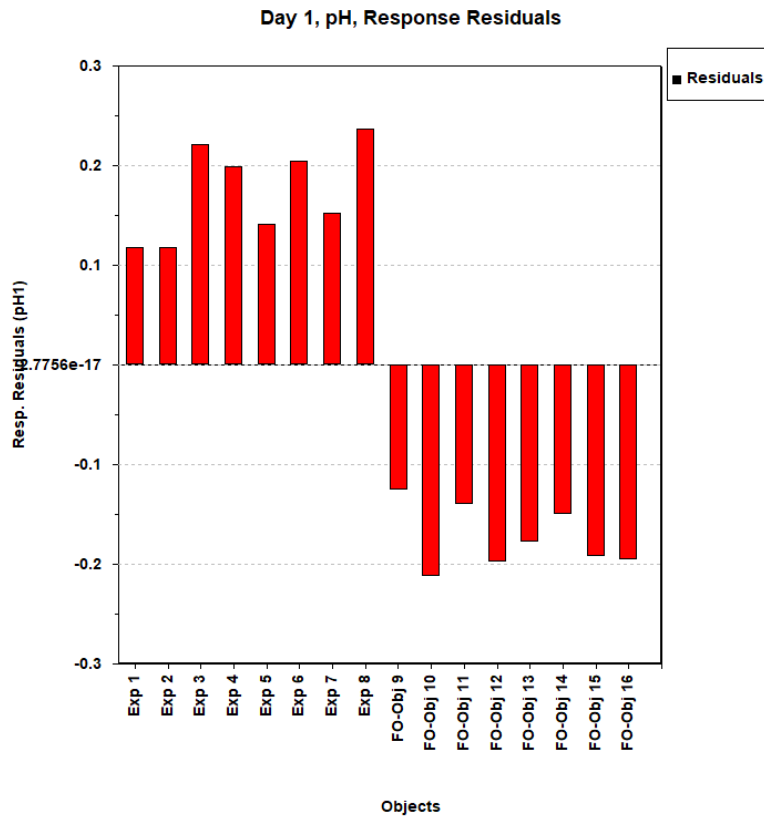


Figure 16: Response residuals for pH day 1 with the significant variables

Significant variables were identified by generating the regression coefficient graph, normal probability plot and half-normal probability plot. The seven fermentation parameters with the interactions were selected, and pH of Day 1 is the response variable. The dependent variable used for Days 7, 10, and 14 is the difference between the final pH and Day 1. To further clarify, for pH Day 7, the difference between pH Day 7 and pH Day 1 was taken as the dependent variable. The reason behind this is to cover the contribution of the previous days' pH without changing the design's dimensionality. Identifying significant variables using the regression coefficient plot is possible by the relative size to each other. Larger values of the regression coefficient signify the importance of the parameter.

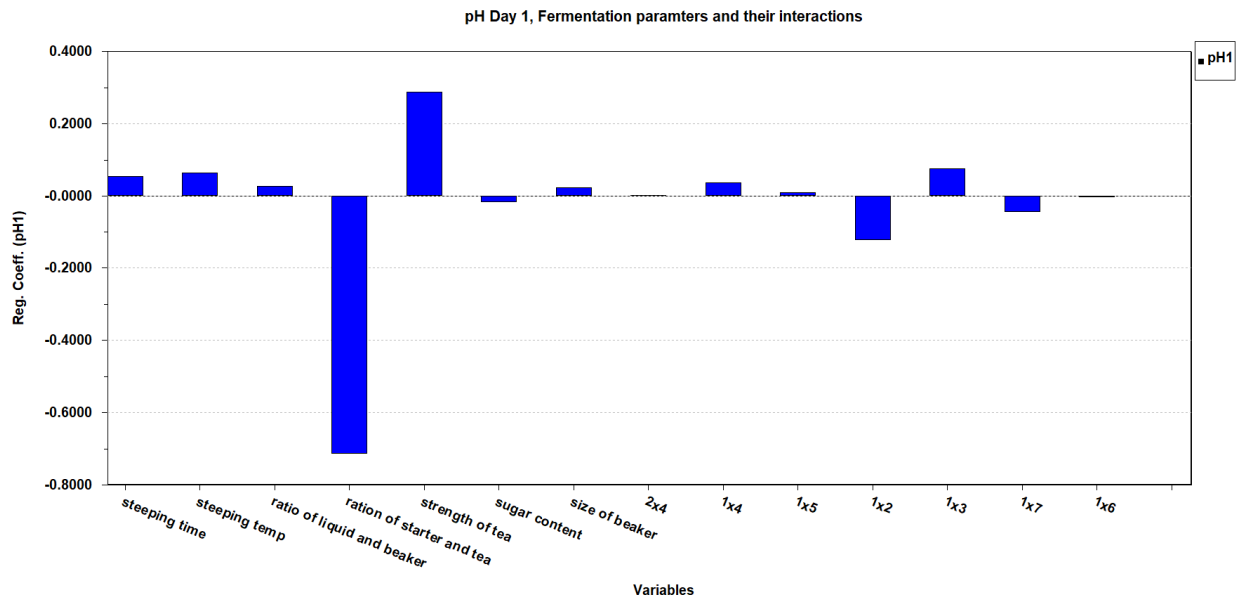


Figure 17: Screening variables for pH Day 1

Figure 17 show that strength of tea, ratio of starter, and tea and interaction 1x2 have the most prominent influence on the pH of kombucha.

A normal probability plot and a half-normal probability plot determine the significant variables through a straight line that passes through the origin and the most number of points. The variables that go outside the line are the significant effects. Figure 18 illustrates that strength of tea, 1x2 interaction and ratio of starter and tea are significant variables for day 1 which is confirmed by Figure 19.

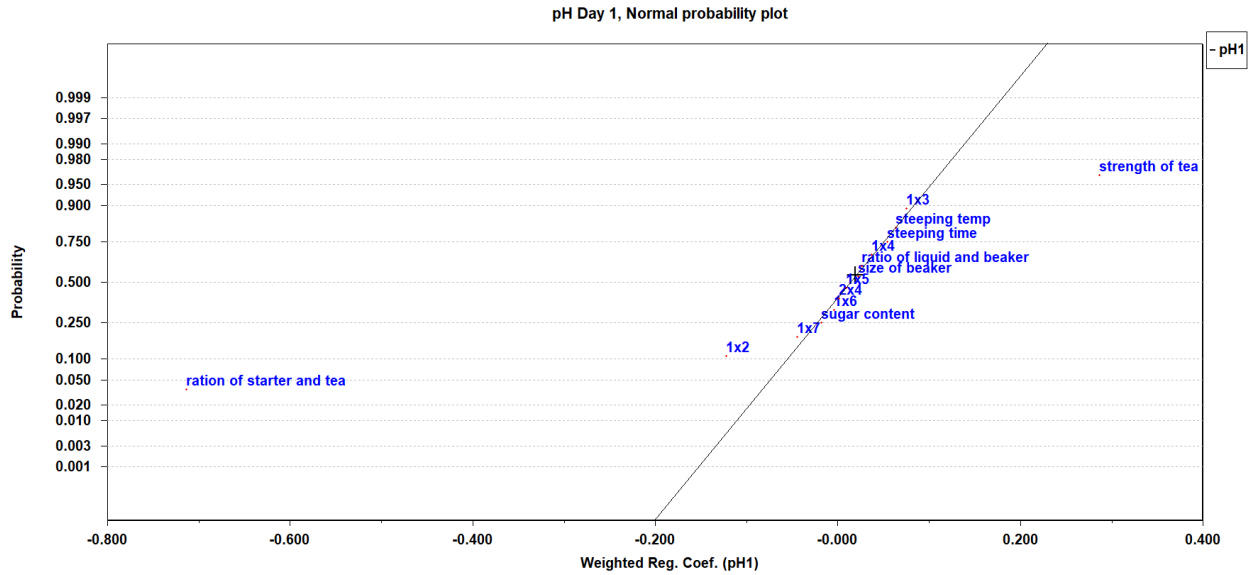


Figure 18: Normal probability plot of screening variables for pH day 1

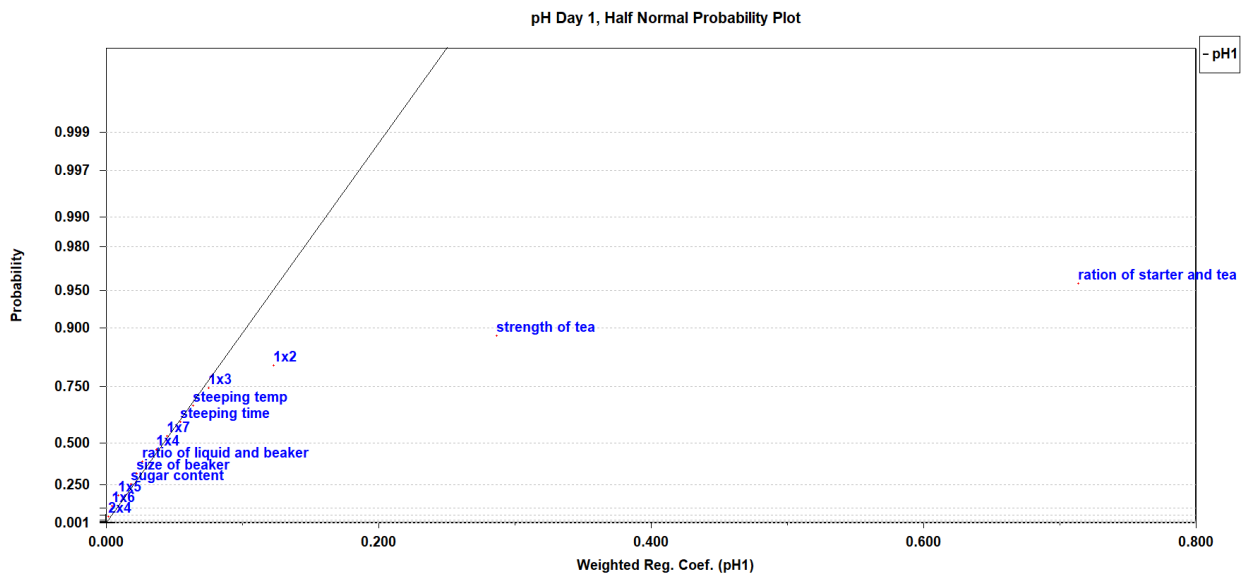


Figure 19: Half normal probability plot for pH day 1

Table 7 summarizes the significant effects of Days 1, 7, 10, and 14. Graphs and plots for Days 7, 10, and 14, similar to Day 1, are in the Appendix. Caffeine is not an important variable as the model improved when this variable was removed, suggesting that caffeine might not stimulate the fermentation process with regards to the pH of Kombucha.

Table 7: Identified significant variables affecting pH on days 1, 7, 10 and 14.

	Day 1 (60.62%)	Day 7 (75.76%)	Day 10 (94.25%)	Day 14 (68.79%)
Steeping Time				
Steeping Temp		—		
Ratio of Liquid and Beaker		+	+	+
Ratio of Starter and Tea	—	+	+	+
Strength of Tea	+	—		
Sugar Content			—	—
Beaker Size		+	+	+
2x4 (BxD)				+
1x4 (AxD)				
1x5 (AxE)				
1x2 (AxB)	—			
1x3 (AxC)		—		
1x7 (AxB)				
1x6 (AxF)				

“+” denotes significant variables that are positively correlated; “—” denotes significant variables that are negatively correlated

As expected, the ratio of starter and tea plays the most critical role in the pH of the sample, due to the execution of the design and also since the starter is old kombucha. The signs from pH Day 7 to pH Day 14 flipped compared to Day 1, since the pH is the difference between the corresponding day and pH Day 1. This is also in line with a study conducted by Lončar et al. where they noted a faster consumption of the sugars and acidification with 15% starter versus 10% starter. They suggest that the higher inoculum accelerates the elaboration kinetics⁸⁴.

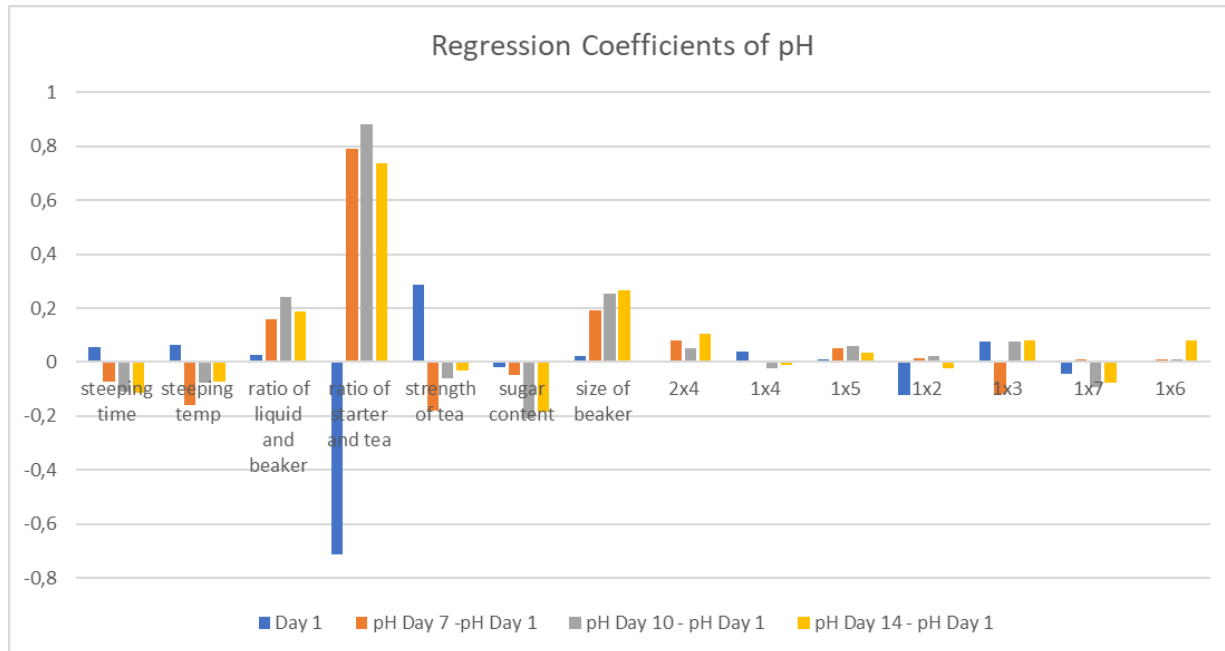


Figure 20: Regression coefficients for pH from day 1, day 7, 10 and 14

Variables concerning the space occupied by the liquid were found to be significant on Day 7 up until Day 14. Figure 20 shows that the regression coefficient for the size of the beaker and ratio of starter and tea grew significantly as compared to Day 1. Studies show that dimensions of the container and space consumed by kombucha can affect the pH^{31,32}. For example, a study by Malbaša showed that different sizes influence the pH more as the fermentation days progress. They reasoned that uncertainty in homogeneity increases, especially for solutions that are not agitated. Thus, nutrients for the microorganisms are not distributed uniformly, affecting the properties of kombucha. Apart from pH, they found that content of acids, sugars, and total acids also depend on the container's size³¹.

In addition, a larger surface of liquid to volume of liquid to ratio contributes to faster acidification because there is better oxygen access for AAB, which can be achieved by reducing the volume of liquid¹⁰. Thus, the earlier observation of why BKB's pH is higher than the ones found in this study despite the similarity in the ingredients can be linked to the size of the container and the ratio of the liquid and container. Furthermore, it proves that scaling up and downsizing kombucha production is not straightforward.

The importance of the strength of tea also decreases as the days pass. It was found to be influential on the first day and decreases in the later days. Opposite to this trend is the sugar content, which was not found to be significant in the first week, only on Day 10 and Day 14. It can be due to the fermentation of the sugar content to organic acids, and the organic acid content is increasing, influencing the pH and buffering capacity³².

Comparing the variables that seem to affect the pH from the profiles and the experimental design, they are similar to each other except that in the fractional factorial design, the ratio of liquid and beaker is significant.

3.3 Caffeine

This section is divided to four parts:

- (i) Method validation of caffeine content by HPLC
- (ii) Conversion from standard addition to external calibration
- (iii) Caffeine content
- (iv) Factors affecting caffeine content

3.3.1 Method validation of caffeine content by HPLC

Modifications were made to the procedure due to the availability of resources and the nature of the sample. Thus, validation was conducted. The kombucha was also almost impossible to filter directly for HPLC using the available syringe filter, despite filtering the drink through filter paper prior. Hence, it was diluted to 1 in 10 before filtering into the HPLC vials. A hypothesis is that the original method had tea leaves in the concentration of 1.5 g/L, while this study has 2.5 g/L and 10 g/L, thus contributing to a more concentrated solution. Criteria was based on an HPLC caffeine content validated procedure for tea and coffee⁷⁹ and obtained values are in Table 8. Some raw data are in Appendix: 7.5 Method validation

Table 8: Method validation for caffeine content criteria and values

Parameter	Criteria	Values
Selectivity	The caffeine peak in the kombucha sample has a resolution ≥ 1.5 .	2.5
	Retention time difference between the caffeine peak from the sample and standard should be within 2.0%	Complies
Linearity and range	$R^2 \geq 0.99$, 2 to 60 ppm	0.9993
Accuracy	Recovery: 80%-120%.	5 ppm: 105.4%; 10 ppm: 96.4%; 15 ppm: 97.2%
	Conducting t-test between the recovered and the actual spiked concentration should not have a significant difference when t-test is conducted at 95% confidence interval.	No significant difference.
Precision	Six injections of 28 ppm on the same day with $CV \leq 2.0\%$	0.42%

3.3.2 Conversion from standard addition to external calibration method

To save time and resources, standard addition can be converted to external calibration. Rodriguez et al has achieved this and his journal was followed step-by-step in this study⁸¹.

Table 9 shows the parameters calculated for conversion through the calibration curve for standard calibration, standard addition calibration, and variations in the sample. The standard error from the standard calibration curve (SC) represents the standard error of all three-calibration curve because it has the most number of measurements.

Table 9: Descriptive statistics for conversion of standard addition to external calibration

Parameter	Standard calibration (SC)	Standard addition calibration (SA)	Variations in the concentration of the sample (YC)
Number of samples	48	12	12
Intercept	-5.27	1310.09	4.96
Slope	39.21	37.86	1333.47
Standard Error	18.83	24.42	47.76

First, the similarity between the standard calibration and standard addition slopes was compared by student t-test (8).

$$t(b) = \frac{|b_s - b_A|}{s_s \sqrt{\frac{1}{\sum (c_{i,s} - \bar{c}_s)^2} + \frac{1}{\sum (c_{i,A} - \bar{c}_A)^2}}} \quad (8)$$

where: $t(b)$ = statistic for slope

b_s = slope of standard calibration

b_A = slope of standard addition

S_s = regression standard deviation of standard calibration

$c_{i,s}$ = concentration of standard set used in standard calibration

\bar{c}_s = average concentration of standard set used in standard calibration

$c_{i,A}$ = concentration of added-standard set used in standard addition calibration

\bar{c}_A = average concentration of added-standard set used in standard addition calibration

The degree of freedom used is 56 with a 1% significance level, as the journal claims this method is quite robust. Since computed $t(b)=1.39$ is smaller than the t_{crit} (2.67), the standard calibration curve can represent both the standard calibration and standard addition.

After establishing the similarity of the slope between standard calibration and standard addition, the intercept between SC and YC was investigated. They will always differ because they are different matrices and cannot be compared directly. Thus, the journal uses confidence interval at 1% to determine whether intercept of YC is in the confidence interval of the intercept of SC (9).

$$a_Y \in a_s \pm t_a s_s \sqrt{\frac{\sum c_{i,s}^2}{n \sum (c_{i,s} - \bar{c}_s)^2}} \quad (9)$$

a_Y = Intercept of YC

a_s = Intercept of SC

t_a = t-test statistic, where (n=46, at 1% significance level; 2.410)

Using (10), the intercept of the YC sample ($a_Y = 4.96$) in kombucha is in the confidence interval of the intercept of the SC ($a_S = -5.27$). Thus, the intercept of the standard calibration curve is used as the intercept and there is no need correct to for the matrix.

To check for accuracy, the concentration of caffeine was determined from the standard calibration curve (10) and standard addition curve (11).

$$c_{x,S} = \frac{R_x - a_Y}{b_S} \quad (10)$$

$c_{x,S}$ = solution analyte concentration from SC

R_x = Sample analytical signal

YB = Variations in the concentration of the sample

$$c_{x,A} = \frac{(a_A - YB) - a_S}{b_S} = \frac{a_A - a_Y}{b_S} \quad (11)$$

$c_{x,A}$ = Solution analyte concentration from AC

a_A = Intercept of AC

The average concentration ($n=3$) obtained from (10) is 33.37, while for (11) is 33.27. To compare this, t-test is used (13).

$$t(c) = \frac{|c_{x,S} - c_{x,A}|}{\frac{s_S}{b_S} \sqrt{\frac{1}{n_S} + \frac{1}{n_A}}} \quad (13)$$

$t(c)$ = Statistic for concentration

n_S = Number of measurements used for standard calibration

n_A = Number of measurements used for standard addition

Since $t_{\text{stat}} (0.64) < t_{\text{crit}} (2.002)$, the converted method can be used as an external calibration.

Figure 21 shows a chromatogram of kombucha for caffeine content.

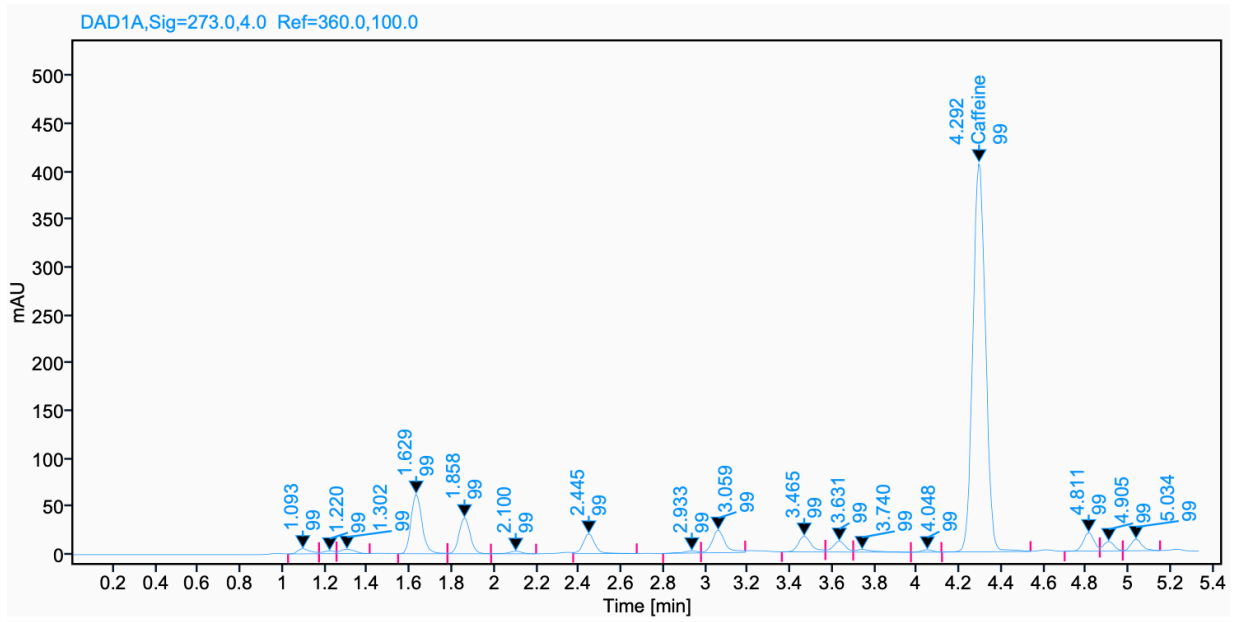


Figure 21: Chromatogram of kombucha for caffeine content

3.3.3 Caffeine content

Compared to pH, caffeine in kombucha is less widely studied. Caffeine serves as an additional source of nutrients for the SCOBY. Myths also arise among kombucha brewers that caffeine stimulates the fermentation process²³. For human consumption, caffeine is mainly related to being a stimulant. Figure 22 to 24 show the trends of kombucha over the 14-day fermentation period.

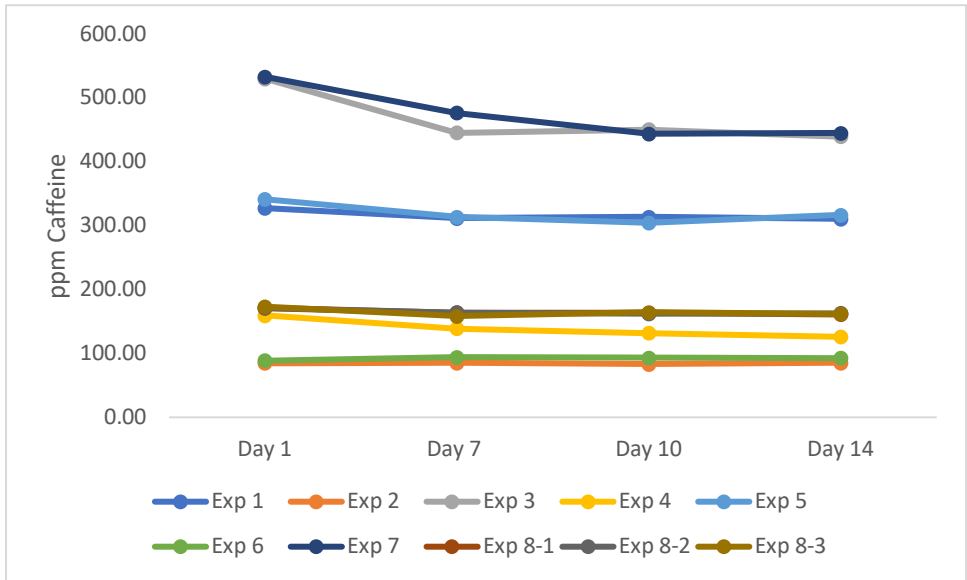


Figure 22: Caffeine profile over 14 days Set 1

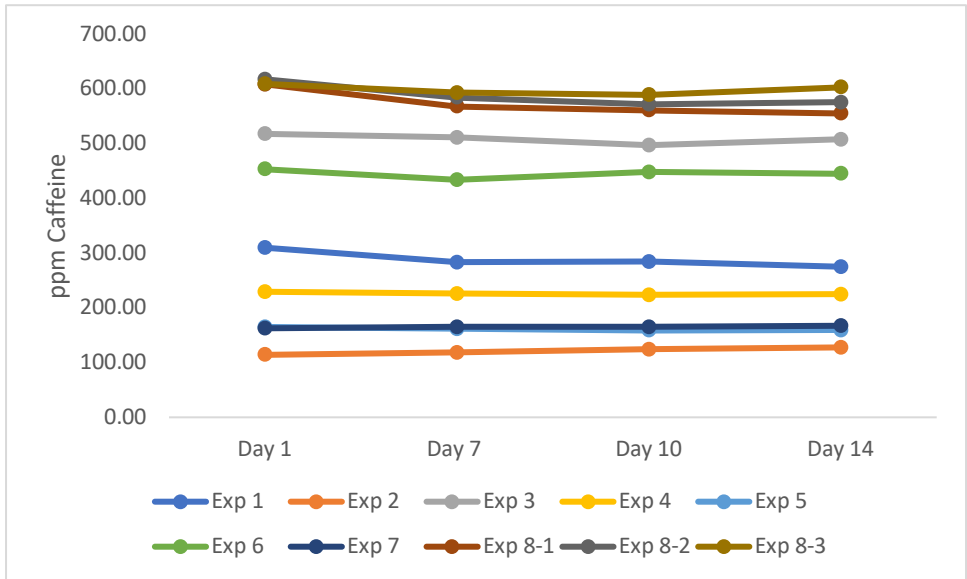


Figure 23: Caffeine profile over 14 days Set 2

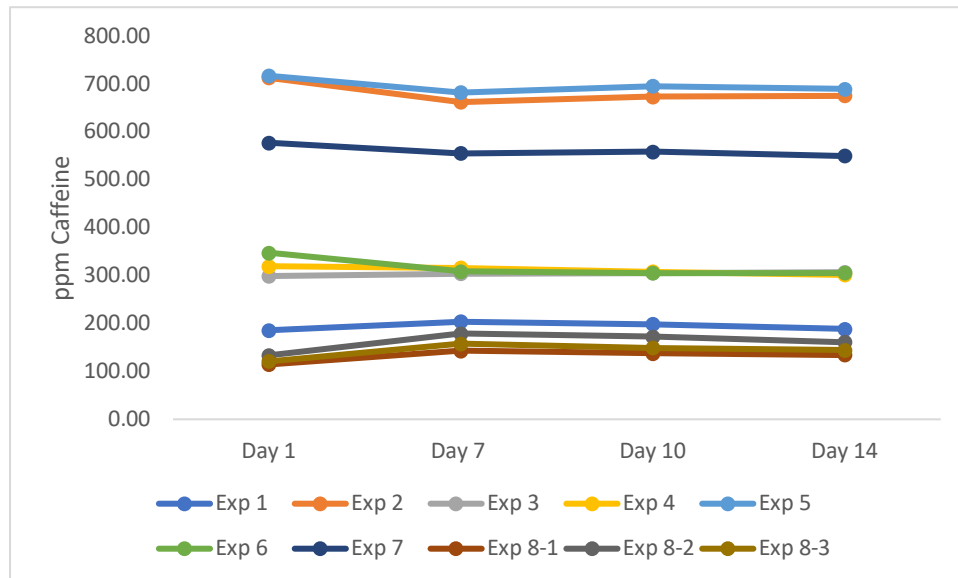


Figure 24:Caffeine profile over 14 days Set 3

Unlike pH, where there is a drastic decrease in the values, the caffeine content does not seem to change as much. Studies suggest that the SCOBY feeds on caffeine for nutrients⁶. However, some notable set-ups have increased caffeine content by more than 10% in the 14 days, such as Set 2: Experiment 2 and Set 3: Experiment 8. However, when comparing Set 2: experiment 2 with its counterpart in Set 1, they do not manifest the same behavior. Instead, Set 1 retains the caffeine content. Thus, it may be attributed to the starter or SCOBY on each set, as these are the only differences. As for Set 3: Experiment 8, all three replicates show an increase in caffeine content of 14-20%. This set-up contains all the negative parameters of kombucha; thus, it was quite unexpected to observe such behavior in all three replicates. As of writing, no other studies have encountered this situation in the early days of fermentation. However, there are studies that show an increase in caffeine content after decreasing for a period of time, and then increased again^{85,86}. These studies do not also explain the mechanism behind, thus this observation can be investigated further.

3.3.4 Factors affecting caffeine content

Factors significant to the caffeine content of kombucha over days 1, 7, 10, and 14 were also explored. In Table 10, the value in the parenthesis beside day is the percent explained variance of the model using the identified significant variables.

Table 10: Identified significant variables affecting caffeine on days 1, 7, 10 and 14.

	Day 1 (93.52%)	Day 7 (94.83%)	Day 10 (95.52%)	Day 14 (95.11%)
Steeping Time	+		+	
Steeping Temp	+	—	—	—
Ratio of Liquid and Beaker			—	
Ratio of Starter and Tea	+	—	—	—
Strength of Tea	+	—	—	—
Sugar Content		—	—	—
Beaker Size			—	
2x4 (BxD)		—		—
1x4 (AxD)		+	+	+
1x5 (AxE)	+	—	—	—
1x2 (AxB)	—			
1x3 (AxC)				
1x7 (AxG)				
1x6 (AxF)	+			

“+” denotes significant variables that are positively correlated; “—” denotes significant variables that are negatively correlated

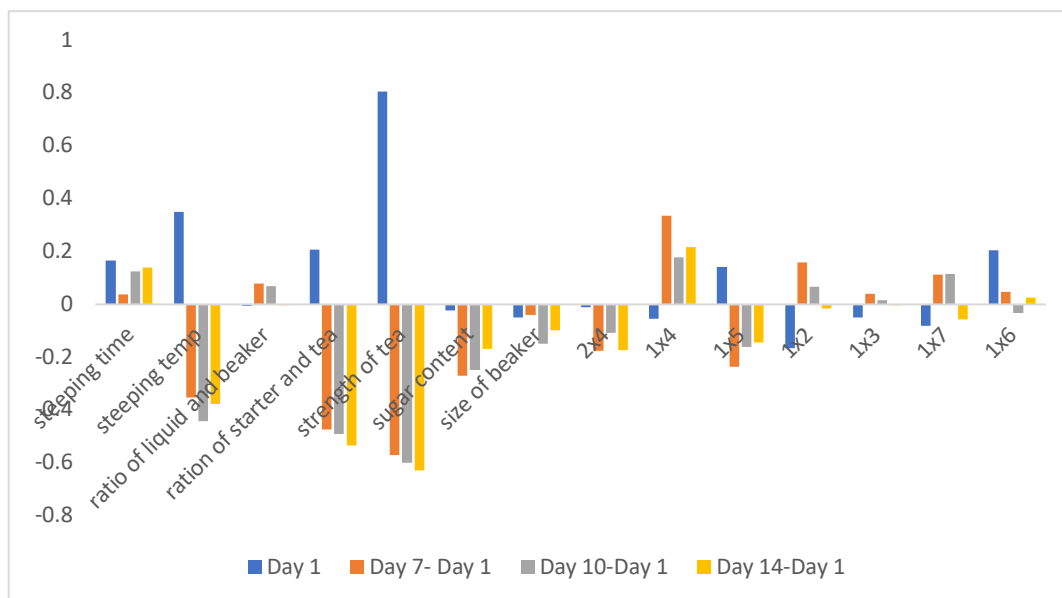


Figure 25: Regression coefficients for caffeine content from day 1, day 7, 10 and 14

Noticeably, the models generated for caffeine content explain the variances more than the ones from pH (Table 10). Figure 25 illustrates the identified significant factors from the four-day sample points throughout the fermentation 14-day period. These are steeping temperature, ratio of starter and tea, strength of tea, and the 1x5 (AxE) interaction. Similar to pH, ratio of starter and tea is a significant variable but it might be more pronounced due to the execution of the design. The starter is highly probably a contributor as this starter has a higher caffeine content at around 344.9 ± 8.1 ppm versus the second set with 191.9 ± 4.2 ppm. The interaction 1x5 (AxE) is most probably driven by steeping time and strength of the tea.

This implies that steeping temperature is more effective in extracting caffeine from the tea leaves over steeping time. Parameters such as sugar content and 1x4(AxD) became essential from day 7 until day 14. 1x4(AxD) can be studied further as this is not clear in this experimental design.

3.4 Raman spectroscopy

3.4.1 Raw data

There are 125 samples having three replicate spectra each equaling to 375 spectra. Following the experimental design in Table 2 and Table 3, there are ten experiments from each set, with

withdrawal points on Day 1, Day 7, Day 10 and Day 14. Apart from the samples of the experiments from the experimental design, the Raman spectra of each starter were obtained on Day 1. Thus, each set has 123 spectra. Spectra of a commercially produced kombucha were obtained from BKB with six replicate spectra. Table 11 describes the format naming of each spectra.

Table 11: Naming format of the Raman spectra from kombucha

		Spectra format naming	Number of Samples
Set 1/ Set 2/ Set 3	Day 1	[set#]1[exp #][replicate#]	10 each set
	Day 7	[set#]7[exp #][replicate#]	10 each set
	Day 10	[set#]10[exp #][replicate#]	10 each set
	Day 14	[set#]14[exp #][replicate#]	10 each set
Starter	Set 1	100[replicate#]	1
	Set 2	200[replicate#]	1
	Set 3	300[replicate#]	1
BKB		1000[replicate#]	1
		2000[replicate#]	1

Figure 26 is characterized by an intense peak from the Rayleigh scattering, but analysis starts after this intense peak at the Stokes scattering. Figure 27 shows a zoomed in Raman spectra, focusing on the spectra after the Rayleigh scattering. It exhibits a curvature that goes upwards and slopes down again, which is the fluorescence that is present in all the Kombucha Raman spectra. The spectra also shows some odd negative peaks at around 300 cm^{-1} , 1476 cm^{-1} and 2135 cm^{-1} , which become greater in magnitude as the vertical offset increases. A hypothesis for these negative peaks could be from the settings of the Raman spectra.

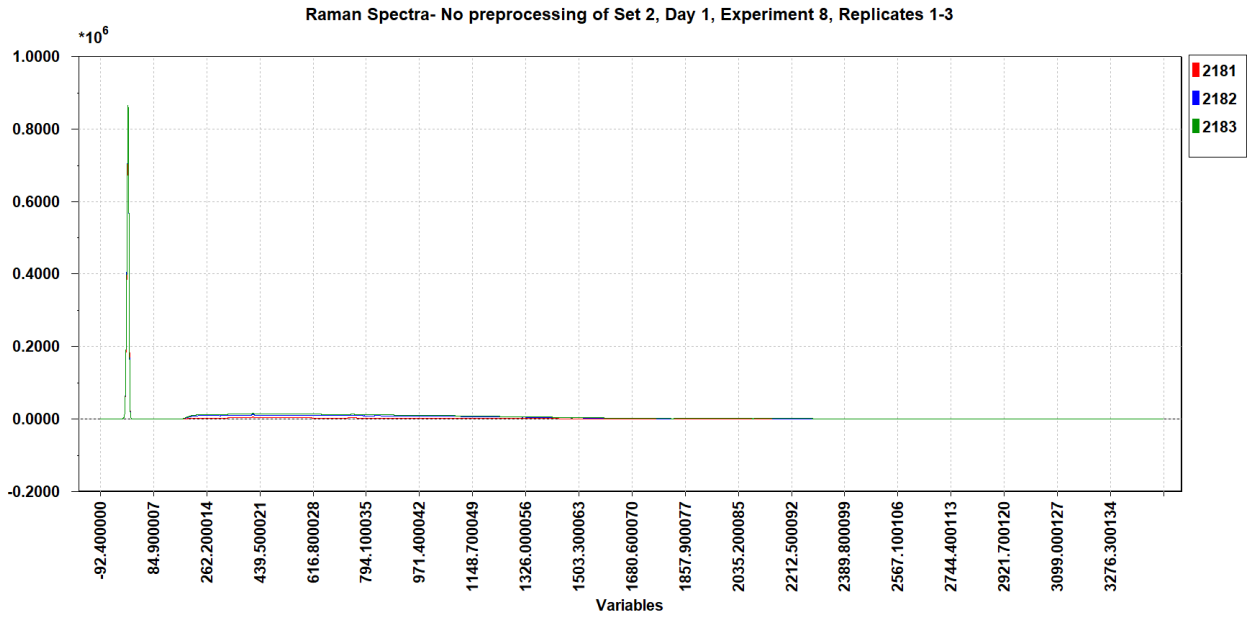


Figure 26: Sample Raman spectra of kombucha

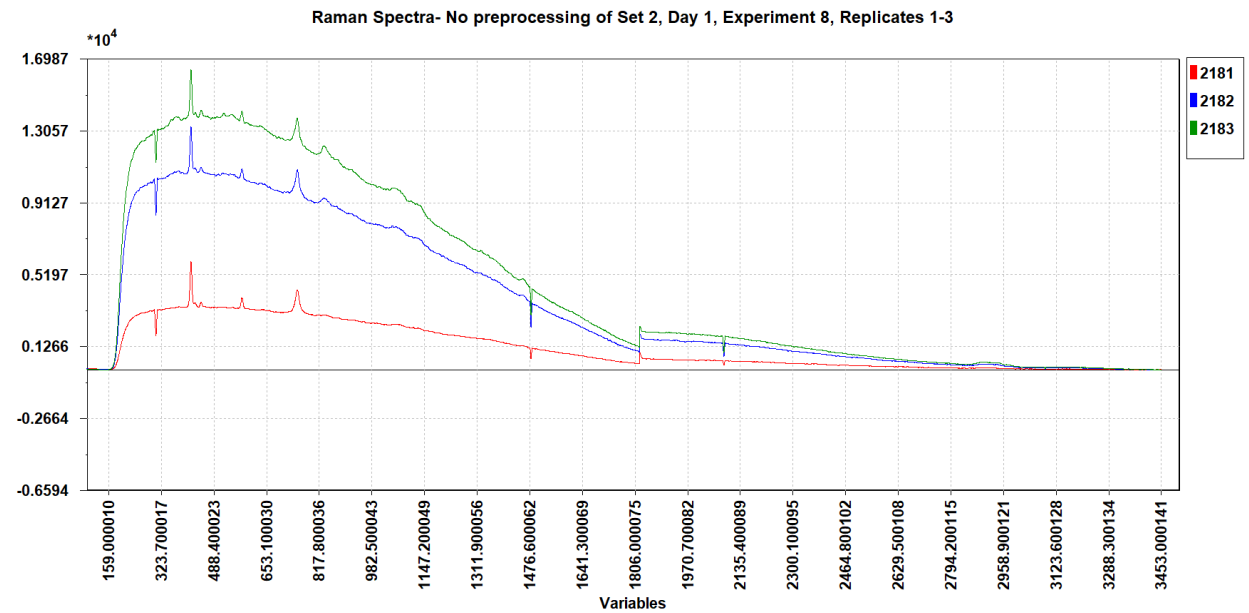


Figure 27: Sample Raman spectra of kombucha zoomed in

Most samples visually exhibit replicates that have significant differences in intensity and variations from different parts of the spectra (Figure 27). There is no observed pattern of whether the first, second, or third replicates are usually the outliers under one sample. Due to the relatively small peaks of Raman shifts occurring compared to Rayleigh scattering, reproducibility

is a disadvantage of Raman spectra⁵⁹. Pre-processing techniques can reduce such differences, which will be discussed in the following sections.

3.4.2 Exploratory analysis

Using Principal Component Analysis (PCA) for exploratory analysis through Sirius, the data is mean-centered, and weighting is set at 1.

Visually, the intense peak (Rayleigh scattering) was not accounted for since this is not the region of interest and the higher wavenumber do not have information (Figure 27). Thus, the only wavelengths retained are 200 to 1813 cm^{-1} . Without pre-processing (Figure 28), the PCA shows a slight separation between Set 3 and Sets 1 and 2. Interestingly, Set 1 and Set 2 seem to overlap each other.

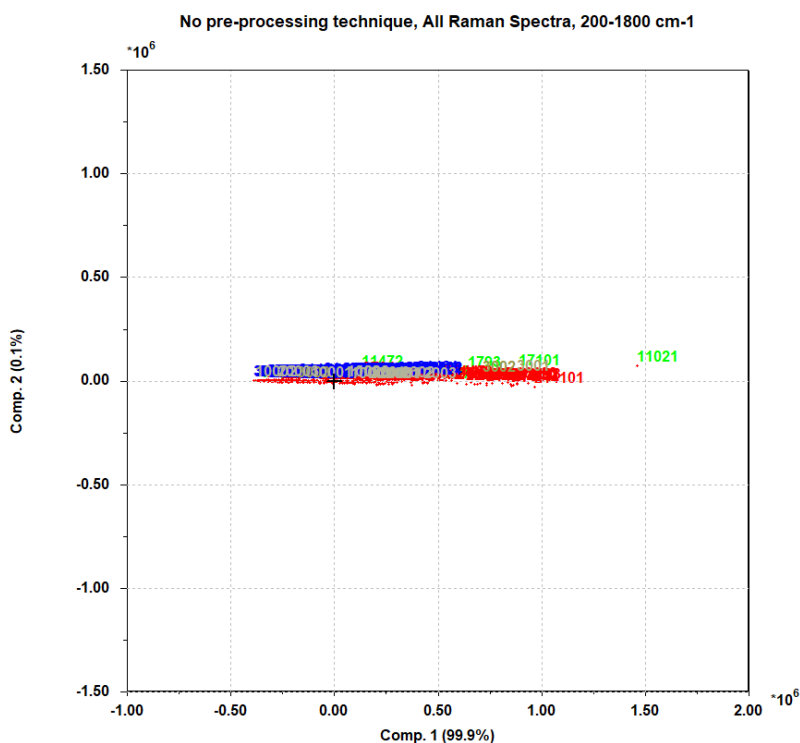


Figure 28: Score plot of all samples and replicates without pre-treatment

Figure 28 shows that despite the different parameters in each set-up, the spectra are almost all similar. Set 3, colored in blue, is grouped on the upper left side of the PCA, while Sets 1 and 2 (green and red, respectively) are more spread out.

An outlier spectra is also noted with Sample 11021 (Set 1, Day 10, Experiment 2, Replicate 1). Removing this sample, the score plot still looks similar (Figure 29).

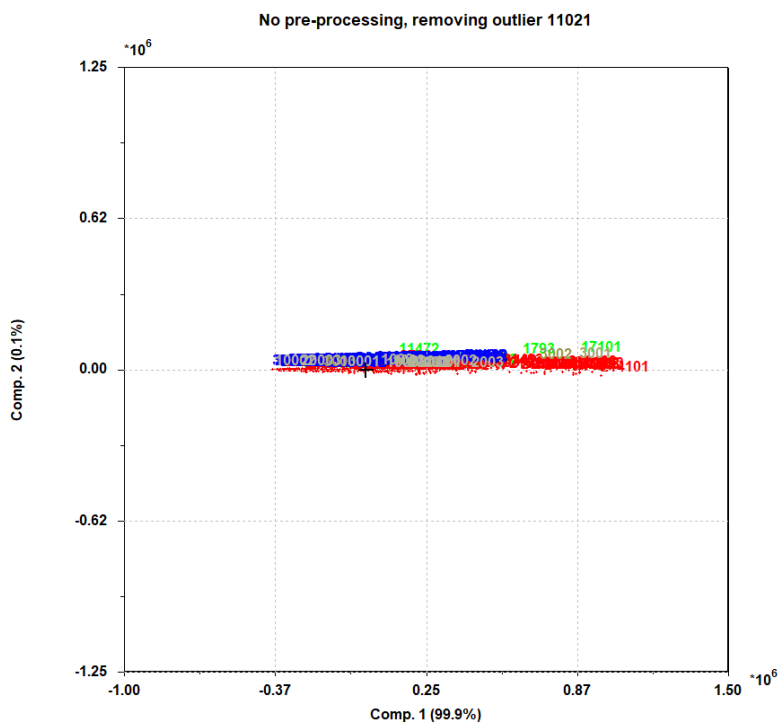


Figure 29: Score plot of unprocessed Raman spectra, removing outlier

3.4.3 Data preprocessing

Pre-treatment might aid the poor replicates from Figure 29 and make groupings from the Raman spectra. Several pre-treatments and combinations thereof, were attempted. Significant time was

spent in rolling ball due to its premise (Figure 30). However, it was difficult to determine a suitable ball radius due to the peak shapes change and lack of not so well-defined peaks.

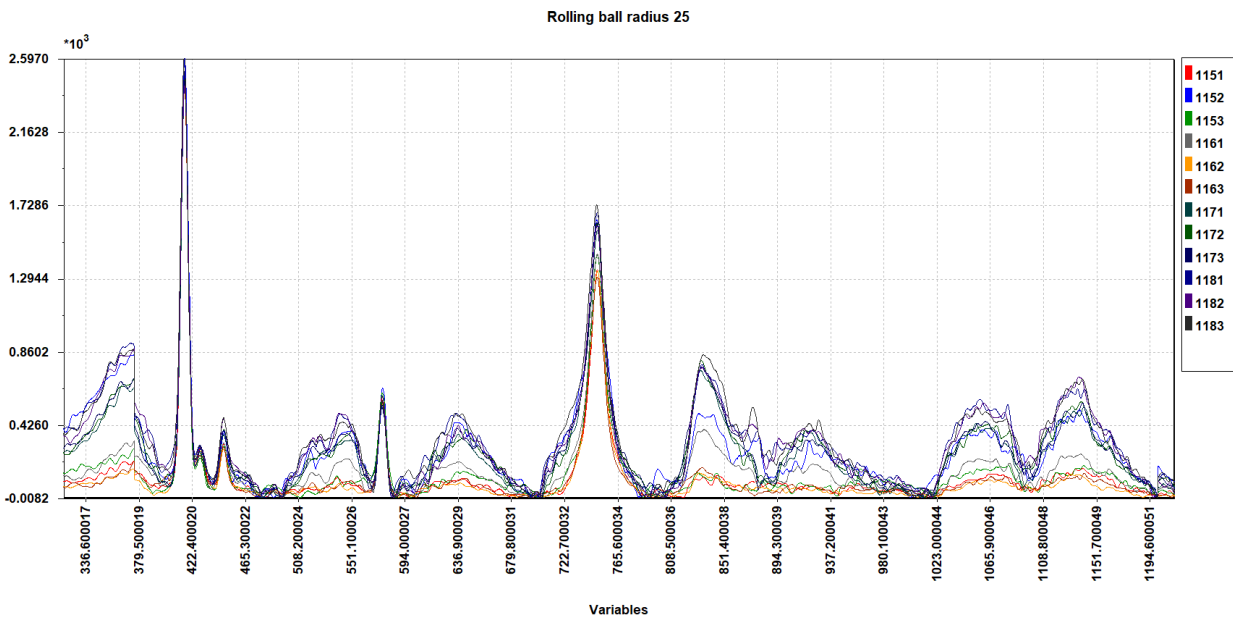


Figure 30: Example of a rolling ball spectra

Figure 30 shows 12 spectra from four samples. However, the spectra do not show replicates of the sets from each other, nor does it show any peaks relating to caffeine or pH.

Numerical differentiation or differentiation by Savitzky-Golay by the first derivative was found to be the best option. Derivatives (1st to 4th), window sizes (5 to 17) and degree of polynomial (1 to 4) were also played around and there was no significance changes found in terms of variance explained. A usual combination paired with Savitzky-Golay, EMSC, was found to not much have difference in the score plot, and with the variances it can explain. Thus, 11 window size at degree 2 (Figure 31) which showed the most promise in grouping the kombucha was chosen and most

notably using PC2 and PC3, which explains only 16.8% of the variance (Figure 32).

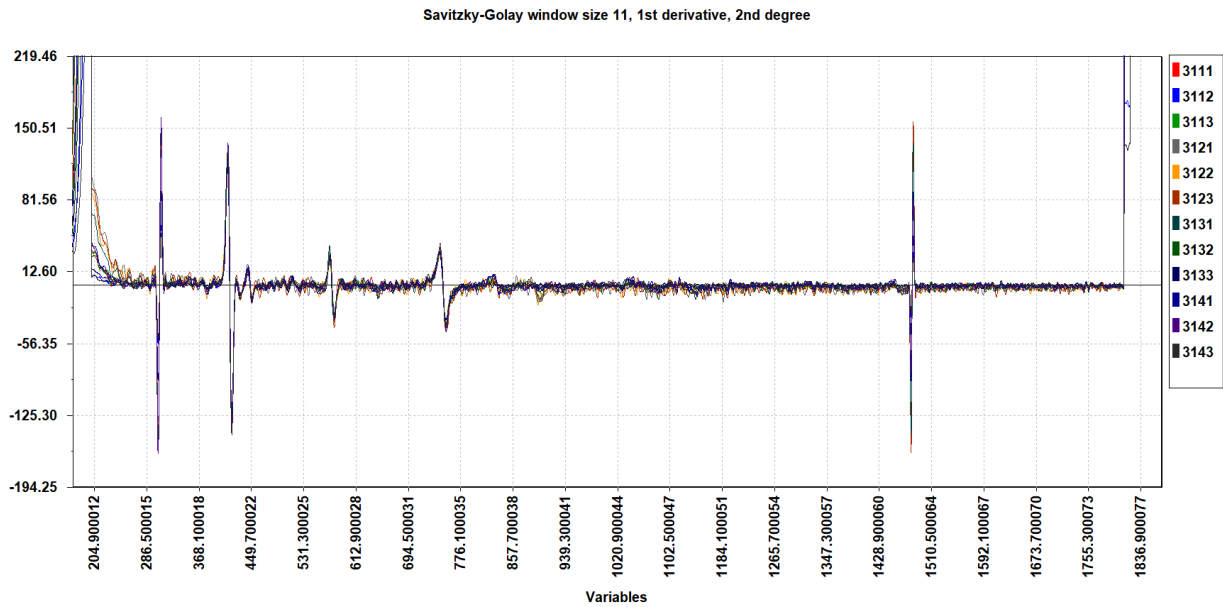


Figure 31: Raman spectra pre-processed using Savitzky-Golay 1st Derivative, Window Size 11, Degree 2

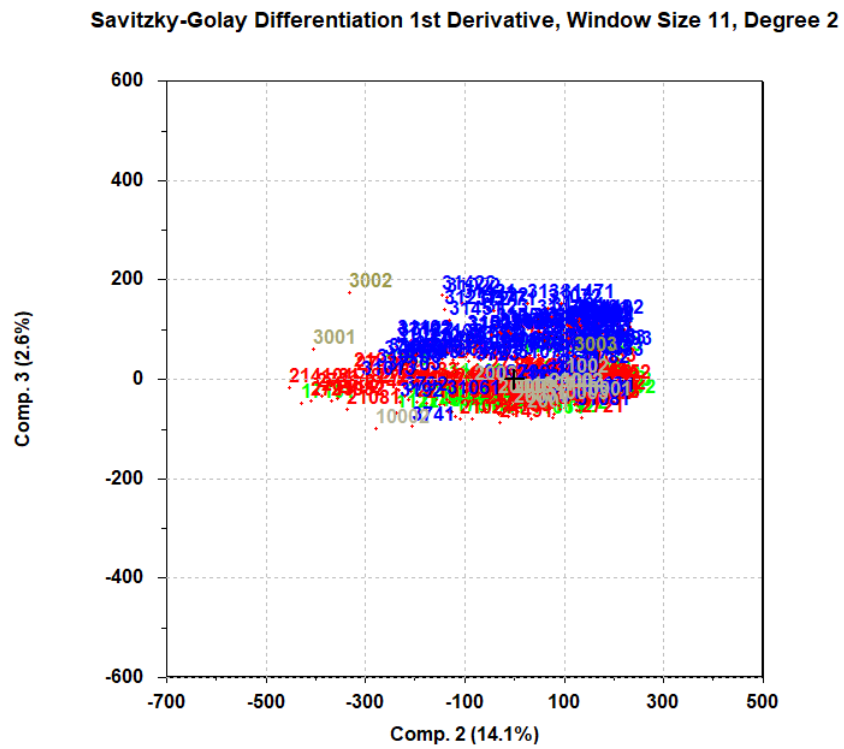


Figure 32: PCA plot for all samples and replicates of kombucha

In Figure 32, most of the sample replicates are also apart, showing that most spectra are not replicates of each other. A reason could be the samples were unfiltered when it was subjected to Raman spectroscopy; thus, the suspended particles in the solution could have affected the repeatability of the replicates¹⁰.

The loadings plot (Figure 33) shows that the separation can be most attributed to 400-500 cm^{-1} . It was hypothesized that the separation might be driven by pH since the pH of the samples in Set 3 is lower than in Sets 1 and 2.

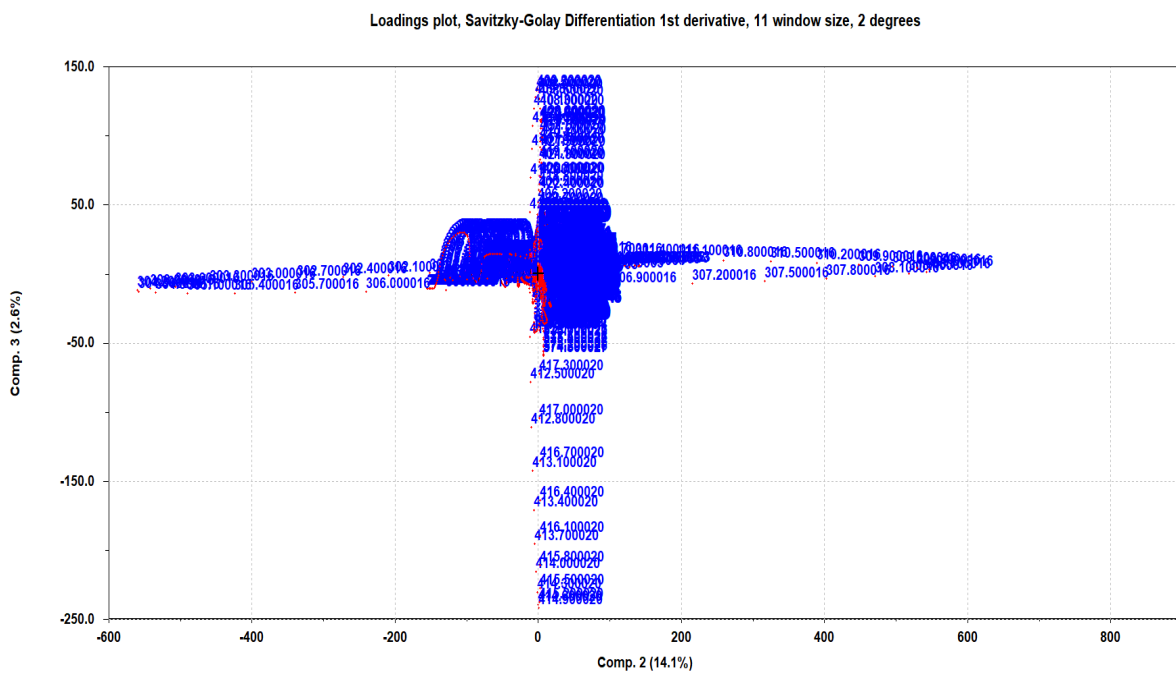


Figure 33: Loadings plot of the kombucha samples

The color gradient was attempted to see if this is possible; however, it is difficult to tell for sure as the pH ranges is small; thus, the color differences are less prominent (Figure 34). In Figure 34, blue is less acidic while red is more acidic.

on the Raman spectra and PCA, only a minimal difference was detected between the experiments under each set. The Raman spectra of BKB are also located on the side of Sets 1 and 2, suggesting that BKB's sample is more similar to these sets than Set 3. Variable selection can be attempted to further explore the slight separation as noise from the has been subjected to PCA.

3.4.4 Partial least squares

Partial Least Squares was attempted to determine suitable pre-processing techniques because of the difficulty in understanding the samples' behavior using PCA. Variations of selecting the training sets were explored such as:

- a. each of the replicates
- b. two of the replicates
- c. first brewing set with all three replicates and two of the all positives and negatives.

Cross-validation is used to evaluate the performance of a model. The software was set by leaving every fourth object. Number of iterations was set at 40. The maximum number of compositions selected is 10. The validation level is at 0.401. When a model has been generated, the following were observed:

- a. number of components generated and their respective p-MC
- b. the RMSEP and R^2 where low RMSEP and R^2 near 1 is ideal in the predicted versus measured plot of the training set and predicting set,

Pre-processing techniques stated earlier were attempted for both pH and caffeine, however none of the models were successful as they all had low R^2_{CV} and R^2_P and/or high RMSEP, despite removing outliers PLS tabular results (Appendix: 7.10 PLS tabular results).

Another strategy used is inputting a random numbers for caffeine and pH and comparing with the actual result. The dataset with the random numbers should have lower variations obtained and high p-MC values, while the actual values would have higher percentage of variation explained in the components generated, and lower p-MC values. This was also not successful because the variations between the random values and actual values do not have a big difference

between them. A big difference would signal that there is a relationship between the actual results and the spectra obtained.

Due to the difficulty in generating a predictive model from PLS for caffeine content and pH, standards and spiked samples were analyzed (Figure 36). Comparing 1000 ppm caffeine and water, there are no significant peaks from the caffeine standard. Adding more caffeine to the 1000 ppm caffeine standard (red) showed more significant peaks. Also, spiking caffeine to kombucha of more than 1000 ppm in total concentration shows more peaks in the spectra (green). This suggests that the instrument can detect at concentrations higher than 1000 ppm. It is important to note that the highest caffeine content is around 800 ppm (yellow), which also resembles the spectra of water.

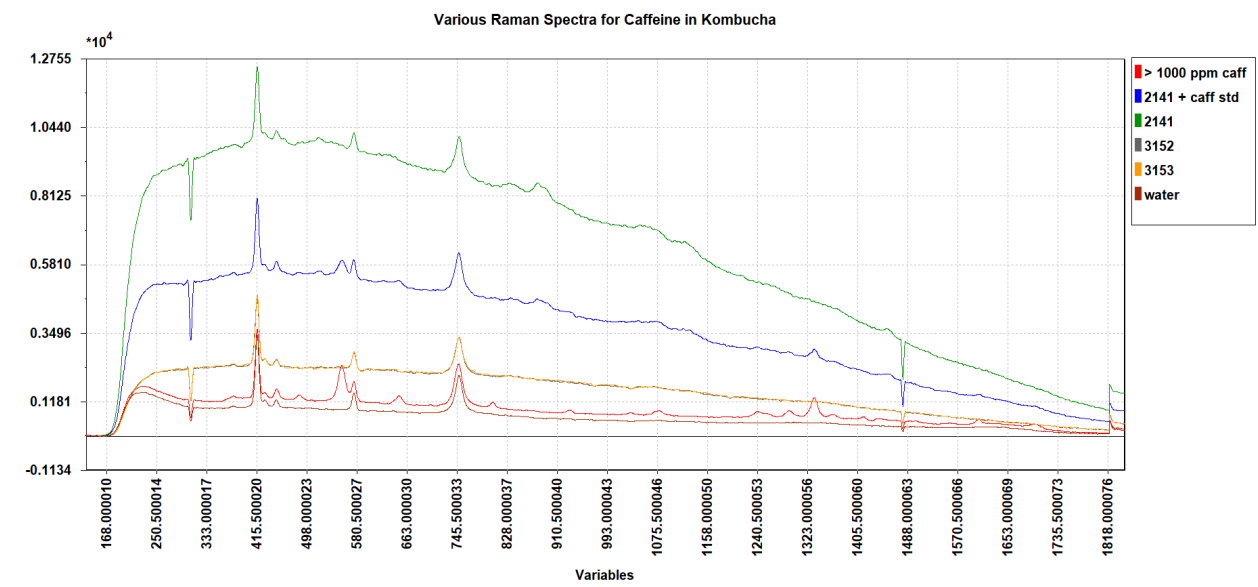


Figure 36: Various Raman spectra of caffeine content in kombucha

Since it has been established that the concentration range for caffeine content in kombucha for this study is too low for detection, using Raman spectroscopy to model pH is futile since pH is a simple method. However, to observe the Raman spectra profile when pH is manipulated 0.1 M NaOH and acetic acid were added to kombucha (Figure 37). Sodium hydroxide was used as the choice for the basic solution since this is Raman inactive and readily available. On the other hand, acetic acid was chosen since this is the dominant acid in kombucha.

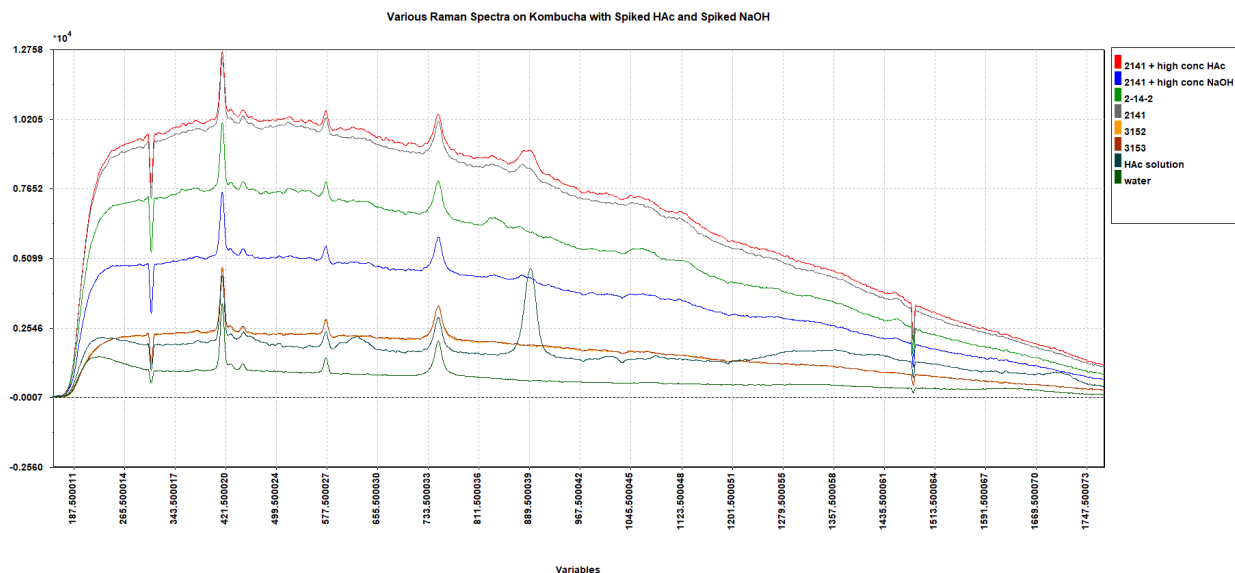


Figure 37: Raman spectra of kombucha spiked with acetic acid (HAc) and NaOH

Comparing the Raman spectra of acetic acid with the Raman spectra of other kombucha, models relating to acetic acid content can be generated from the Raman spectra between 574 to 962 cm^{-1} . This also suggests that acetic acid might not be one of the reasons why Set 3 is separated from Set 1 and Set 2 in the PCA generated.

From this experiment, Raman spectroscopy is not a suitable instrument for this range of fermentation parameters since the spectra generated do not seem to vary much. The instrument's specifications are also not compatible with the range of caffeine in the experiment also suggesting that the solution is too dilute for this Raman method to detect any significant variations between the experiments. Another type of Raman, Surface-enhanced Raman Spectroscopy (SERS) can be attempted, as this was found to be more sensitive than the conventional Raman^{20,59}.

4 Conclusion

The main objective of this study is to understand the profile and fermentation parameters of Kombucha white tea and its effect on caffeine and pH. In relation to this, an HPLC method determining caffeine content was validated for use. Additionally, the possibility of using Raman spectroscopy was explored to understand and predict kombucha behavior.

Different parameters explored over fourteen (14) days were steeping time, steeping temperature, the strength of tea, ratio of starter and tea, ratio of tea and liquid, sugar content, and size of the beaker. Through this experiment, preparing kombucha with different parameters affects the drink's physical quality.

As for pH, general behavior shows a sudden decrease from Day 1 to Day 7, then a gradual decrease until Day 14. The ratio of starter and tea is a consistent significant parameter affecting the pH. For a week, the strength of tea influences the pH, while sugar content starts to affect the pH on days 10 and 14. Parameters relating to space affect pH at days 7 to 14. There are no interactions that affect the pH consistently throughout the days.

Using the HPLC method for quantifying caffeine content, most experiments either stayed consistent or decreased in caffeine content, which is consistent with most studies—however, Set 3. Experiment 8 with all its replicates (all the negative parameters) showed increased caffeine content in all replicates, which should be investigated more. The main effects of steeping temperature, starter and tea ratio, tea strength, and 1x5(AxE) affect the caffeine content for all sampling points. On the seventh day, sugar content and 1x4 (AxD) also contribute to the caffeine content.

Despite the several pre-processing techniques employed on the Raman spectroscopy of kombucha, only little information can be gathered except for the separation of Sets 3 from Sets 1 and 2 in PCA, using Savitzky-Golay differentiation by the first derivative and 11 window size. It is not determined what drives this; however, certainly, it is not caffeine or pH through the PLS.

5 Recommendations

With the end of this study, there are several recommendations that can be explored. Some recommendations for this study could be using the same starter for all experiments. The apparent separation between the experimental design and its fold-over creates limitations in the analysis of the design. It was incredibly challenging for Day 1 since the data is clearly separated between Sets 2 and 3. Another option is to incorporate blocking in the experimental design to consider the different starters that will be used in the duration of the study.

Relating to the physical properties of kombucha, it can be recommended to conduct a more quantitative approach in determining color and appearance. Methods such as a spectrometer or having a panel to judge the color and appearance can be explored. Also, other organoleptic parameters such as smell, taste and desirability can be explored since these are other aspects that concern consumers of kombucha.

Concerning the experimental design, the values of the selected parameters mainly revolves closely around the fermentation parameter value of BKB. Wider ranges should be experimented to see better how the parameters affect each other. From this, a study can be executed on optimizing kombucha's fermentation. The identified interactions can also be investigated to understand the behavior of kombucha better. Also, the microbial composition of the SCOBY and the starter should be considered since this plays a prominent role in the physical aspects and health compounds of kombucha.

Another recommendation is with regards to the Raman spectrometer. Reproducibility of the spectra between replicates was a problem, thus filtering the solution prior Raman analysis can be attempted. More advanced Raman spectrometer and other parameters can be explored to enhance the variations from kombucha and enable detection caffeine content or other compounds, which may have better results in the future. Lastly, variable selection can be used to explore the PCA results further.

6 References

- (1) Villarreal-Soto, S. A.; Beaufort, S.; Bouajila, J.; Souchard, J.-P.; Taillandier, P. Understanding Kombucha Tea Fermentation: A Review: Understanding Kombucha Tea Fermentation.... *J. Food Sci.* **2018**, *83* (3), 580–588. <https://doi.org/10.1111/1750-3841.14068>.
- (2) Jayabalan, R.; Malbaša, R. V.; Lončar, E. S.; Vitas, J. S.; Sathishkumar, M. A Review on Kombucha Tea-Microbiology, Composition, Fermentation, Beneficial Effects, Toxicity, and Tea Fungus: A Review on Kombucha.... *Compr. Rev. Food Sci. Food Saf.* **2014**, *13* (4), 538–550. <https://doi.org/10.1111/1541-4337.12073>.
- (3) Kaewkod, T.; Bovonsombut, S.; Tragoolpua, Y. Efficacy of Kombucha Obtained from Green, Oolong, and Black Teas on Inhibition of Pathogenic Bacteria, Antioxidation, and Toxicity on Colorectal Cancer Cell Line. *Microorganisms* **2019**, *7* (12), 700. <https://doi.org/10.3390/microorganisms7120700>.
- (4) Kaashyap, M.; Cohen, M.; Mantri, N. Microbial Diversity and Characteristics of Kombucha as Revealed by Metagenomic and Physicochemical Analysis. *Nutrients* **2021**, *13* (12), 4446. <https://doi.org/10.3390/nu13124446>.
- (5) Bishop, P.; Pitts, E. R.; Budner, D.; Thompson-Witrick, K. A. Chemical Composition of Kombucha. *Beverages* **2022**, *8* (3), 45. <https://doi.org/10.3390/beverages8030045>.
- (6) Chakravorty, S.; Bhattacharya, S.; Chatzinotas, A.; Chakraborty, W.; Bhattacharya, D.; Gachhui, R. Kombucha Tea Fermentation: Microbial and Biochemical Dynamics. *Int. J. Food Microbiol.* **2016**, *220*, 63–72. <https://doi.org/10.1016/j.ijfoodmicro.2015.12.015>.
- (7) Fortune Business Insights. The Global Kombucha Market Size Stood at USD 1.84 Billion in 2019 and Is Projected to Reach USD 10.45 Billion by 2027, Exhibiting a CAGR of 23.2% during the Forecast Period. <https://www.fortunebusinessinsights.com/industry-reports/kombucha-market-100230>.
- (8) Freitas, A.; Sousa, P.; Wurlitzer, N. Alternative Raw Materials in Kombucha Production. *Int. J. Gastron. Food Sci.* **2022**, *30*, 100594. <https://doi.org/10.1016/j.ijgfs.2022.100594>.
- (9) Phung, L. T.; Kitwetcharoen, H.; Chamnipa, N.; Boonchot, N.; Thanonkeo, S.; Tippayawat, P.; Klanrit, P.; Yamada, M.; Thanonkeo, P. Changes in the Chemical Compositions and Biological

Properties of Kombucha Beverages Made from Black Teas and Pineapple Peels and Cores. *Sci. Rep.* **2023**, *13* (1), 7859. <https://doi.org/10.1038/s41598-023-34954-7>.

- (10) Tran, T.; Grandvalet, C.; Verdier, F.; Martin, A.; Alexandre, H.; Tourdot-Maréchal, R. Microbiological and Technological Parameters Impacting the Chemical Composition and Sensory Quality of Kombucha. *Compr. Rev. Food Sci. Food Saf.* **2020**, *19* (4), 2050–2070. <https://doi.org/10.1111/1541-4337.12574>.
- (11) Amarasinghe, H.; Weerakkody, N. S.; Waisundara, V. Y. Evaluation of Physicochemical Properties and Antioxidant Activities of Kombucha “Tea Fungus” during Extended Periods of Fermentation. *Food Sci. Nutr.* **2018**, *6* (3), 659–665. <https://doi.org/10.1002/fsn3.605>.
- (12) Neffe-Skocińska, K.; Sionek, B.; Ścibisz, I.; Kołożyn-Krajewska, D. Acid Contents and the Effect of Fermentation Condition of Kombucha Tea Beverages on Physicochemical, Microbiological and Sensory Properties. *CyTA - J. Food* **2017**, *15* (4), 601–607. <https://doi.org/10.1080/19476337.2017.1321588>.
- (13) Bishop, P.; Pitts, E. R.; Budner, D.; Thompson-Witrick, K. A. Kombucha: Biochemical and Microbiological Impacts on the Chemical and Flavor Profile. *Food Chem. Adv.* **2022**, *1*, 100025. <https://doi.org/10.1016/j.focha.2022.100025>.
- (14) Harris, D. C.; Lucy, C. A. *Quantitative Chemical Analysis*, Tenth edition.; Macmillan Learning: Austin Boston New York Plymouth, 2020.
- (15) Wang, B.; Rutherford-Markwick, K.; Zhang, X.-X.; Mutukumira, A. N. Kombucha: Production and Microbiological Research. *Foods* **2022**, *11* (21), 3456. <https://doi.org/10.3390/foods11213456>.
- (16) Goh, W.N., Rosma A., Kaur, B., Fazilah, A., Karim A.A. and *; Rajeev Bhat. Fermentation of Black Tea Broth (Kombucha): I. Effects of Sucrose Concentration and Fermentation Time on the Yield of Microbial Cellulose. *Int. Food Res. J.* **2012**, *19* (1), 109–117.
- (17) Food and Drug Administration. Food Code 2022 Recommendations of the United States Public Health Service Food and Drug Administration, 2023. <https://www.fda.gov/media/164194/download> (accessed 2023-06-18).

- (18) Kombucha Brewers International. *Kombucha Brewers International Code of Practice*. Kombucha Code of Practice. <https://kombuchabrewers.org/kombucha-code-of-practice/> (accessed 2023-08-14).
- (19) Nyhan, L. M.; Lynch, K. M.; Sahin, A. W.; Arendt, E. K. Advances in Kombucha Tea Fermentation: A Review. *Appl. Microbiol.* **2022**, *2* (1), 73–101. <https://doi.org/10.3390/applmicrobiol2010005>.
- (20) Zareef, M.; Mehedi Hassan, M.; Arslan, M.; Ahmad, W.; Ali, S.; Ouyang, Q.; Li, H.; Wu, X.; Chen, Q. Rapid Prediction of Caffeine in Tea Based on Surface-Enhanced Raman Spectroscopy Coupled Multivariate Calibration. *Microchem. J.* **2020**, *159*, 105431. <https://doi.org/10.1016/j.microc.2020.105431>.
- (21) Fontana, J. D.; Franco, V. C.; De Souza, S. J.; Lyra, I. N.; De Souza, A. M. Nature of Plant Stimulators in the Production of *Acetobacter Xylinum* (“Tea Fungus”) Biofilm Used in Skin Therapy. *Appl. Biochem. Biotechnol.* **1991**, *28–29* (1), 341–351. <https://doi.org/10.1007/BF02922613>.
- (22) Greenwalt, C. J.; Steinkraus, K. H.; Ledford, R. A. Kombucha, the Fermented Tea: Microbiology, Composition, and Claimed Health Effects. *J. Food Prot.* **2000**, *63* (7), 976–981. <https://doi.org/10.4315/0362-028X-63.7.976>.
- (23) Majumder, S. Stimulants of Tea Infusion Are Completely Withdrawn by Scoby during Kombucha Fermentation: A Biochemical Investigation. *Int. J. Food Ferment. Technol.* **2020**, *10* (2). <https://doi.org/10.30954/2277-9396.02.2020.7>.
- (24) Miranda, B.; Lawton, N. M.; Tachibana, S. R.; Swartz, N. A.; Hall, W. P. Titration and HPLC Characterization of Kombucha Fermentation: A Laboratory Experiment in Food Analysis. *J. Chem. Educ.* **2016**, *93* (10), 1770–1775. <https://doi.org/10.1021/acs.jchemed.6b00329>.
- (25) Kallel, L.; Desseaux, V.; Hamdi, M.; Stocker, P.; Ajandouz, E. H. Insights into the Fermentation Biochemistry of Kombucha Teas and Potential Impacts of Kombucha Drinking on Starch Digestion. *Food Res. Int.* **2012**, *49* (1), 226–232. <https://doi.org/10.1016/j.foodres.2012.08.018>.
- (26) Narko, T.; Wibowo, M. S.; Damayanti, S.; Wibowo, I. EFFECT OF KOMBUCHA CULTURE ON CAFFEINE AND CHLOROGENIC ACID CONTENT IN FERMENTATION OF ROBUSTA GREEN

COFFEE BEANS (*Coffea Canephora* L.). *Rasayan J. Chem.* **2020**, *13* (02), 1181–1186. <https://doi.org/10.31788/RJC.2020.1325675>.

- (27) Pastoriza, S.; Pérez-Burillo, S.; Rufián-Henares, J. Á. How Brewing Parameters Affect the Healthy Profile of Tea. *Curr. Opin. Food Sci.* **2017**, *14*, 7–12. <https://doi.org/10.1016/j.cofs.2016.12.001>.
- (28) Castiglioni, S.; Damiani, E.; Astolfi, P.; Carloni, P. Influence of Steeping Conditions (Time, Temperature, and Particle Size) on Antioxidant Properties and Sensory Attributes of Some White and Green Teas. *Int. J. Food Sci. Nutr.* **2015**, *66* (5), 491–497. <https://doi.org/10.3109/09637486.2015.1042842>.
- (29) Watawana, M. I.; Jayawardena, N.; Waisundara, V. Y. Enhancement of the Functional Properties of Coffee Through Fermentation by “Tea Fungus” (Kombucha): Functional Properties of Fermented Coffee. *J. Food Process. Preserv.* **2015**, *39* (6), 2596–2603. <https://doi.org/10.1111/jfpp.12509>.
- (30) Vitas, J. S.; Cvetanović, A. D.; Mašković, P. Z.; Švarc-Gajić, J. V.; Malbaša, R. V. Chemical Composition and Biological Activity of Novel Types of Kombucha Beverages with Yarrow. *J. Funct. Foods* **2018**, *44*, 95–102. <https://doi.org/10.1016/j.jff.2018.02.019>.
- (31) Malbaša, R.; Lončar, E.; Djurić, M.; Klašnja, M.; Kolarov, L. J.; Markov, S. Scale-Up of Black Tea Batch Fermentation by Kombucha. *Food Bioprod. Process.* **2006**, *84* (3), 193–199. <https://doi.org/10.1205/fbp.05061>.
- (32) Cvetković, D.; Markov, S.; Djurić, M.; Savić, D.; Velićanski, A. Specific Interfacial Area as a Key Variable in Scaling-up Kombucha Fermentation. *J. Food Eng.* **2008**, *85* (3), 387–392. <https://doi.org/10.1016/j.jfoodeng.2007.07.021>.
- (33) Savary, O.; Mounier, J.; Thierry, A.; Poirier, E.; Jourden, J.; Maillard, M.-B.; Penland, M.; Decamps, C.; Coton, E.; Coton, M. Tailor-Made Microbial Consortium for Kombucha Fermentation: Microbiota-Induced Biochemical Changes and Biofilm Formation. *Food Res. Int.* **2021**, *147*, 110549. <https://doi.org/10.1016/j.foodres.2021.110549>.
- (34) Zhou, S.; Zhang, J.; Ma, S.; Ou, C.; Feng, X.; Pan, Y.; Gong, S.; Fan, F.; Chen, P.; Chu, Q. Recent Advances on White Tea: Manufacturing, Compositions, Aging Characteristics and

- Bioactivities. *Trends Food Sci. Technol.* **2023**, *134*, 41–55.
<https://doi.org/10.1016/j.tifs.2023.02.016>.
- (35) Yang, C.; Hu, Z.; Lu, M.; Li, P.; Tan, J.; Chen, M.; Lv, H.; Zhu, Y.; Zhang, Y.; Guo, L.; Peng, Q.; Dai, W.; Lin, Z. Application of Metabolomics Profiling in the Analysis of Metabolites and Taste Quality in Different Subtypes of White Tea. *Food Res. Int.* **2018**, *106*, 909–919.
<https://doi.org/10.1016/j.foodres.2018.01.069>.
- (36) Yilmaz, B.; Acar-Tek, N. White Tea: Its History, Composition, and Potential Effects on Body Weight Management. *eFood* **2023**, *4* (3), e89. <https://doi.org/10.1002/efd2.89>.
- (37) Malbaša, R.; Lončar, E.; Djurić, M.; Došenović, I. Effect of Sucrose Concentration on the Products of Kombucha Fermentation on Molasses. *Food Chem.* **2008**, *108* (3), 926–932.
<https://doi.org/10.1016/j.foodchem.2007.11.069>.
- (38) Chu, S.-C.; Chen, C. Effects of Origins and Fermentation Time on the Antioxidant Activities of Kombucha. *Food Chem.* **2006**, *98* (3), 502–507.
<https://doi.org/10.1016/j.foodchem.2005.05.080>.
- (39) Miller, J. N.; Miller, J. C. *Statistics and Chemometrics for Analytical Chemistry*, 5. ed., [Nachdr.]; Pearson Prentice Hall: Harlow, England, 2009.
- (40) Lundstedt, T.; Seifert, E.; Abramo, L.; Thelin, B. *Experimental Design and Optimization*. **1998**.
- (41) Montgomery, D. C. *Design and Analysis of Experiments*, Tenth edition.; Wiley: Hoboken, NJ, 2020.
- (42) LaCourse, M. E.; LaCourse, W. R. General Instrumentation in HPLC *. In *Liquid Chromatography*; Elsevier, 2017; pp 417–429. <https://doi.org/10.1016/B978-0-12-805393-5.00017-8>.
- (43) Marina, M. L.; García, M. A. CHROMATOGRAPHY: LIQUID | Micellar Liquid Chromatography. In *Encyclopedia of Separation Science*; Elsevier, 2000; pp 726–737.
<https://doi.org/10.1016/B0-12-226770-2/01811-1>.
- (44) Moldoveanu, S. C.; David, V. *Selection of the HPLC Method in Chemical Analysis*; Elsevier: Amsterdam, Netherlands Cambridge, MA, United States, 2017.

- (45) Valcárcel, M.; Cárdenas, S.; Simonet, B. M.; Carrillo-Carrión, C. Principles of Qualitative Analysis in the Chromatographic Context. *J. Chromatogr. A* **2007**, *1158* (1–2), 234–240. <https://doi.org/10.1016/j.chroma.2007.03.034>.
- (46) USP. 〈1225〉 *Validation of Compendial Procedures*. In: USP - NF. Rockville, MD.: USP; August 1, 2017. https://doi.org/10.31003/USPNF_M99945_04_01.
- (47) Konieczka, P. The Role of and the Place of Method Validation in the Quality Assurance and Quality Control (QA/QC) System. *Crit. Rev. Anal. Chem.* **2007**, *37* (3), 173–190. <https://doi.org/10.1080/10408340701244649>.
- (48) *Fundamentals of Analytical Chemistry*, 9. ed., International ed.; Skoog, D. A., West, D. M., Holler, F. J., Crouch, S. R., Eds.; Brooks/Cole, Cengage Learning: Melbourne, 2014.
- (49) USP. 〈1858〉 *Raman Spectroscopy-Theory and Practice*. In: USP - NF. Rockville, MD.: USP; November 1, 2020. https://doi.org/10.31003/USPNF_M1017_02_01.
- (50) Magdas, D. A.; Guyon, F.; Feher, I.; Pinzaru, S. C. Wine Discrimination Based on Chemometric Analysis of Untargeted Markers Using FT-Raman Spectroscopy. *Food Control* **2018**, *85*, 385–391. <https://doi.org/10.1016/j.foodcont.2017.10.024>.
- (51) Butler, H. J.; Ashton, L.; Bird, B.; Cinque, G.; Curtis, K.; Dorney, J.; Esmonde-White, K.; Fullwood, N. J.; Gardner, B.; Martin-Hirsch, P. L.; Walsh, M. J.; McAinsh, M. R.; Stone, N.; Martin, F. L. Using Raman Spectroscopy to Characterize Biological Materials. *Nat. Protoc.* **2016**, *11* (4), 664–687. <https://doi.org/10.1038/nprot.2016.036>.
- (52) Vankeirsbilck, T.; Vercauteren, A.; Baeyens, W.; Van Der Weken, G.; Verpoort, F.; Vergote, G.; Remon, J. P. Applications of Raman Spectroscopy in Pharmaceutical Analysis. *TrAC Trends Anal. Chem.* **2002**, *21* (12), 869–877. [https://doi.org/10.1016/S0165-9936\(02\)01208-6](https://doi.org/10.1016/S0165-9936(02)01208-6).
- (53) Schmid, T.; Dariz, P. Raman Microspectroscopic Imaging of Binder Remnants in Historical Mortars Reveals Processing Conditions. *Heritage* **2019**, *2* (2), 1662–1683. <https://doi.org/10.3390/heritage2020102>.
- (54) Ferraro, J. R.; Nakamoto, K.; Brown, C. W. *Introductory Raman Spectroscopy*, 2nd ed.; Academic Press: Amsterdam ; Boston, 2003.

- (55) Opilik, L.; Schmid, T.; Zenobi, R. Modern Raman Imaging: Vibrational Spectroscopy on the Micrometer and Nanometer Scales. *Annu. Rev. Anal. Chem.* **2013**, *6* (1), 379–398. <https://doi.org/10.1146/annurev-anchem-062012-092646>.
- (56) Xu, Y.; Zhong, P.; Jiang, A.; Shen, X.; Li, X.; Xu, Z.; Shen, Y.; Sun, Y.; Lei, H. Raman Spectroscopy Coupled with Chemometrics for Food Authentication: A Review. *TrAC Trends Anal. Chem.* **2020**, *131*, 116017. <https://doi.org/10.1016/j.trac.2020.116017>.
- (57) Muehlethaler, C.; Massonnet, G.; Esseiva, P. The Application of Chemometrics on Infrared and Raman Spectra as a Tool for the Forensic Analysis of Paints. *Forensic Sci. Int.* **2011**, *209* (1–3), 173–182. <https://doi.org/10.1016/j.forsciint.2011.01.025>.
- (58) Riolo, D.; Piazza, A.; Cottini, C.; Serafini, M.; Lutero, E.; Cuoghi, E.; Gasparini, L.; Botturi, D.; Marino, I. G.; Aliatis, I.; Bersani, D.; Lottici, P. P. Raman Spectroscopy as a PAT for Pharmaceutical Blending: Advantages and Disadvantages. *J. Pharm. Biomed. Anal.* **2018**, *149*, 329–334. <https://doi.org/10.1016/j.jpba.2017.11.030>.
- (59) Martin, C.; Bruneel, J.-L.; Guyon, F.; Médina, B.; Jourdes, M.; Teissedre, P.-L.; Guillaume, F. Raman Spectroscopy of White Wines. *Food Chem.* **2015**, *181*, 235–240. <https://doi.org/10.1016/j.foodchem.2015.02.076>.
- (60) Guo, S.; Popp, J.; Bocklitz, T. Chemometric Analysis in Raman Spectroscopy from Experimental Design to Machine Learning–Based Modeling. *Nat. Protoc.* **2021**, *16* (12), 5426–5459. <https://doi.org/10.1038/s41596-021-00620-3>.
- (61) Barbosa, C. D.; Baqueta, M. R.; Rodrigues Santos, W. C.; Gomes, D.; Alvarenga, V. O.; Teixeira, P.; Albano, H.; Rosa, C. A.; Valderrama, P.; Lacerda, I. C. A. Data Fusion of UPLC Data, NIR Spectra and Physicochemical Parameters with Chemometrics as an Alternative to Evaluating Kombucha Fermentation. *LWT* **2020**, *133*, 109875. <https://doi.org/10.1016/j.lwt.2020.109875>.
- (62) Bocklitz, T.; Walter, A.; Hartmann, K.; Rösch, P.; Popp, J. How to Pre-Process Raman Spectra for Reliable and Stable Models? *Anal. Chim. Acta* **2011**, *704* (1–2), 47–56. <https://doi.org/10.1016/j.aca.2011.06.043>.

- (63) Lai, C. W.; Schwab, M.; Hill, S. C.; Santarpià, J.; Pan, Y.-L. Raman Scattering and Red Fluorescence in the Photochemical Transformation of Dry Tryptophan Particles. *Opt. Express* **2016**, *24* (11), 11654. <https://doi.org/10.1364/OE.24.011654>.
- (64) Barton, B.; Thomson, J.; Lozano Diz, E.; Portela, R. Chemometrics for Raman Spectroscopy Harmonization. *Appl. Spectrosc.* **2022**, *76* (9), 1021–1041. <https://doi.org/10.1177/00037028221094070>.
- (65) Brandt, N. N.; Brovko, O. O.; Chikishev, A. Y.; Paraschuk, O. D. Optimization of the Rolling-Circle Filter for Raman Background Subtraction. *Appl. Spectrosc.* **2006**, *60* (3), 288–293. <https://doi.org/10.1366/000370206776342553>.
- (66) Kneen, M. A.; Annegarn, H. J. Algorithm for Fitting XRF, SEM and PIXE X-Ray Spectra Backgrounds. *Nucl. Instrum. Methods Phys. Res. Sect. B Beam Interact. Mater. At.* **1996**, *109–110*, 209–213. [https://doi.org/10.1016/0168-583X\(95\)00908-6](https://doi.org/10.1016/0168-583X(95)00908-6).
- (67) Sternberg. Biomedical Image Processing. *Computer* **1983**, *16* (1), 22–34. <https://doi.org/10.1109/MC.1983.1654163>.
- (68) Engel, J.; Gerretzen, J.; Szymańska, E.; Jansen, J. J.; Downey, G.; Blanchet, L.; Buydens, L. M. C. Breaking with Trends in Pre-Processing? *TrAC Trends Anal. Chem.* **2013**, *50*, 96–106. <https://doi.org/10.1016/j.trac.2013.04.015>.
- (69) Santos Panero, P. D.; Santos Panero, F. D.; Santos Panero, J. D.; Bezerra Da Silva, H. E. Application of Extended Multiplicative Signal Correction to Short-Wavelength near Infrared Spectra of Moisture in Marzipan. *J. Data Anal. Inf. Process.* **2013**, *01* (03), 30–34. <https://doi.org/10.4236/jdaip.2013.13005>.
- (70) Martens, H.; Nielsen, J. P.; Engelsen, S. B. Light Scattering and Light Absorbance Separated by Extended Multiplicative Signal Correction. Application to Near-Infrared Transmission Analysis of Powder Mixtures. *Anal. Chem.* **2003**, *75* (3), 394–404. <https://doi.org/10.1021/ac020194w>.
- (71) Dos Santos, H. T. L.; De Oliveira, A. M.; De Melo, P. G.; Freitas, W.; De Freitas, A. P. R. Chemometrics: Theory and Application. In *Multivariate Analysis in Management, Engineering and the Sciences*; Freitas, L., Ed.; InTech, 2013. <https://doi.org/10.5772/53866>.

- (72) Guo, S.; Rösch, P.; Popp, J.; Bocklitz, T. Modified PCA and PLS: Towards a Better Classification in Raman Spectroscopy–Based Biological Applications. *J. Chemom.* **2020**, *34* (4). <https://doi.org/10.1002/cem.3202>.
- (73) USP. ⟨1039⟩ *Chemometrics*. In: USP - NF. Rockville, MD.: USP; May 1, 2020. https://doi.org/10.31003/USPNF_M2345_02_01.
- (74) Lever, J.; Krzywinski, M.; Altman, N. Principal Component Analysis. *Nat. Methods* **2017**, *14* (7), 641–642. <https://doi.org/10.1038/nmeth.4346>.
- (75) Miller, J. N.; Miller, J. C. *Statistics and Chemometrics for Analytical Chemistry*, 5th ed.; Pearson/Prentice Hall: Harlow, England ; New York, 2005.
- (76) Bro, R.; Smilde, A. K. Principal Component Analysis. *Anal Methods* **2014**, *6* (9), 2812–2831. <https://doi.org/10.1039/C3AY41907J>.
- (77) Kvalheim, O. M. History, Philosophy and Mathematical Basis of the Latent Variable Approach – from a Peculiarity in Psychology to a General Method for Analysis of Multivariate Data. *J. Chemom.* **2012**, *26* (6), 210–217. <https://doi.org/10.1002/cem.2427>.
- (78) Borman, P.; Elder, D. Q2(R1) Validation of Analytical Procedures: Text and Methodology. In *ICH Quality Guidelines*; Teasdale, A., Elder, D., Nims, R. W., Eds.; Wiley, 2017; pp 127–166. <https://doi.org/10.1002/9781118971147.ch5>.
- (79) Pokhrel, P.; Shrestha, S.; Rijal, S. K.; Rai, K. P. A Simple HPLC Method for the Determination of Caffeine Content in Tea and Coffee. *J. Food Sci. Technol. Nepal* **2016**, *9*, 74–78. <https://doi.org/10.3126/jfstn.v9i0.16200>.
- (80) USP. ⟨621⟩ *Chromatography*. In: USP - NF. Rockville, MD.: USP; April 1, 2023. https://doi.org/10.31003/USPNF_M99380_07_01.
- (81) Rodríguez, L. C.; Campaña, A. M. G.; Barrero, F. A.; Linares, C. J.; Ceba, M. R. Validation of an Analytical Instrumental Method by Standard Addition Methodology. *J. AOAC Int.* **1995**, *78* (2), 471–476. <https://doi.org/10.1093/jaoac/78.2.471>.
- (82) Essawet, N.; Cvetkovic, D.; Velicanski, A.; Canadanovic-Brunet, J.; Vulic, J.; Maksimovic, V.; Markov, S. Polyphenols and Antioxidant Activities of Kombucha Beverage Enriched with Coffeeberry® Extract. *Chem. Ind. Chem. Eng. Q.* **2015**, *21* (3), 399–409. <https://doi.org/10.2298/CICEQ140528042E>.

- (83) Malbaša, R. V.; Lončar, E. S.; Vitas, J. S.; Čanadanović-Brunet, J. M. Influence of Starter Cultures on the Antioxidant Activity of Kombucha Beverage. *Food Chem.* **2011**, *127* (4), 1727–1731. <https://doi.org/10.1016/j.foodchem.2011.02.048>.
- (84) Lončar, E.; Djurić, M.; Malbaša, R.; Kolarov, L. J.; Klašnja, M. Influence of Working Conditions Upon Kombucha Conducted Fermentation of Black Tea. *Food Bioprod. Process.* **2006**, *84* (3), 186–192. <https://doi.org/10.1205/fbp.04306>.
- (85) La Torre, C.; Fazio, A.; Caputo, P.; Plastina, P.; Caroleo, M. C.; Cannataro, R.; Cione, E. Effects of Long-Term Storage on Radical Scavenging Properties and Phenolic Content of Kombucha from Black Tea. *Molecules* **2021**, *26* (18), 5474. <https://doi.org/10.3390/molecules26185474>.
- (86) Jayabalan, R.; Marimuthu, S.; Thangaraj, P.; Sathishkumar, M.; Binupriya, A. R.; Swaminathan, K.; Yun, S. E. Preservation of Kombucha Tea—Effect of Temperature on Tea Components and Free Radical Scavenging Properties. *J. Agric. Food Chem.* **2008**, *56* (19), 9064–9071. <https://doi.org/10.1021/jf8020893>.

7 Appendix

7.1 Brewing

Table 12: Actual Values for Brewing kombucha in the Experimental Design

Experiment	Temp H ₂ O (°C)	Volume Water (mL)	Weight sugar (g)	Weight tea (g)	Steeping time (mins)	Volume of beaker (mL)	Starter Vol. (mL)
Exp 1	60	275	66.35	5.53	5	921.47	275
Exp 2	60	1655	227.21	4.73	15	3155.73	235
Exp 3	95	1655	113.61	18.93	5	3155.73	235
Exp 4	95	275	33.17	1.38	15	921.47	275
Exp 5	60	1260	151.48	6.31	5	3155.73	1260
Exp 6	60	645	44.23	7.36	15	921.47	90
Exp 7	95	645	88.46	1.84	5	921.47	90
Exp 8-1	95	1260	302.95	25.24	15	3155.73	1260
Exp 8-2	95	1260	302.95	25.24	15	3155.73	1260
Exp 8-3	95	1260	302.95	25.24	15	3155.73	1260
FO-Obj 9	95	2210	151.55	6.31	15	3155.73	315
FO-Obj 10	95	370	44.19	7.38	5	921.47	370
FO-Obj 11	60	370	88.48	1.85	15	921.47	370
FO-Obj 12	60	2210	302.98	25.23	5	3155.73	315
FO-Obj 13	95	485	66.4	5.55	15	921.47	70
FO-Obj 14	95	945	227.38	4.72	5	3155.73	945
FO-Obj 15	60	945	113.6	18.95	15	3155.73	945
FO-Obj 16-1	60	485	33.16	1.4	5	921.47	70
FO-Obj 16-2	60	485	33.16	1.39	5	921.47	70
FO-Obj 16-3	60	485	33.16	1.38	5	921.47	70

7.2 Color and Appearance

Table 13: Organoleptic properties of different kombucha set-ups (Sets 1-3) and time points

	Before starter	Day 1	Day 7	Day 10	Day 14
Set 1					
Exp 1	Yellow, slightly turbid	Orange yellow, slightly turbid	Yellow, slightly turbid	Brownish yellow, clear	Brownish yellow, clear
Exp 2	Yellow orange, clear	Yellow orange, clear	Yellow, clear	Orange yellow, slightly turbid	Yellow, clear
Exp 3	Reddish brown, turbid	Orange yellow, turbid	Yellow orange, clear	Orange brownish, turbid	Yellow brown, slightly turbid
Exp 4	Orange brown, Slightly turbid	Yellow orange, slightly turbid	Orange yellow, slightly turbid	Brownish yellow, clear	Yellow brown, slightly turbid
Exp 5	Yellowish brown, turbid	Brown yellow, turbid	Yellowish brown, turbid	Yellow brown, turbid	Orange yellow, slightly turbid
Exp 6	Golden yellow, clear	Orange yellow, clear	Yellow, clear	Yellow, clear	Yellow, slightly turbid
Exp 7	Orange yellow, turbid	Brown, turbid	Yellow brown, slightly turbid	Brown yellow, turbid	Yellow orange, slightly turbid
Exp 8-T1	Red brown, slightly turbid	Brown orange, turbid	Yellow orange, turbid	Orange yellow, Slightly turbid	Yellow orange, slightly turbid
Exp 8-T2	Red brown, slightly turbid	Red orange, turbid	Yellow brown, turbid	Red orange, slightly turbid	Brownish yellow, slightly turbid
Exp 8-T2	Red brown, slightly turbid	Red orange, turbid	Orange yellow, turbid	Orange yellow, slightly turbid	Yellow orange, slightly turbid
Set 2					
Exp 1	Yellow, slightly turbid	Orange Yellow, turbid	Yellow orange, clear	Brownish yellow, slightly turbid	Orange yellow, slightly turbid
Exp 2	Orange yellow, slightly turbid	Yellow, slightly turbid	Yellow turbid	Orange yellow, turbid	Orange yellow, turbid
Exp 3	Red orange, turbid	Orange turbid	Orange turbid	Orange turbid	Orange, slightly turbid
Exp 4	Orange, slightly turbid	Brownish yellow, slightly turbid	Yellow orange, clear	Yellow orange, turbid	Orange yellow, slightly turbid

Exp 5	Yellow, clear	Orange turbid	yellow,	Yellow turbid	orange,	Yellow turbid	orange	Yellow turbid	orange,	
Exp 6	Orange, turbid	Gold turbid	yellow,	Gold turbid	yellow,	Golden slightly turbid	yellow	Yellow, turbid	slightly	
Exp 7	Yellow orange, slightly turbid	Yellow, turbid		Yellow turbid	orange,	Orange slightly turbid	yellow,	Yellow, turbid	slightly	
Exp 8-T1	Brown, turbid	Yellow turbid	brown,	Orange turbid	brown	Orange turbid	brown,	Brownish turbid	orange,	
Exp 8-T2	Brown, turbid	Red turbid	orange,	Orange turbid	brown	Orange turbid	brown,	Brownish turbid	orange,	
Exp 8-T2	Brown, turbid	Red turbid	orange,	Orange turbid	brown	Orange turbid	brown,	Brownish turbid	orange,	
Set 3										
FO-Obj 9	Red brown, turbid	Orange slightly turbid	brown,	Orange clear	brown,	Orange clear	brown,	Orange clear	brown,	
FO-Obj 10	Orange turbid	Orange turbid	brown,	Orange turbid	brown,	Orange slightly turbid	brown,	Orange slightly turbid	brown,	
FO-Obj 11	Yellow slightly turbid	Yellow turbid	orange,	Yellow clear	orange,	Yellow clear	orange,	Yellow clear	orange,	
FO-Obj 12	Orange slightly turbid	Orange, turbid		Yellow turbid	orange,	Yellow turbid	orange	Yellow slightly turbid	orange,	
FO-Obj 13	Red brown, clear	Red brown, turbid	orange	Brown, clear		Orange slightly turbid	brown, turbid,	Orange clear	brown,	
thin film										
FO-Obj 14	Orange clear	Orange turbid	brown,	Orange clear	brown,	Orange turbid	brown,	Orange turbid	Orange turbid	
FO-Obj 15	Orange turbid	Orange turbid	brown	Orange turbid	brown,	Orange slightly turbid	brown,	Orange turbid	brownish,	
FO-Obj 16-T1	Yellow, clear	Yellow turbid		Yellow clear, thin film		Yellow clear, thin film		Yellow clear,		
FO-Obj 16-T2	Yellow, clear	Yellow turbid		Yellow clear, thin film		Yellow clear, thin film		Yellow clear,		
FO-Obj 16-T3	Yellow, clear	Yellow turbid		Yellow clear, thin film		Yellow clear, thin film		Yellow clear,		

7.3 Pictures of kombucha



Figure 38: Set 1 Day 7: Experiments 1 ,4, 7 and 6



Figure 39: SCOBY to be laid on one of the Kombucha set-ups

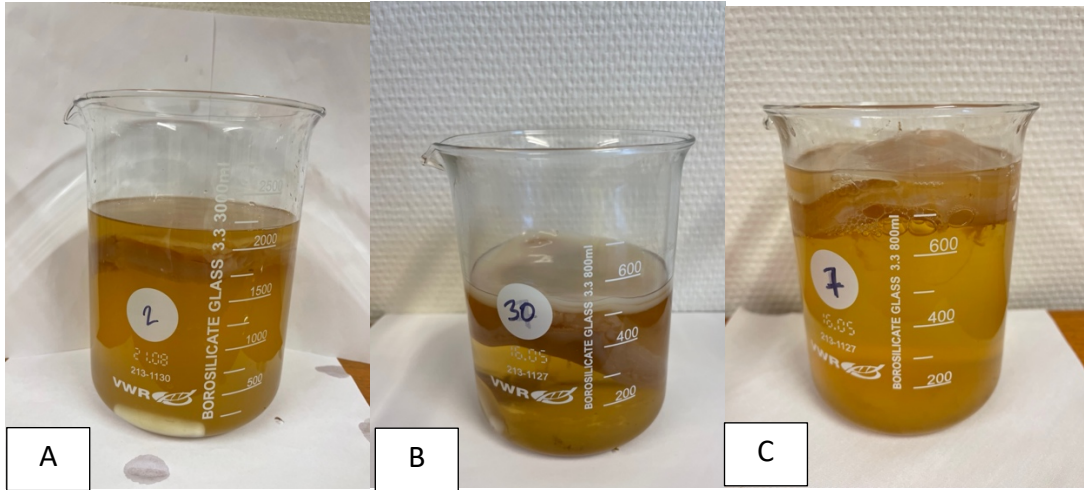


Figure 40: Random kombucha experiments: A) Set 2, Day 1, Experiment 2 B) Set 3, Day 10, Experiment 10 C) Set 2, Day 7, Experiment 7



Figure 41: Set 2, Day 10, Experiments 1 to 10 (Exp 8-3) in sample bottles

7.4 pH

Table 14: Obtained pH results for Sets 1, 2 and 3 over 1st, 7th, 10th and 14th day

Set	Exp	Day 1	SD	Day 7	SD	Day 10	SD	Day 14	SD	
1*	Starter	2.78								
	Exp 1	3.26		2.99		2.87		2.77		
	Exp 2	3.58		3.14		2.88		2.78		
	Exp 3	3.77		3.22		3.09		3.06		
	Exp 4	3.00		2.84		2.71		2.67		
	Exp 5	3.22		3.07		2.98		2.97		
	Exp 6	3.58		3.12		2.98		2.93		
	Exp 7	3.79		3.25		3.11		3.05		
	Exp 8-T1	3.07		2.99		2.88		2.76		
	Exp 8-T2	3.04		2.98		2.92		2.81		
	Exp 8-T3	3.02		2.92		2.88		2.82		
	2	Starter	2.75	0.00						
		Exp 1	3.03	0.00	2.83	0.01	2.79	0.01	2.59	0.01
Exp 2		3.34	0.02	3.07	0.02	2.94	0.02	2.76	0.00	
Exp 3		3.61	0.01	3.24	0.02	3.27	0.01	3.11	0.00	
Exp 4		2.95	0.00	2.78	0.01	2.74	0.01	2.55	0.01	
Exp 5		2.89	0.00	2.84	0.03	2.86	0.01	2.70	0.00	
Exp 6		3.59	0.01	3.27	0.01	3.27	0.00	3.07	0.00	
Exp 7		3.38	0.00	3.07	0.01	2.97	0.00	2.73	0.00	
Exp 8-T1		3.15	0.02	2.95	0.01	2.96	0.02	2.84	0.00	
Exp 8-T2		3.13	0.00	2.98	0.02	2.99	0.01	2.85	0.00	
Exp 8-T3		3.07	0.02	2.99	0.06	3.01	0.02	2.86	0.00	
3	Starter	2.52	0.01							
	FO-Obj 9	3.03	0.01	2.83	0.01	2.75	0.01	2.67	0.01	
	FO-Obj 10	2.77	0.01	2.70	0.01	2.64	0.01	2.62	0.01	
	FO-Obj 11	2.68	0.01	2.62	0.01	2.53	0.00	2.49	0.00	
	FO-Obj 12	3.12	0.00	2.95	0.01	2.82	0.01	2.78	0.01	
	FO-Obj 13	3.14	0.01	2.86	0.01	2.71	0.01	2.61	0.01	
	FO-Obj 14	2.67	0.01	2.63	0.01	2.56	0.01	2.54	0.01	
	FO-Obj 15	2.79	0.01	2.75	0.01	2.66	0.01	2.63	0.01	
	FO-Obj 16-T1	2.96	0.00	2.75	0.01	2.63	0.01	2.56	0.02	
	FO-Obj 16-T2	2.94	0.02	2.70	0.00	2.57	0.01	2.49	0.01	
	FO-Obj 16-T3	2.94	0.01	2.71	0.01	2.58	0.01	2.52	0.02	
BKB sample	3.22	0.00								

*Set 1 only has one trial

7.5 Method validation

7.5.1 Linearity and range

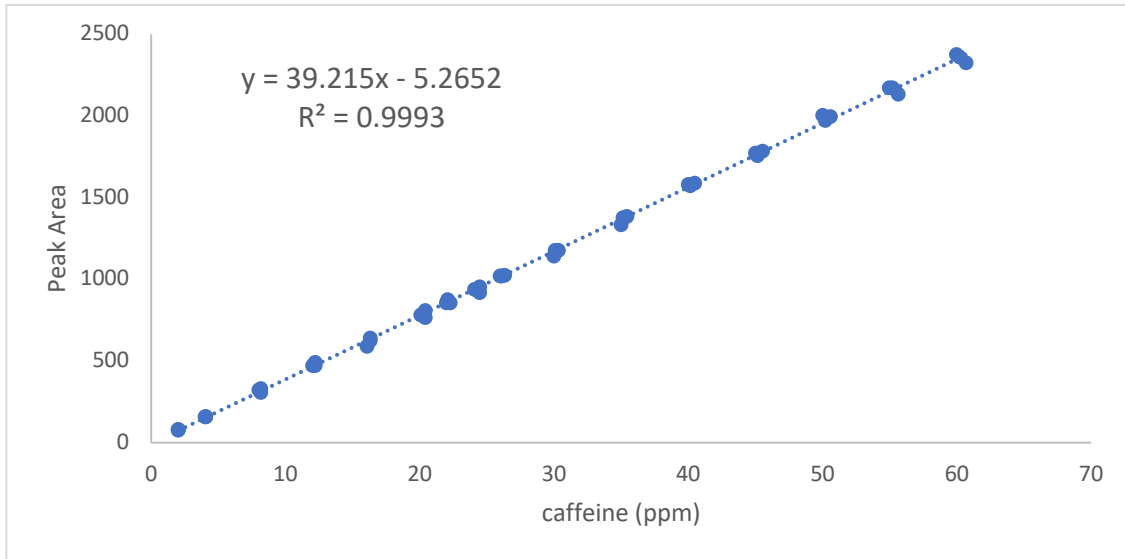


Figure 42: Calibration curve peak area vs caffeine concentration (ppm)

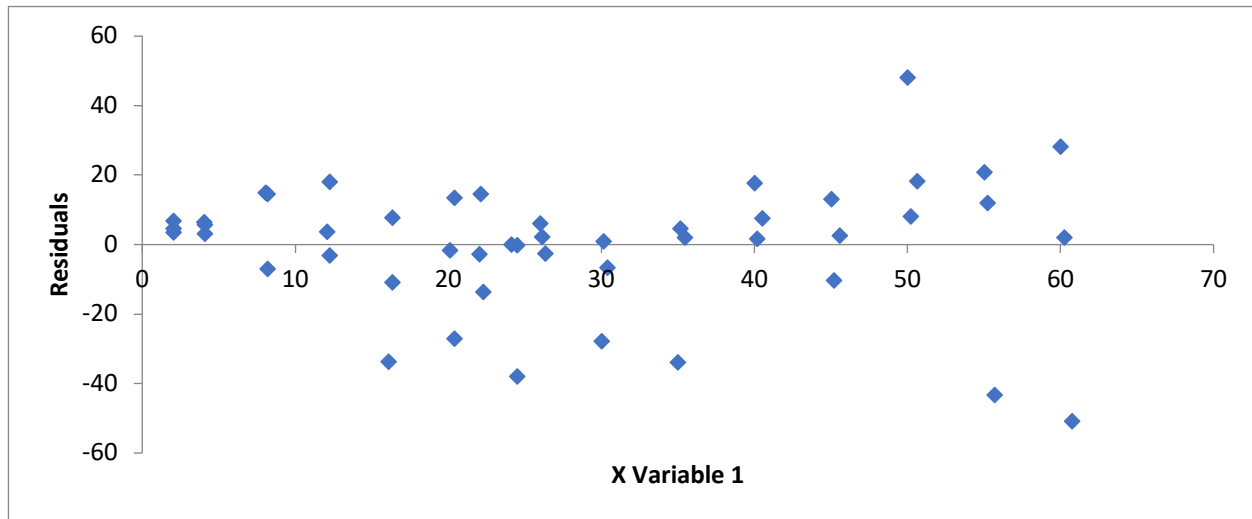


Figure 43: Residual plot of calibration curve from Figure 42

7.5.2 Precision

Table 15: Raw data for precision study of caffeine content

Standard Solution concentration	Peak area
28 ppm	1105.2512
28 ppm	1105.3089
28 ppm	1106.1656
28 ppm	1106.3928
28 ppm	1104.9109
28 ppm	1105.851
CV	0.42%

7.5.3 Accuracy

Table 16: Data for accuracy studies of kombucha for caffeine content

Average spiked (c_{det})	Average theoretical concentration (C_{theor})	Average %recovery	t_{stat}	t_{crit}
5.07	5.35	105.4	-0.91	2.77
10.15	9.78	96.4	-0.83	
15.22	14.80	97.2	-1.89	

7.6 Caffeine Content

Table 17: Obtained caffeine content (ppm) results for Sets 1, 2 and 3 over 1st, 7th, 10th and 14th day

Set	Exp	Day 1	SD	Day 7	SD	Day 10	SD	Day 14	SD
1*	Starter	119.33	1.00						
	Exp 1	327.91	11.31	312.10	3.38	314.20	2.04	311.17	2.87
	Exp 2	84.86	1.33	85.58	1.77	83.62	2.61	85.15	1.34
	Exp 3	530.70	6.20	446.23	1.88	450.91	12.65	439.83	4.07
	Exp 4	159.87	1.56	139.19	4.91	132.20	1.07	126.15	1.82
	Exp 5	341.80	3.21	314.04	8.41	304.89	4.63	317.16	3.86
	Exp 6	88.72	2.14	94.38	3.27	93.23	1.61	93.10	0.23
	Exp 7	533.77	6.24	477.10	15.90	444.52	6.25	445.40	6.91
	Exp 8-T1	170.99	1.26	164.30	2.85	163.49	1.24	161.18	2.19
	Exp 8-T2	171.60	1.02	164.33	2.63	162.51	1.57	163.34	2.05
	Exp 8-T2	173.42	3.78	158.79	3.21	164.83	1.23	161.97	2.27
2	Starter	191.88	4.15						
	Exp 1	310.16	2.44	283.30	1.01	284.72	0.85	275.38	3.11
	Exp 2	114.24	2.32	118.60	0.41	124.55	0.99	127.86	1.44
	Exp 3	518.30	1.83	511.51	5.22	497.65	4.00	508.13	8.20
	Exp 4	229.60	3.68	226.00	2.69	224.10	0.51	224.71	3.59
	Exp 5	165.29	5.08	161.95	0.25	158.71	0.94	159.34	1.10
	Exp 6	453.56	3.06	434.31	6.42	448.60	4.71	445.64	4.55
	Exp 7	162.79	3.67	165.14	2.03	165.02	1.43	167.40	2.26
	Exp 8-T1	608.94	8.52	568.75	0.98	561.52	2.04	555.63	6.11
	Exp 8-T2	618.08	5.93	584.70	16.08	572.31	13.77	576.10	2.20
	Exp 8-T2	609.67	7.80	593.54	5.73	589.56	8.88	603.86	10.57
3	Starter	344.90	8.11						
	FO-Obj 9	186.17	0.81	203.87	1.88	198.86	2.42	189.03	1.20
	FO-Obj 10	713.56	8.08	662.94	10.71	674.54	8.44	676.12	17.65
	FO-Obj 11	299.43	2.11	304.60	0.97	305.93	5.36	307.56	2.35
	FO-Obj 12	320.01	2.17	316.64	1.67	308.45	2.56	301.73	2.74
	FO-Obj 13	717.91	4.78	682.85	1.39	696.03	12.98	690.04	10.19
	FO-Obj 14	348.20	4.91	309.18	10.72	306.02	3.31	305.60	4.04
	FO-Obj 15	578.05	3.50	555.65	1.68	558.95	7.65	550.24	3.90
	FO-Obj 16-T1	114.70	0.38	143.61	1.03	137.66	0.56	134.59	4.93
	FO-Obj 16-T2	133.73	2.01	179.43	1.95	172.91	0.46	161.46	0.84
	FO-Obj 16-T3	121.01	0.64	158.24	1.98	149.37	2.27	144.88	2.65
	BKB sample	133.62	2.36						

7.7 Experimental Design pH

7.7.1 pH day 1

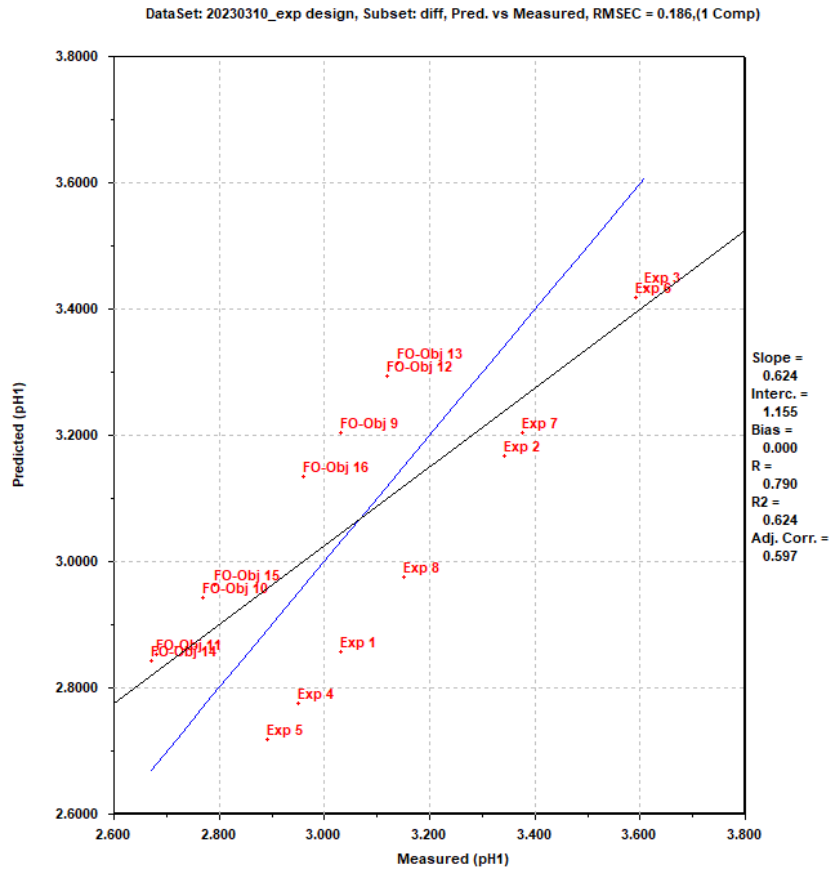


Figure 44: Predicted versus measured pH day 1 all screening variables

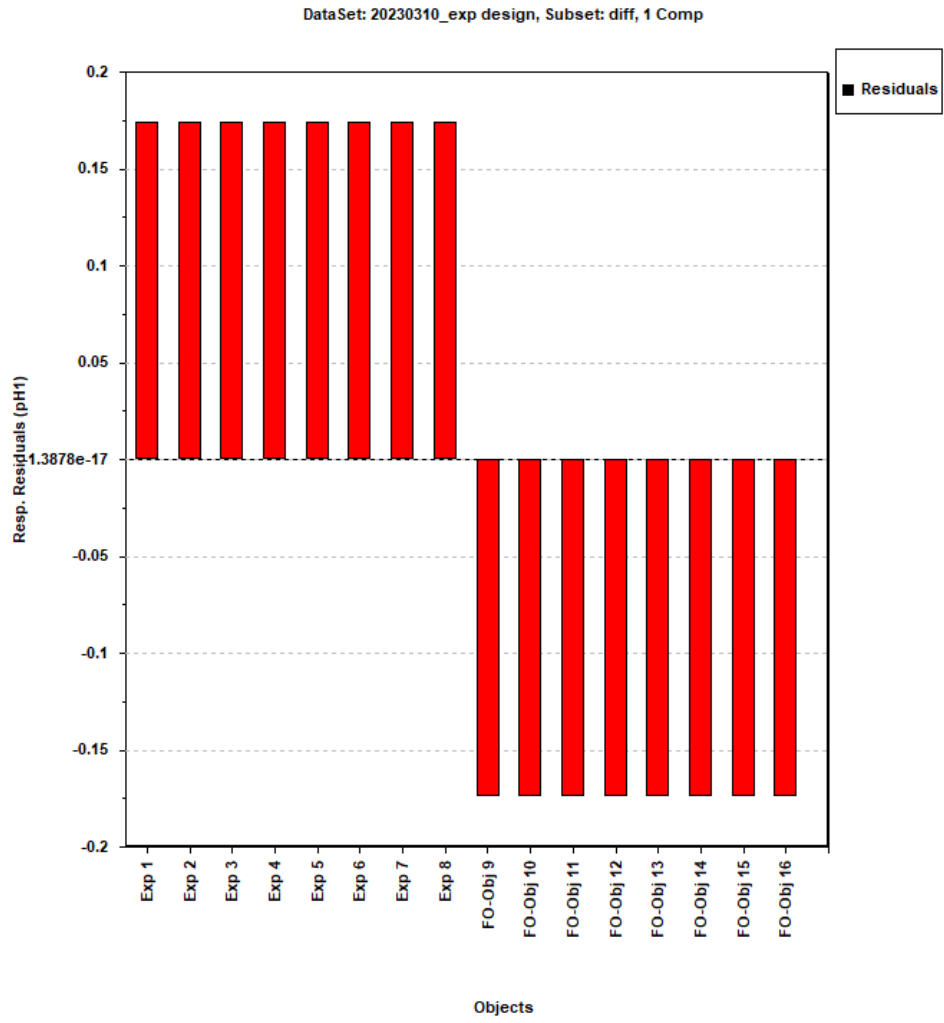


Figure 45: Response residuals of pH day 1- all screening variables

7.7.2 pH day 7

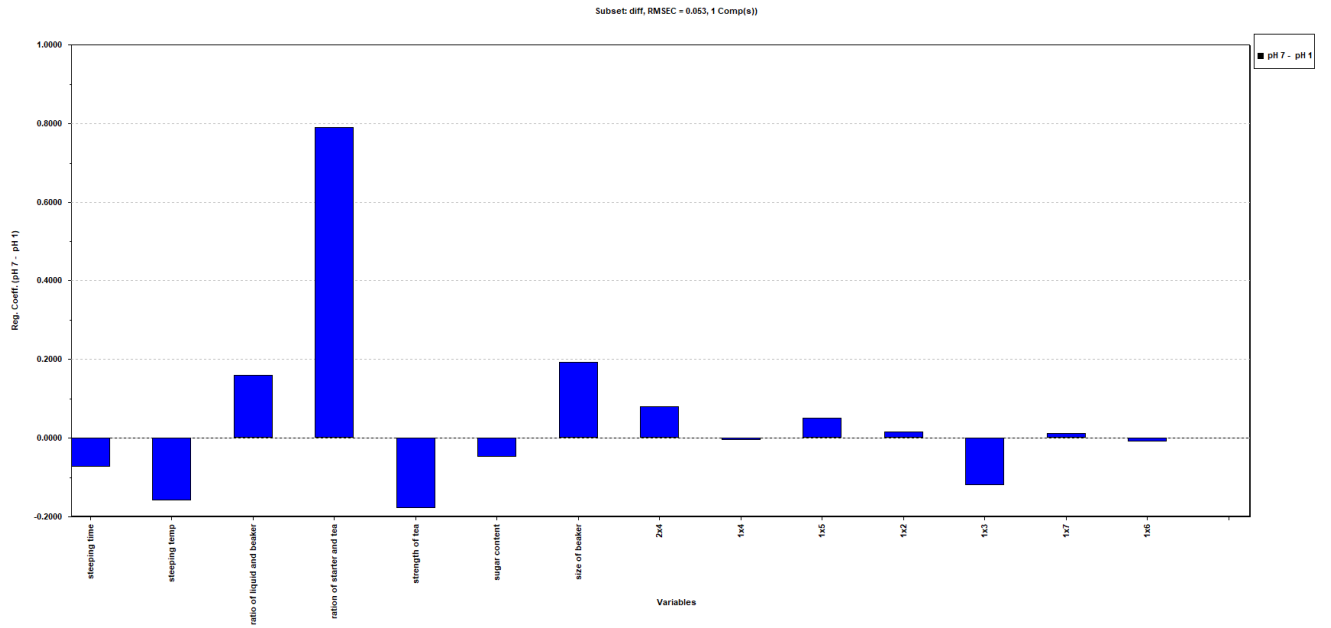


Figure 46: Screening variables for pH difference Day 7 and Day 1 (77.51%)

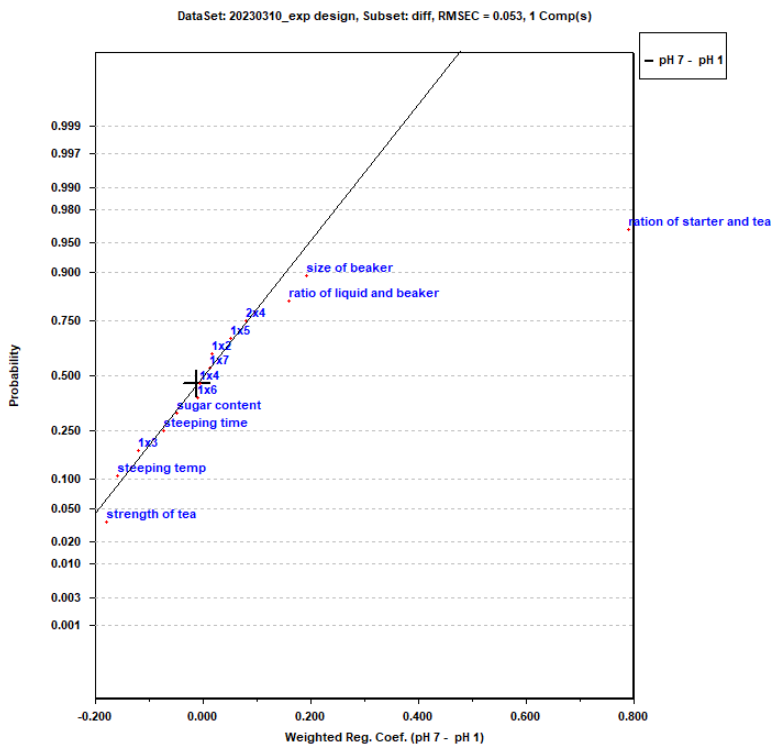


Figure 47: Normal probability plot of screening variables for pH day 7-day 1

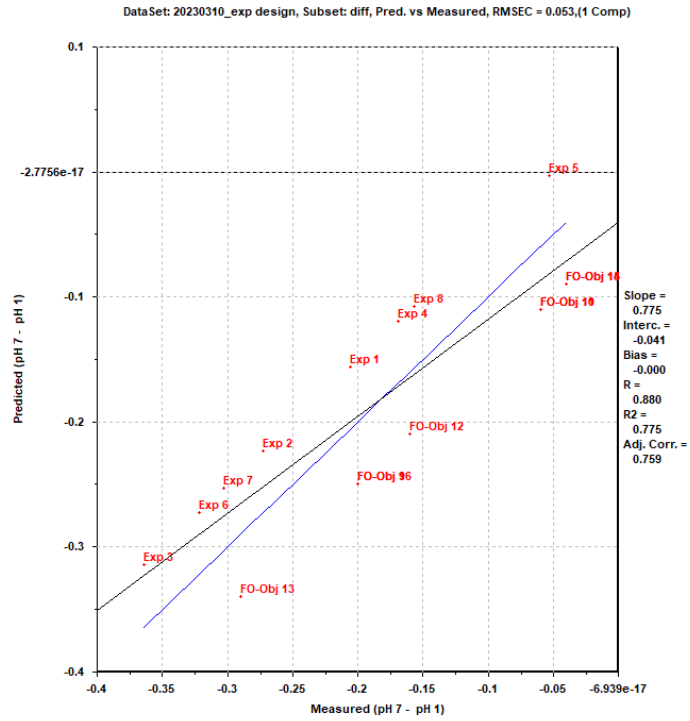


Figure 48: Predicted vs Measured for pH day 7- pH day 1- all significant variables

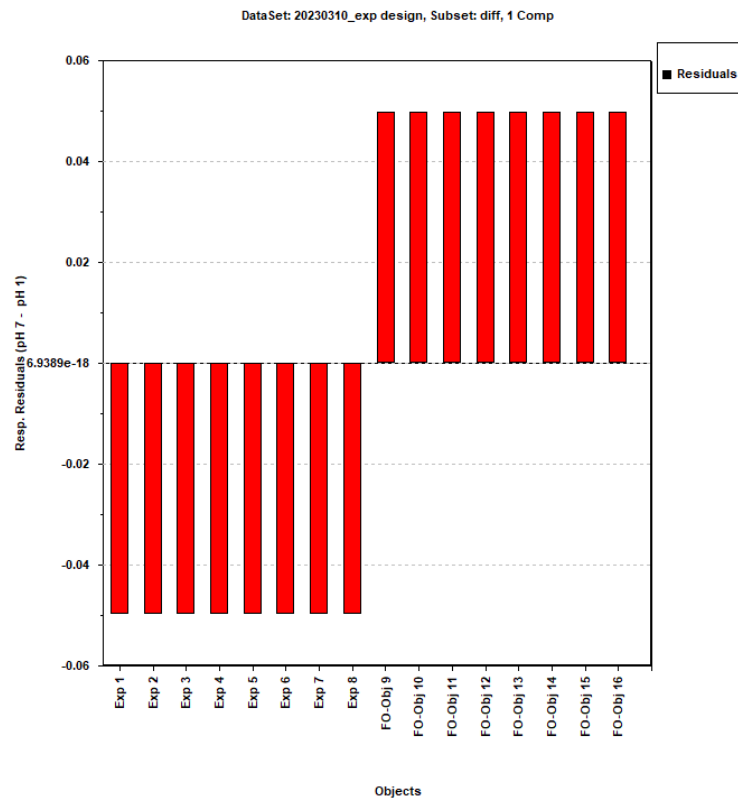


Figure 49: Response residuals pH day 7- pH day 1-all significant variables

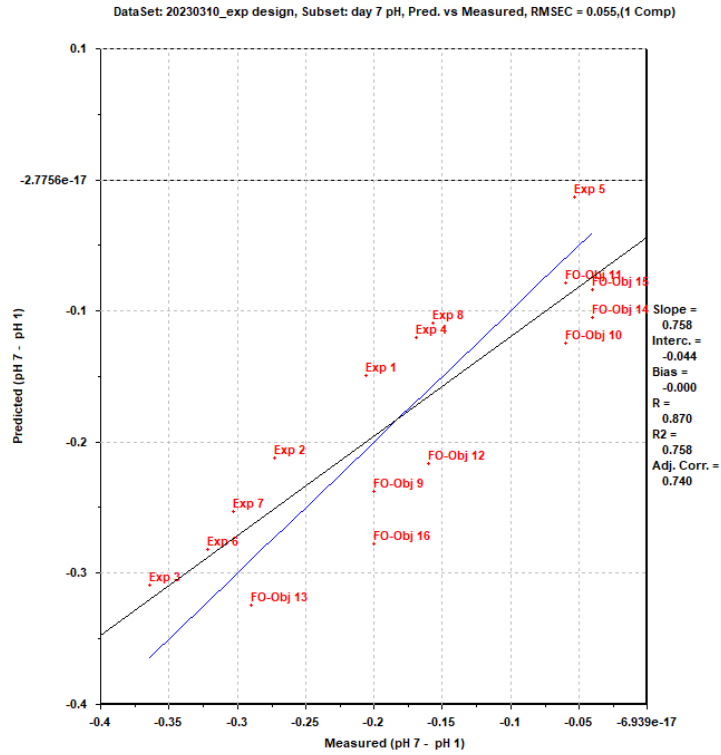


Figure 50: Predicted versus Measured pH day 7- pH day 1, 6 significant variables

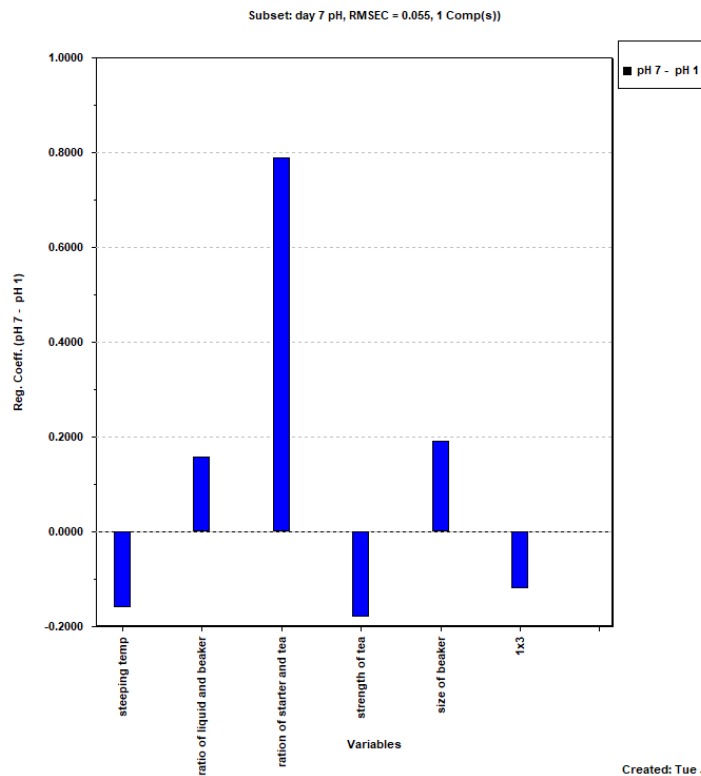


Figure 51: 6 Significant variables under pH day 7 - pH day 1 (75.76%)

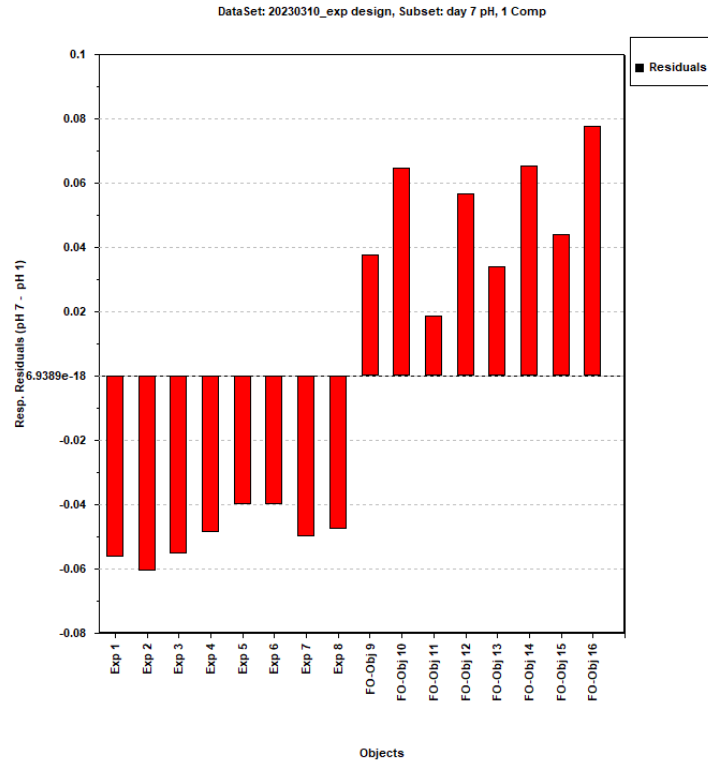


Figure 52: Response Residuals Day 7, 6 significant variables

7.7.3 pH day 10

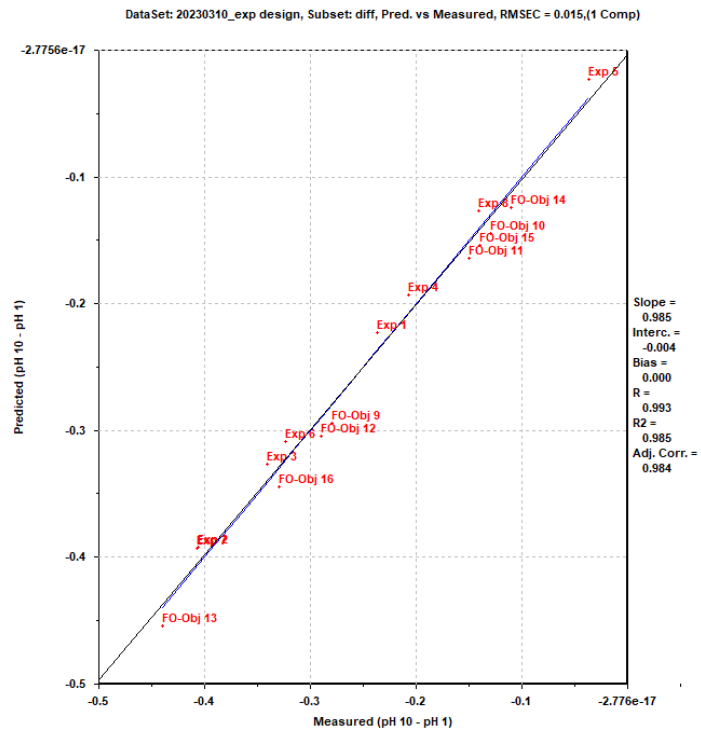


Figure 53: Predicted vs Measured pH day 10-all significant variables

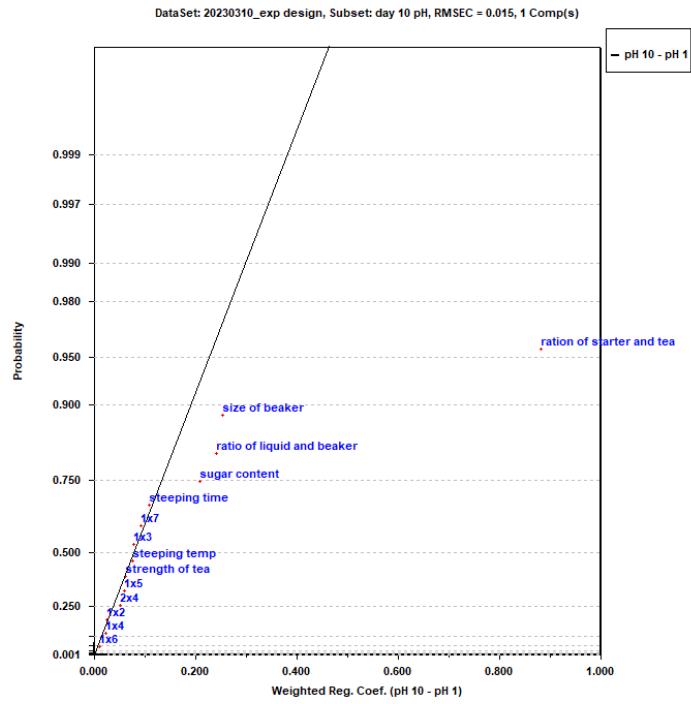


Figure 54: Half normal probability for screening significant variables Day 10

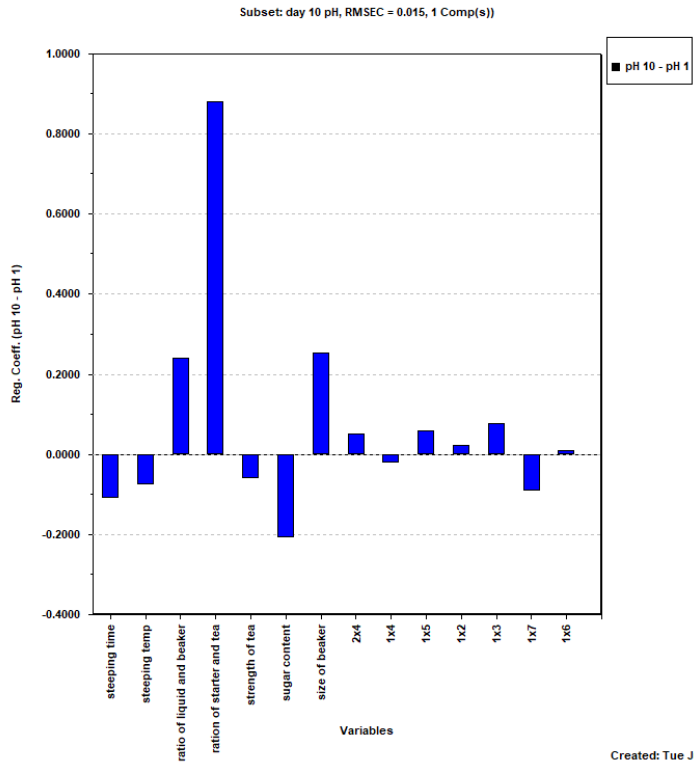


Figure 55: Screening variables for pH of Day 10 (98.53%)

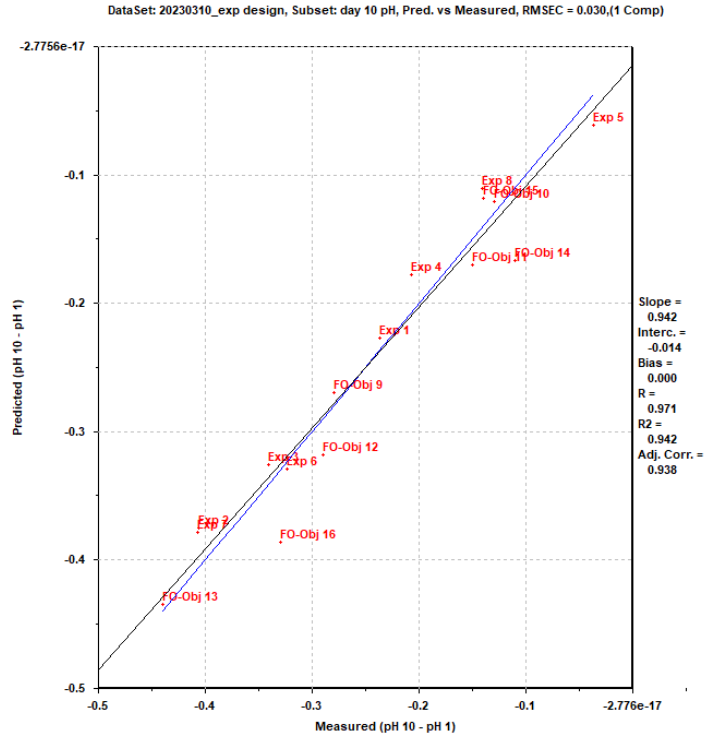


Figure 56: Predicted vs Measured Day 10 - 4 significant variables

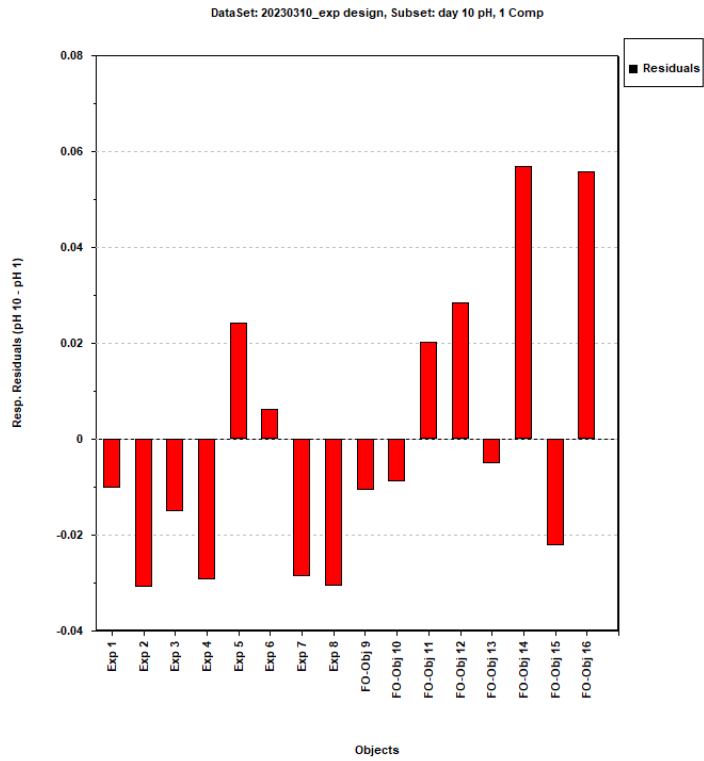


Figure 57: Response residuals pH Day 10-4 significant variables

7.7.4 pH day 14

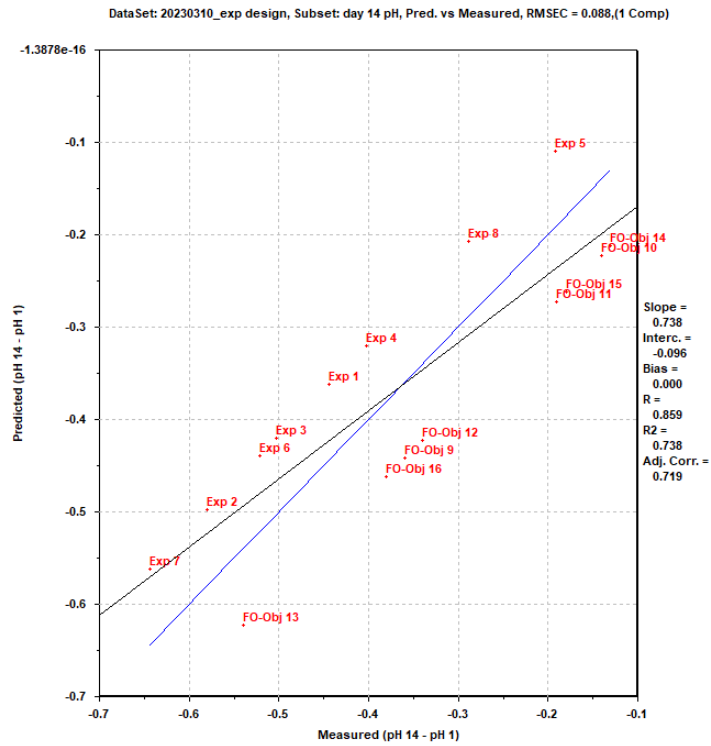


Figure 58: Predicted vs Measured pH day 14-all significant variables

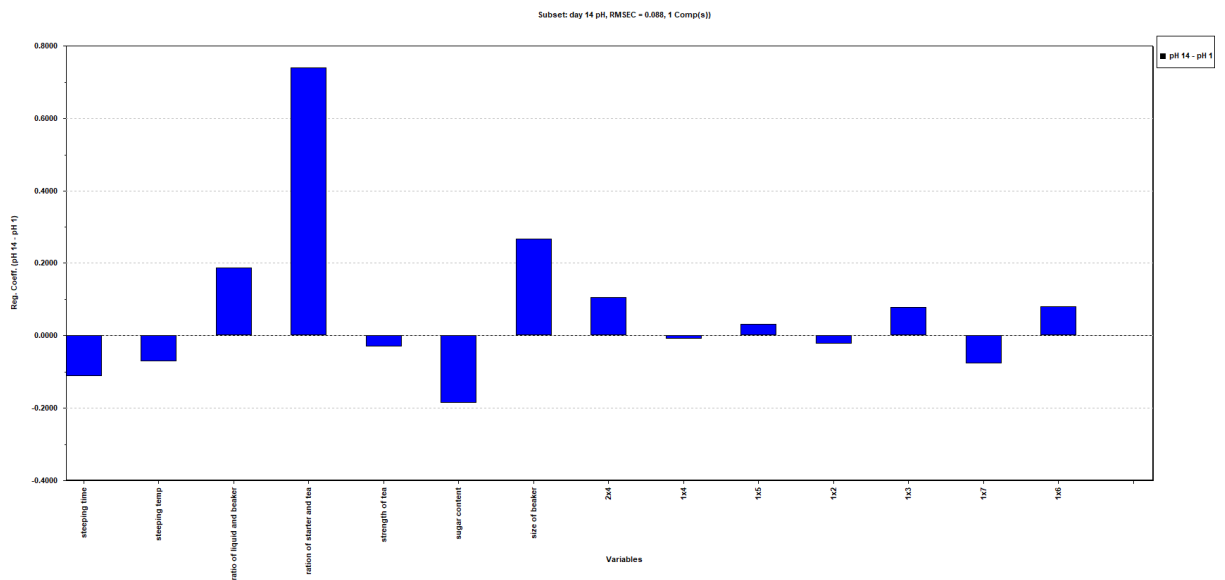


Figure 59: Screening variables for pH of Day 14 (73.79%)-all significant variables

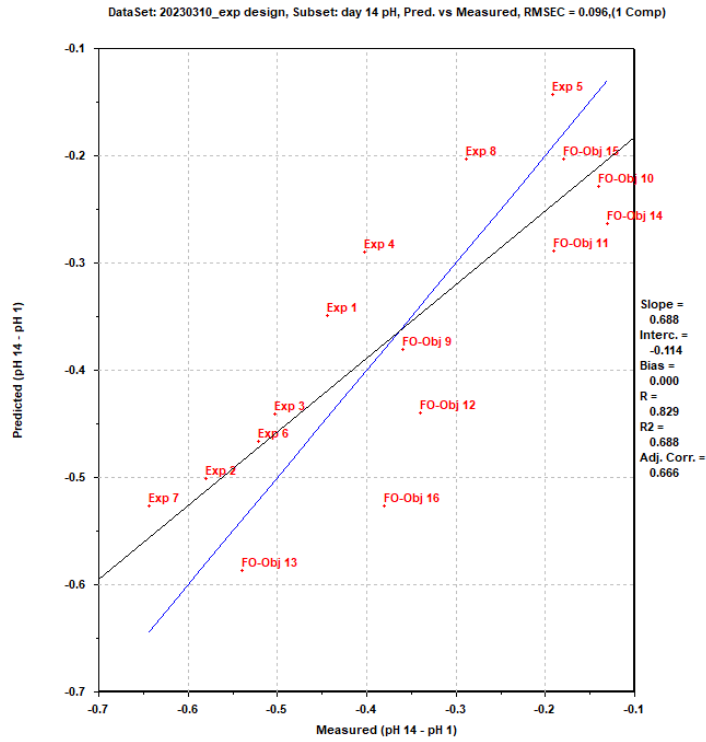


Figure 60: Predicted vs. Measured for pH Day 14-4 significant variables

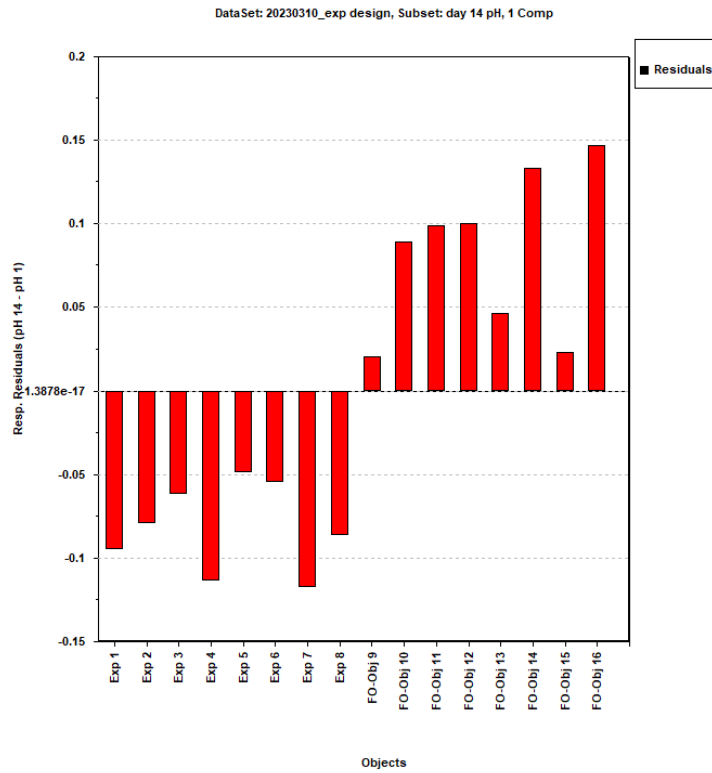


Figure 61: Response residuals for pH Day 14 - 4 significant variables

7.8 Experimental Design Caffeine

7.8.1 Caffeine day 1

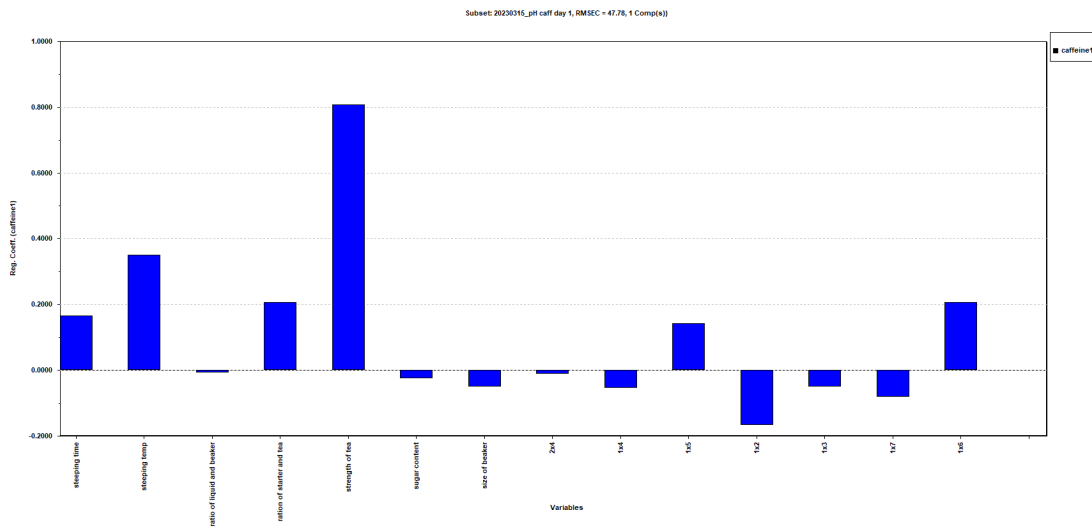


Figure 62: Screening variables for Caffeine content day 1

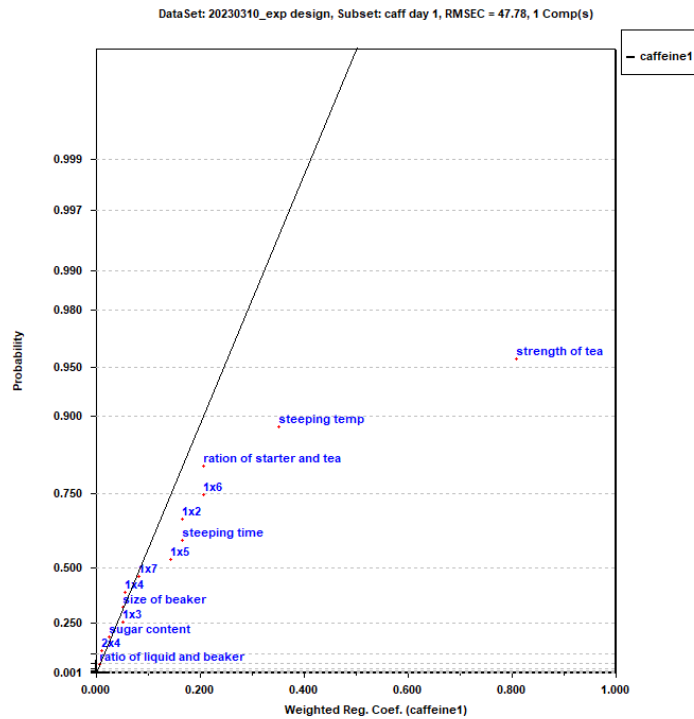


Figure 63: Half normal probability plot of Caffeine Day 1

DataSet: 20230310_exp design, Subset: 20230315_pH caff day 1, Pred. vs Measured, RMSEC = 47.78,(1 Comp)

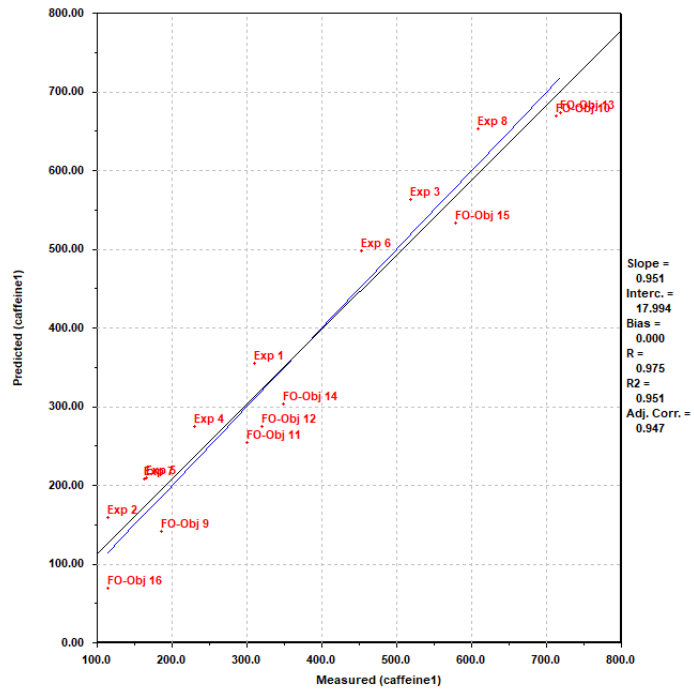


Figure 64: Predicted versus Measured for Caffeine day 1

7.8.2 Caffeine day 7

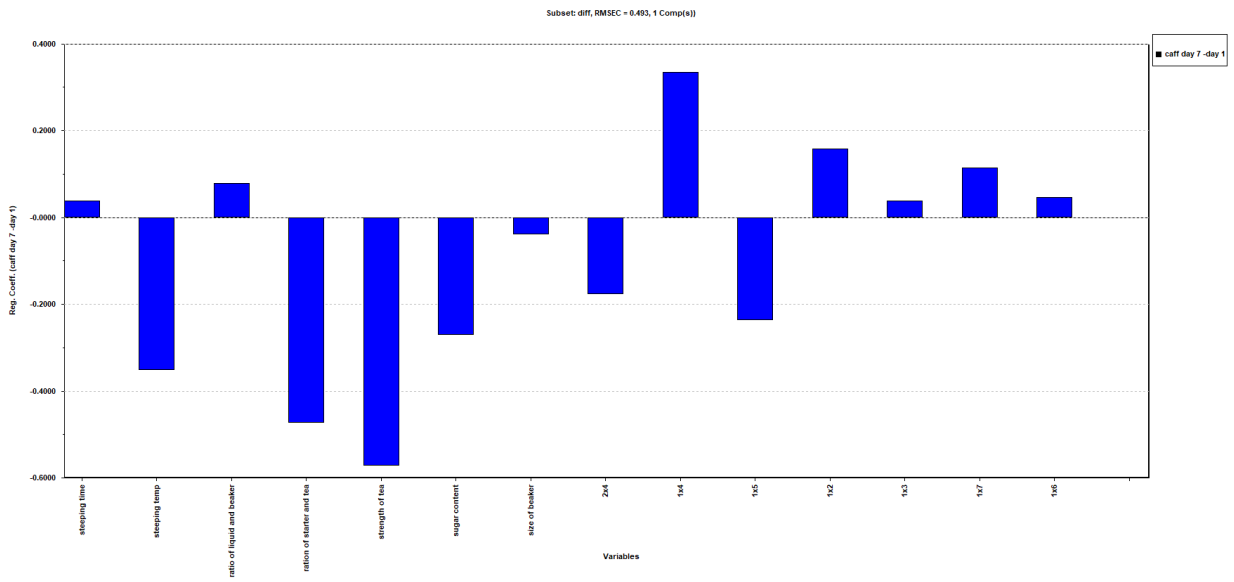


Figure 65: Screening variables for significant variables for caffeine day 7- caffeine day 1

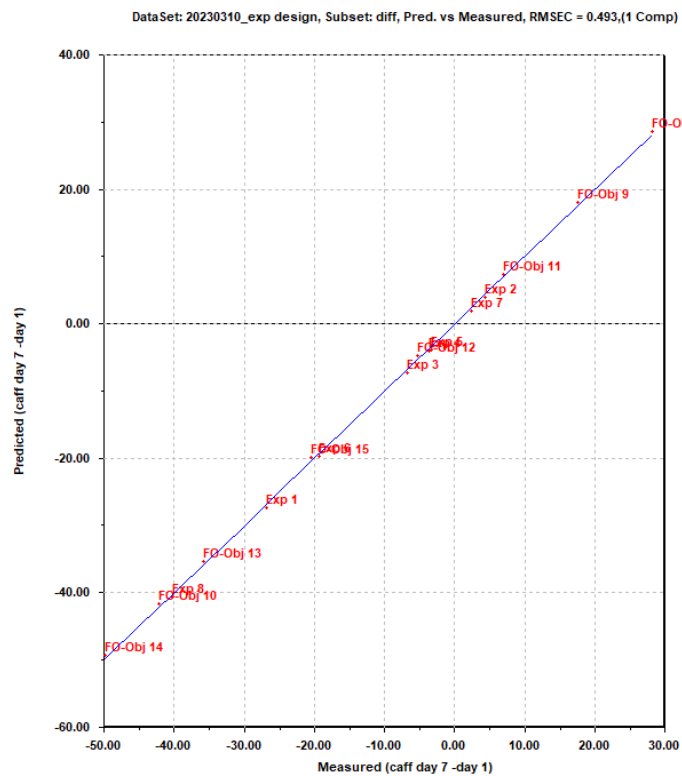


Figure 66: Predicted vs measured caffeine day 7- caffeine day 1

7.8.3 Caffeine day 10

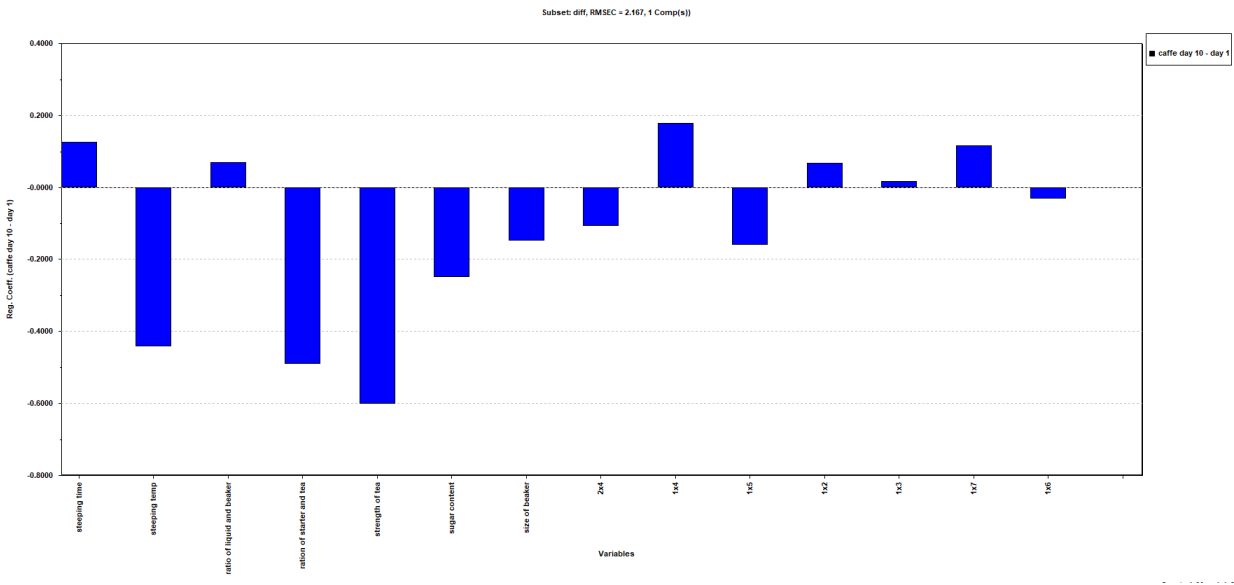


Figure 67: Screening variables caff day 10 - caff day 1 (explains: 99.08%)

7.8.4 Caffeine day 14

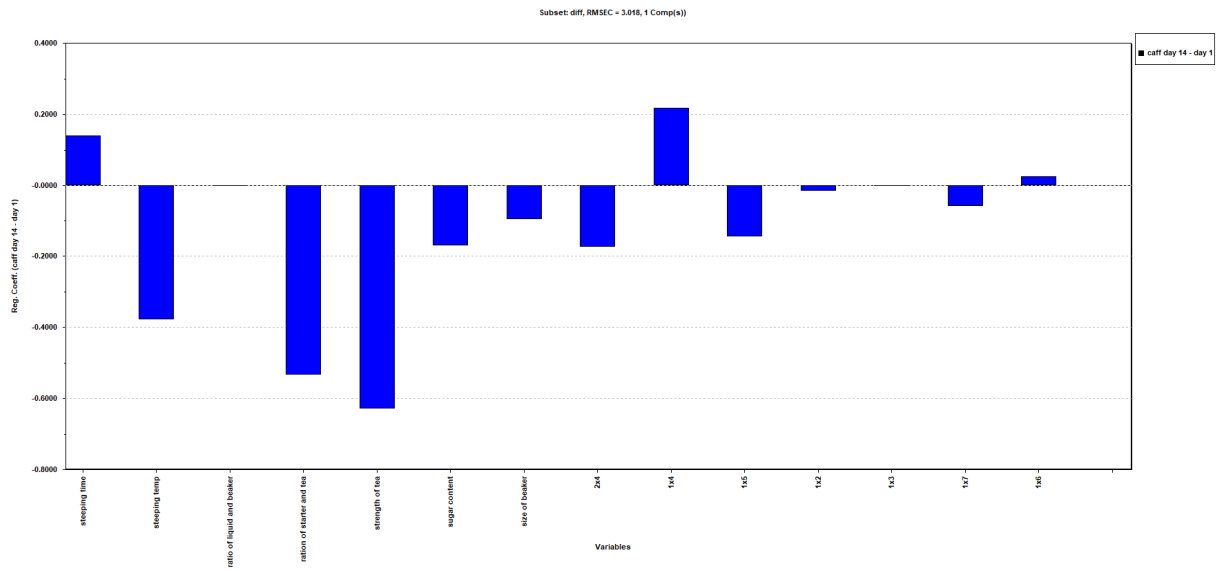


Figure 68: Screening variables caffeine day 14- caffeine day 1 (98.42%)

7.9 Pre-processing

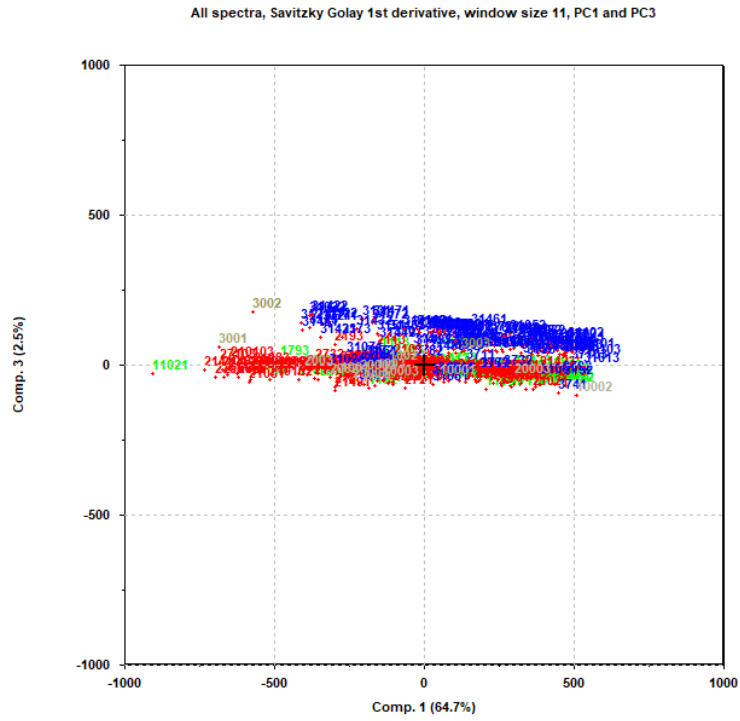


Figure 69: PCA scores PC1 and PC3, Savitzky Golay window 11, 1st derivative

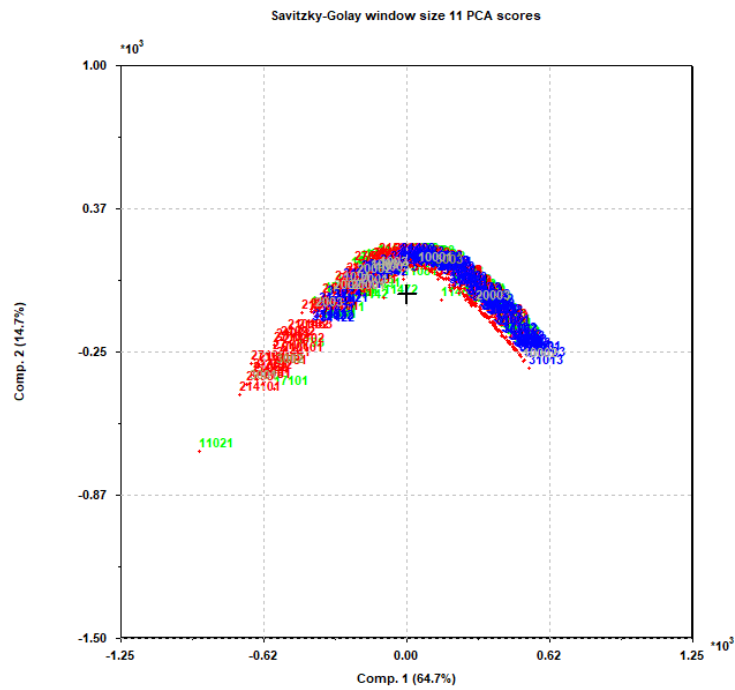


Figure 70: PCA scores PC1 and PC2, Savitzky Golay window 11, 1st derivative

Component Information (Independent and Dependent Block)					
1	- 98.52%	(98.52%)	- 4.66%	(4.66%)	- p-MC = 0.433
2	- 0.43%	(98.95%)	- 17.39%	(22.04%)	- p-MC = 0.300
3	- 0.27%	(99.22%)	- 18.17%	(40.22%)	- p-MC = 0.247
4	- 0.06%	(99.27%)	- 16.42%	(56.64%)	- p-MC = 0.457
5	- 0.02%	(99.28%)	- 16.14%	(78.75%)	- p-MC = 0.550

Figure 71: Component Information Table for the Savitzky Golay Differentiation 1st Derivative Window 11 Degree 2 1st replicates only.

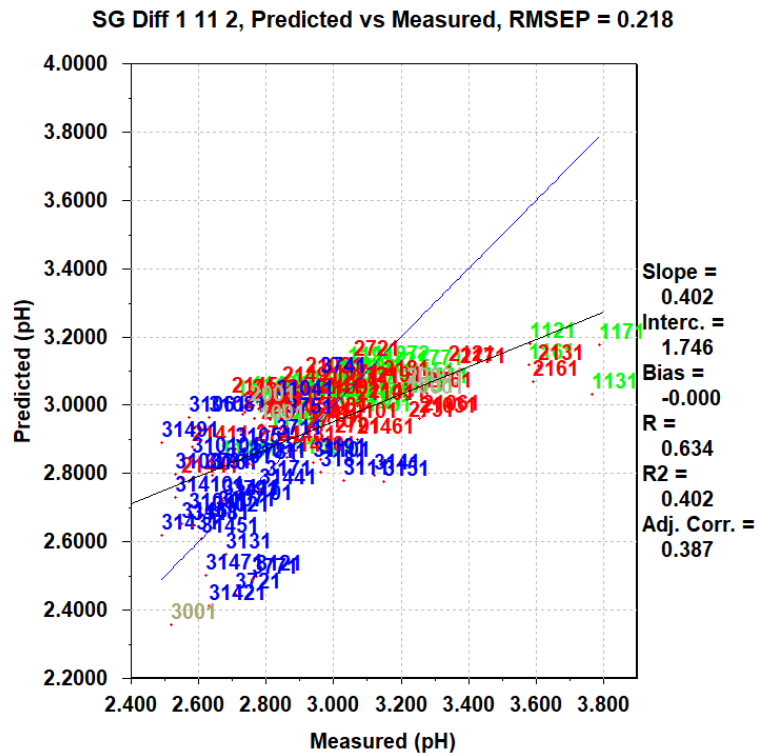


Figure 72: Predicted versus Measured for Savitzky Golay Differentiation 1st Derivative Window 11 Degree 2 with the cross-validation set

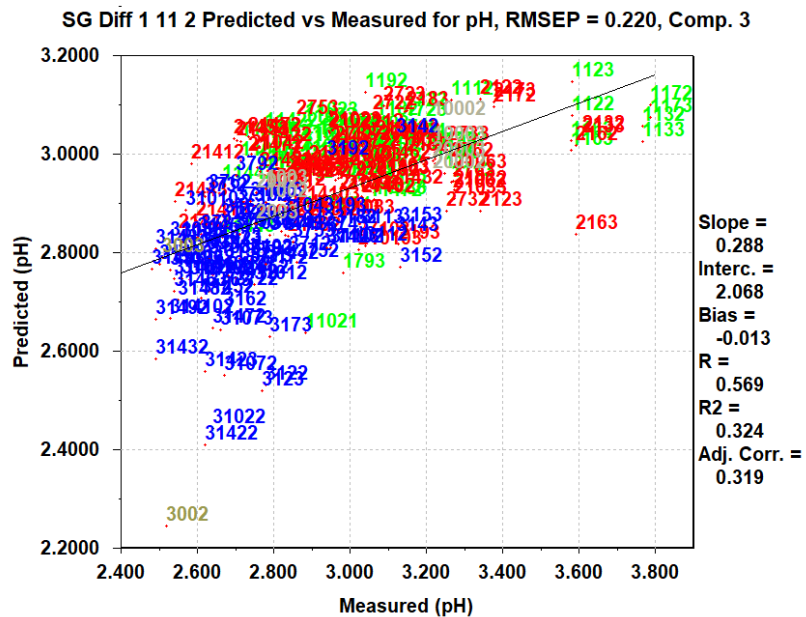


Figure 73: Predicted versus measured for Savitzky Golay Differentiation 1st Derivative Window 11 Degree 2 with the predicting set

7.10 PLS tabular results

Table 18: Examples of Pre-preprocessing techniques on the Raman spectra for pH

Training set	Pre-processing technique	Raman shift	# of components	R^2CV	RMSEP	R^2P	RMSEP
set 1, set 2 exp 8 and 9, starters	rb 10, 0.1; diff 1 11 3	322-1469	4	0.708	0.161	0.586	0.178
First replicates	MSC	322-1469	6	0.885	0.16	0.661	0.149
First replicates	EMSC 2	322-1469	5	0.867	0.17	0.589	0.159
First replicates							

Table 19: Examples of Pre-preprocessing techniques on the Raman spectra for caffeine

Training set	Pre-processing technique	Raman shift	# of components	R^2CV	RMSEP	R^2P	RMSEP
First trials	rollingball 14.999, 0.2999	322-1469	3	0.528	160.7	0.264	152.4
First trials	diff 1 11 3	322-1469	0 (2 manually selected)	0.599	170	0.112	166.777